The Dissertation Committee for Thomas John Van Blarcom Certifies that this is the approved version of the following dissertation:

Antibody Discovery and Engineering using the Anchored Periplasmic Expression (APEx) *Escherichia Coli* Display System with Flow Cytometric Selection

Committee:

George Georgiou, Supervisor

Brent L. Iverson

Andrew D. Ellington

Jennifer A. Maynard

Charles B. Mullins

Antibody Discovery and Engineering using the Anchored Periplasmic Expression (APEx) *Escherichia Coli* Display System with Flow Cytometric Selection

by

Thomas John Van Blarcom, B.S.

Dissertation

Presented to the Faculty of the Graduate School of

The University of Texas at Austin

in Partial Fulfillment

of the Requirements

for the Degree of

Doctor of Philosophy

The University of Texas at Austin

August 2009

Dedication

I dedicate this work to my family and friends whose continuous love and support have made this long and interesting journey possible. Especially my parents, Tom and Dot, who never gave up hope and have made this process more enjoyable. And to Diana, my love and soon to be wife, whose patience and understanding have made me a better person and scientist, and made the writing of this dissertation possible.

Acknowledgements

I would like to thank all past and present BIGG lab members who in one way or another have made me a better scientist, colleague, student, teacher, and friend. Especially Dr. Barrett Harvey, Dr. Laura Segatori, Dr. Karl Griswold, Dr. Robert Mabry, Dr. Yariv Mazor, Dr. Jamie Link, and Dr. Navin Varadarajan, whose mentoring, encouragement, and friendship were paramount to the accomplishment of this work. A special thanks to Prof. Robert Kelly who encouraged me to go to the Lone Star State for graduate school and recommended I work with Prof. George Georgiou. And of course, to George and Brent, who took a chance on me and have been much more than advisors.

Antibody Discovery and Engineering using the Anchored Periplasmic Expression (APEx) *Escherichia Coli* Display System with Flow Cytometric Selection

Publication No._____

Thomas John Van Blarcom, Ph.D.

The University of Texas at Austin, 2009

Supervisor: George Georgiou

The development of recombinant proteins for therapeutic applications has revolutionized the pharmaceutical industry. In particular, monoclonal antibodies are the safest class of all therapeutic molecules and account for the majority of recombinant proteins currently undergoing clinical trials. A variety of technologies exist to engineer antibodies with a desired binding specificity and affinity, both of which are a prerequisite for therapeutic applications. This dissertation describes the implementation of a novel combinatorial library screening technology for the discovery and engineering of antibodies with unique binding properties. Combinatorial library screening technologies are used for the *in vitro* isolation of antibodies from large ensembles of proteins (libraries) typically produced by microorganisms using molecular biology techniques. Our lab has developed a powerful antibody discovery technology that relies on *E. coli* display by anchored periplasmic expression, otherwise known as APEx.

First, I compared the effects of using combinatorial libraries comprising either smaller, monovalent single-chain antibody fragments (scFv), or the much larger, bifunctional full-length IgG antibodies. These technologies were used to isolate a small panel of antigen specific antibodies from the same library of antibody variable domains amplified from a mouse immunized with the Protective Antigen (PA) component from *Bacillus anthracis*, the causative agent of anthrax. Overall, IgG display resulted in the isolation of a broader panel of variable domain sequences. Most of these variable domains exhibited substantially reduced affinity when expressed as scFvs, which is consistent with the finding that none of these could be isolated from the equivalent scFv library. These results indicate that the antibody format used during *in vitro* selection affects which antibody variable domains will be discovered.

Second, I developed several modifications of the APEx methodology to allow for more efficient recovery of antibodies with desired properties. Specifically, the system was reengineered to simultaneously account for antibody binding and expression levels in order to isolate the highest affinity antibodies with favorable expression characteristics.

Third, the new approach, coupled with optimized fluorescence activated cell sorting (FACS) settings, was used to increase the affinity of an antibody by 35-fold resulting in a K_D of 100 pM. It was demonstrated that genetic transfer of this high affinity antibody specific for the V antigen of *Yersinia pestis*, the etiologic agent of the plague, conferred increased protection against intranasal challenge with a 363 LD_{50} of *Y. pestis* in mice.

Table of Contents

List of Tables

List of Figures

Chapter 1.

Engineering Therapeutic Antibodies

INTRODUCTION

Antibodies are produced by the immune system of vertebrates in a defensive response to invasion of foreign agents such as microorganisms and viruses. They have the ability to recognize a diverse array of molecules, referred to as antigens, including proteins, peptides, small molecules, lipids, carbohydrates, and DNA, with an exquisite degree of specificity and affinity. For these reasons, antibodies have been successfully exploited in therapeutic, diagnostic, and analytical applications since the late 19th century (56).

Antibody therapy was revolutionized by the development of the hybridoma cell line in 1975 (86). It circumvented the major limitations of the earlier polyclonal antibody therapies and provided an efficient means to generate monoclonal antibodies. Monoclonal antibodies are produced by individual B cells and are specific for one particular site on an antigen known as an epitope. The interaction between an antibody and antigen *in vivo* can result in a therapeutic benefit. Although the hybridoma technology is still used today, the antibodies they produce are of murine origin and are frequently immunogenic when administered to humans. Fortunately, recent advances in molecular biology have enabled the development of numerous *in vitro* technologies for the discovery and engineering of human antibodies (72). These technologies have been created in an attempt to mimic the *in vivo* generation and selection of antibody diversity by the immune system. They tend to expedite the discovery process, can be parallelized,

and allow the researcher to finely tune antibody properties (72). They also circumvent the biological constraints of antibodies generated *in vivo* which allows the generation of antibodies with higher affinities and toward toxic or non-immunogenic molecules (42, 45). Regardless of the technology used, the overall goal of antibody discovery and engineering is to isolate antigen specific monoclonal antibodies.

Monoclonal antibodies are frequently associated with healthcare since they are being used to treat a wide array of diseases (23). There are currently 18 FDA approved antibodies for use with transplantation, oncology, autoimmune, cardiovascular, and infectious diseases, and several other candidates are being developed for the treatment of a variety of indications (Table 1.1) (58, 99, 129, 154). Antibody-based therapeutics generated $20.6 billion in worldwide sales in 2006, which exceeded prior forecasts (99). This number is even more astonishing since the first FDA approved monoclonal antibody was MabThera™ (Rituximab) in 1997. The rapid growth of the therapeutic antibody market has resulted in over 100 companies generating antibody-based drugs toward hundreds of targets. With more than 150 monoclonal antibodies currently undergoing clinical evaluation, they account for the majority of recombinant protein drugs (24, 99, 129). This growth is predicted to continue because antibodies have established a track record for both safety and efficacy evident by their FDA approval rate being two to three times higher than other drug classes (129). Finally, discoveries in basic pathogenesis are allowing researchers to explore the use of antibodies for alternative treatment strategies (24).

Table 1.1. FDA Approved monoclonal antibodies

Brand name (generic name)	Company	Antibody format	Kd (nM)	Therapeutic Category	Approval Year
Orthoclone OKT3 (muromonab-CD3)	Ortho Biotech Products	Mouse IgG2a	0.83	Immunological	1986
ReoPro (abciximab)	Centocor	Chimeric Fab	5	Hemostasis	1994
Rituxan (rituximab)	Genentech, Biogen Idec	Chimeric IgG1	8	Oncological	1997
Zenapax (daclizumab)	Hoffman-LaRoche	Humanized IgG1	0.3	Immunological	1997
Simulect (basiliximab)	Novartis	Chimeric IgG1	0.1	Immunological	1998
Synagis (palivizumab)	MedImmune, Abbott Laboratories	Humanized IgG1	0.96	Anti-infective	1998
Remicade (infliximab)	Johnson & Johnson, Schering Plough	Chimeric IgG1	0.1	Immunological	1998
Herceptin (trastuzumab)	Genentech, Hoffmann-LaRoche	Humanized IgG1	5	Oncological	1998
Mylotarg (gemtuzumab ozogamicin)	Wyeth	Humanized IgG4, labeled	0.08	Oncological	2000
Campath (alemtuzumab)	Genzyme, Schering	Humanized IgG1	10-32	Oncological	2001
Zevalin (ibritumomab tiuxetan)	Biogen Idec	Mouse IgG1, 90Y-labeled	14-18	Oncological	2002
Humira (adalimumab)	Abbott Laboratories	Human IgG1	0.1	Immunological	2002
Xolair (omalizumab)	Genentech, Novartis	Humanized IgG1	0.17	Immunological	2003
Bexxar (tositumomab-I131)	GlaxoSmithKline	Mouse IgG2a, 131I-labeled	1.4	Oncological	2003
Raptiva (efalizumab)	Genentech, Serono	Humanized IgG1	3	Immunological	2003
Erbitux (cetuximab)	ImClone Systems, Bristol-Myers Squibb	Chimeric IgG1	0.2	Oncological	2004
Avastin (bevacizumab)	Genentech, Hoffmann-LaRoche	Humanized IgG1	1.1	Oncological	2004
Tysabri (natalizumab)	Biogen Idec, Elan	Humanized IgG4	0.3	Immunological	2004
Vectibix (panitumumab)	Amgen	Human IgG2		Oncological	2006

[a]Information obtained from published literature (24, 130, 164).

ANTIBODY STRUCTURE

There are several classes of antibodies known as isotypes, of which the immunoglobulin G (IgG) is the most abundant in human serum. IgG proteins are heterodimers of four covalently linked polypeptides known as the heavy and light chains, which come together and form the classic "Y"-shaped antibody structure. The stem of the "Y" is known as the crystallization or constant fragment (Fc) and the two identical arms are known as the antigen binding fragments (Fab) (Figure 1.1).

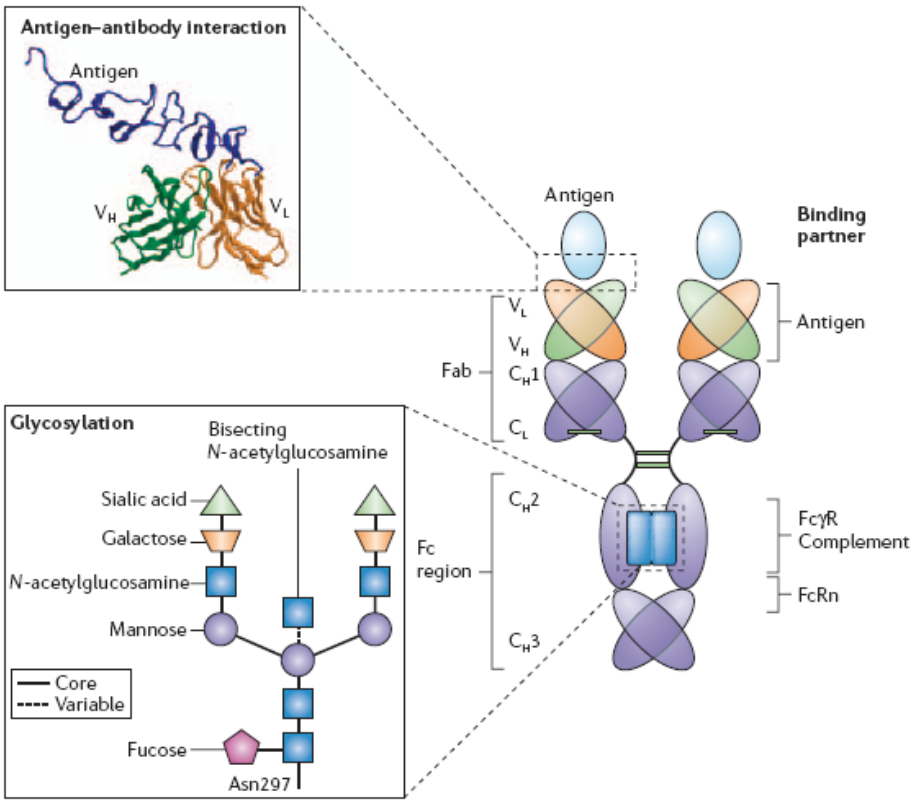

Figure 1.1. Immunoglobulin G (IgG) antibody structure.
The image is reproduced with permission from *Nature* (24).

The Fc is constant for each antibody isotype and is responsible for interacting with the cells of the immune system to initiate antibody mediated effector functions. The Fab, as its name suggests, is responsible for antigen binding, and they can be obtained by proteolytic cleavage from the Fc either as a monomeric species or as a pair ($F(ab')_2$) without altering their original binding properties. Binding occurs through the unique variable domains that are located on the N-terminus of the heavy and light chains, V_H and V_L, respectively. Each variable domain is comprised of three hypervariable loops, otherwise known as complementarity determining regions (CDR), which are supported by four structural framework regions. The vast sequence diversity contained within these variable regions enables antibodies to bind to a diverse array of antigens with both high specificity and affinity.

RECOMBINANT ANTIBODIES

In the late 1980's, molecular biology techniques enabled the facile cloning and expression of recombinant antibodies in bacteria, primarily in the Gram-negative bacterium *Escherichia coli* (146). *E. coli* is an ideal host for the expression of recombinant proteins, including antibodies, because it is easy to genetically manipulate, inexpensive to work with, and requires short periods for growth. However, in early studies it was not possible to produce full-length antibodies in *E. coli* in soluble form due to their size and complexity, thus recombinant antibody fragments are frequently used (106). Recombinant antibody fragments are generated by dissecting full-length antibodies into "minimalistic" binding domains through molecular biology techniques (Figure 1.2). These antibody fragments express well in *E. coli* and typically maintain the binding capabilities of their full-length counterparts (70, 106). Although single V_L and V_H domains can retain binding specificity, they are typically unstable and have lower

affinities than their IgG counterparts (70). Therefore, the most widely used form of a recombinant antibody fragment is the single chain variable fragment (scFv), which is generated by fusing the V_L and V_H domains with a flexible polypeptide linker (13). A variation of the scFv is the single chain antibody (scAb), which is a fusion between a scFv and the light chain kappa constant domain (C_K) (110). Additional forms of recombinant antibodies have also been produced and these are also depicted in Figure 1.2.

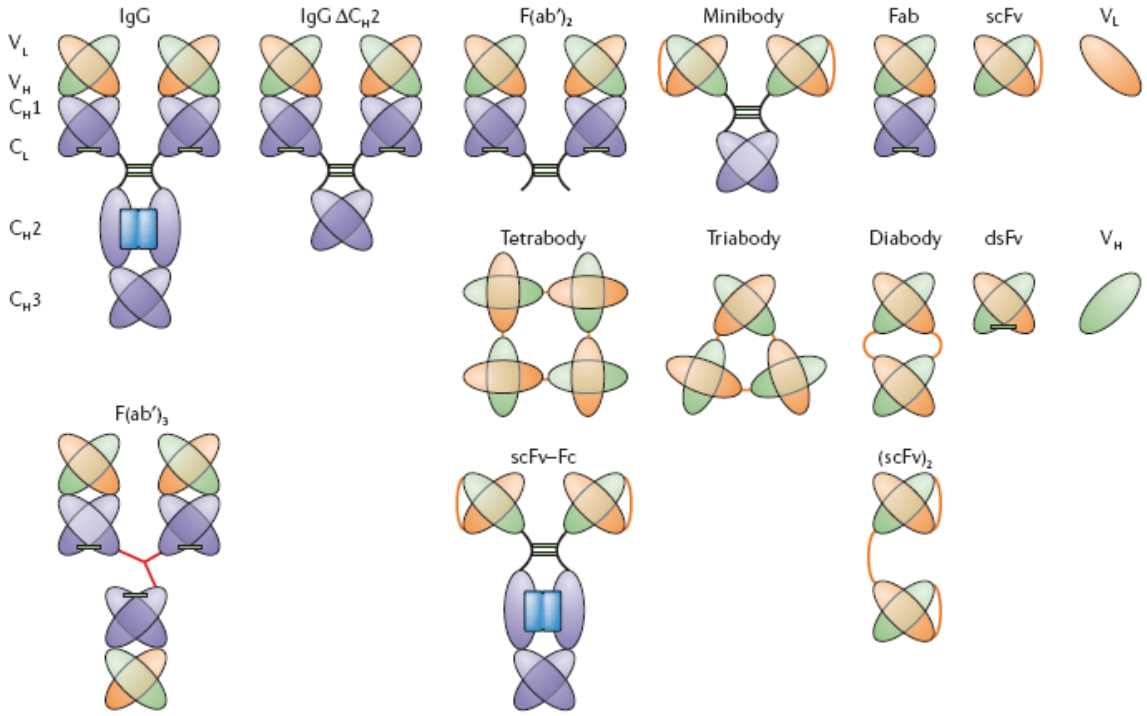

Figure 1.2. Recombinant antibody formats.
The image is reproduced with permission from *Nature* (24).

ANTIBODY SPECIFICITY AND AFFINITY

The two most important features of any form of an antibody, whether it is an IgG or a scFv, are its specificity and affinity for its antigen. This is determined by the amino acid sequences of the light and heavy chain variable domains and particularly the CDR sequences. Specificity is the ability of an antibody to recognize and interact with one particular antigen over another and form an immune complex. The exact region of the antigen that the antibody interacts with is its epitope. Most antigens have multiple epitopes that different antibodies are specific for and can bind to simultaneously, which helps facilitate antigen clearance by the immune system. The immune complexes can be in solution, or they can be insoluble if either the antibody or antigen is immobilized on a surface.

Affinity is the standard performance criterion of an antibody and is defined by an equilibrium binding constant (K_D) as follows:

$$[\text{Antibody}] + [\text{Antigen}] \underset{k_{off}\ (s^{-1})}{\overset{k_{on}\ (M^{-1}s^{-1})}{\rightleftharpoons}} [\text{Antibody:Antibody}]$$

The K_D is a ratio of the dissociation (k_{off}) and association (k_{on}) rate constants of the antigen-antibody complex and results in units of molarity. A higher affinity antibody has a higher propensity to remain in complex with its antigen and results in a lower K_D. Various methods have been created to measure either K_D or the individual rate constants (104). Of these, surface Plasmon resonance (SPR) has emerged as the industry standard since it is capable of real-time measurements over a wide range of affinities (104).

Surface Plasmon resonance (SPR) is an optical technology designed to measure the kinetic interaction between different molecules. It is a label free technology so it avoids the complexity that can arise from labeling the molecules, which can also compromise the integrity of their interaction with the other molecule (133). One

particular SPR instrument that is commonly used is the Biacore^{TM}. It is a microfluidic device in which one molecule (ligand) is covalently immobilized to a derivatized dextran matrix on the surface of sensor chip using primary amine or other standard chemistry. The other molecule (analyte) is injected by a robotic system and flowed across the surface for a set amount of time (Figure 1.3). The change in mass on the surface of the chip as a result of an interaction between the two molecules is monitored by a change in the refractive index of light that is reflected by the surface. This is used to generate in real-time an interaction profile called a sensogram. The sensograms generated under different experimental conditions are analyzed using supplied mathematical software to determine either the association (k_{on}) and dissociation (k_{off}) rate constants or the overall equilibrium constant (K_D).

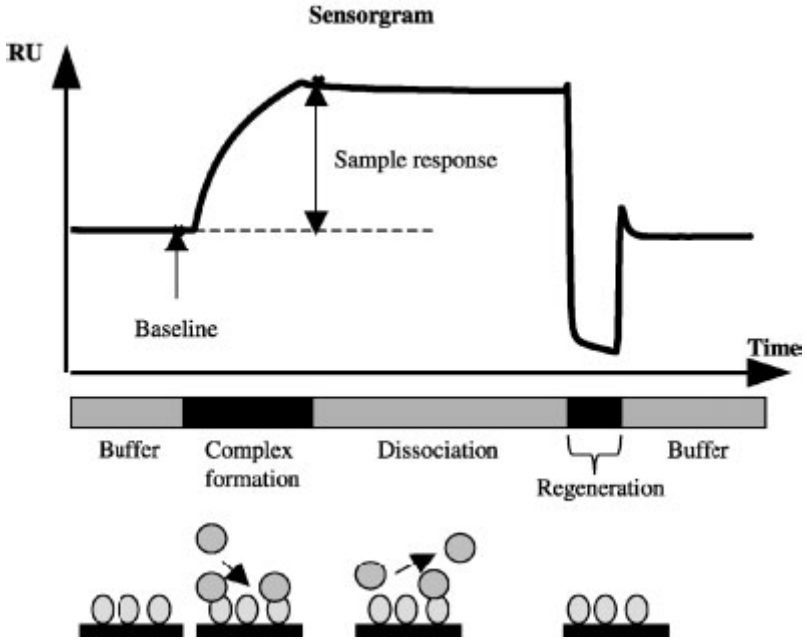

Figure 1.3. Surface Plasmon resonance.
The image is reproduced with permission from *Journal of Molecular Recognition* (84).

ANTIBODY EFFECTOR FUNCTION

Antibodies interact with the innate immune system through their Fc region by binding Fc receptors present on the surface of certain types of leukocytes. The interaction is dependent upon the antibody isotype and often results in effector functions performed by the cells (Figure 1.4). The effector functions eliminate immune complexes by opsonization, antibody dependent cell-mediated cytotoxicity (ADCC), or complement dependent cytotoxicity (CDC). The method of elimination is dependent upon the type of immune complex formed. Additional effector functions involving both cells within and outside of the immune system are antigen independent and are required to maintain antibody serum concentration homeostasis amongst other things (56).

Pathogens, such as a bacterium, have an array of immunogenic surface antigens that can be simultaneously bound by multiple antibodies. The close proximity of these antibody Fc regions allows them to interact simultaneously with multiple Fc receptors on the surface of phagocytes, such as macrophages and neutrophils. This crosslinks the receptors and triggers a signal transduction cascade that enhances phagocytosis and leads to the destruction of the pathogen inside the cell. This process is referred to as opsonization.

Opsonization is not always effective at eliminating immune complexes. Some virus infected, bacterially infected, and cancerous cells that are recognized by antibodies are too large and are destroyed through ADCC. The antibodies interact with Fc receptors on the surface of several cell types including natural killer (NK) cells, macrophages, eosinophils, and neutrophils. These cells destroy the targeted cell through multiple mechanisms leading to cell lysis or apoptosis.

Antibodies can eliminate pathogens and toxins via the complement system, a biochemical defense cascade associated with innate and humoral immunity. The close

proximity of multiple antibody Fc regions on the surface of a pathogen initiates the enzymatic cascade of the classical complement pathway, which ultimately results in formation of the membrane attack complex (MAC). The MAC perforates the bacterial cell membrane resulting in loss of osmotic stability followed by cell lysis. An important byproduct of activating the classical pathway is the activation of complement protein C3b, which binds non-specifically to immune complexes near the site of complement activation. C3b bound to the surface of a pathogen can initiate the alternative complement pathway, another biochemical cascade that results in MAC formation then cell lysis. The bound C3b can also interact with a receptor on the surface of erythrocytes which deliver the immune complexes to the liver and spleen. C3b can also act as an opsonin, initiating phagocytosis by interacting with complement receptors on the surface of immune cells.

IgG also interacts with the neonatal Fc receptors (FcRn) expressed on the surface of a variety of cell types including vascular, pulmonary, and intestinal epithelial cells, as well as antigen presenting cells (136). The expression patterns vary between cells of different species and can be age dependent. FcRn was first discovered as the means by which IgG is transferred from a human mother to her fetus, which is a form of passive immunity. It is now known to be involved in a variety of other biological functions. For example, the prolonged half-life and increased serum concentration of IgG compared to other isotypes are attributed to interactions with FcRn. This ensures that there is a sustained amount of IgG in circulation to efficiently initiate an immune response. In addition, FcRn is responsible for the transcytosis of IgG across intestinal epithelial cells where it can interact with mucosal pathogens and activate an immune response before the pathogen enters circulation.

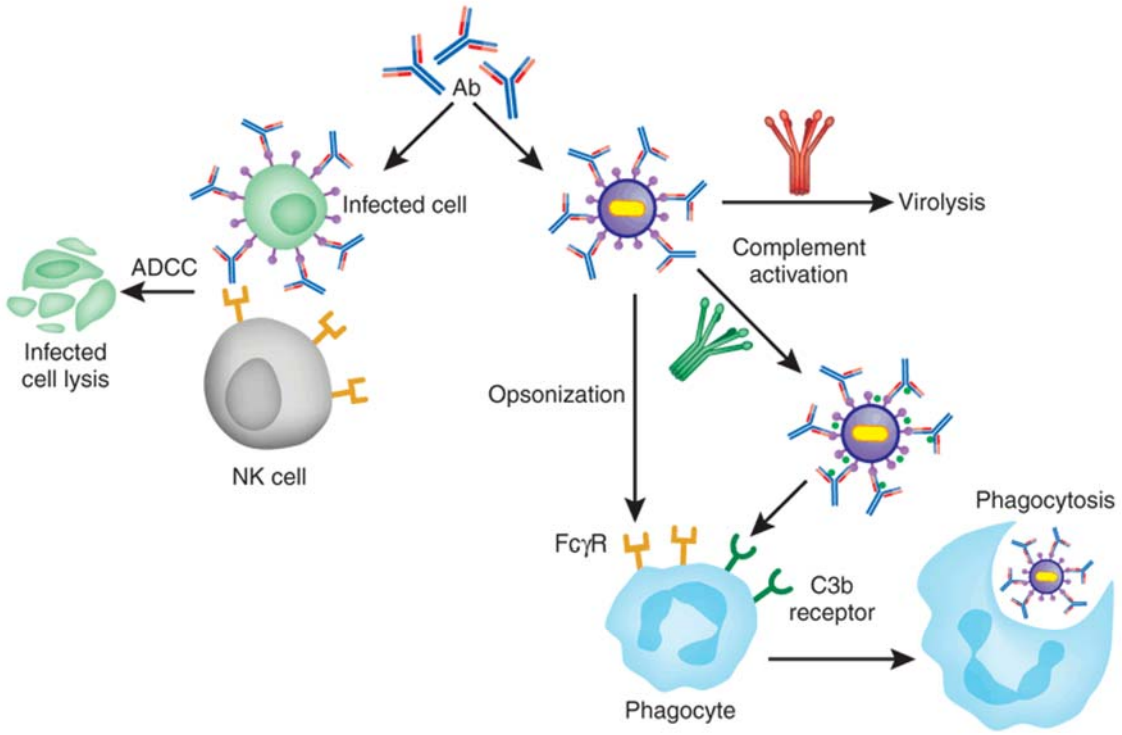

Figure 1.4. Effector functions.
The image is reproduced with permission from *Nature* (100).

ANTIBODY GENERATION *IN VIVO*

The immune system contains primary and secondary defense levels that vary in their specificity and adaptability. The innate immune system is the broadly specific and non-adapting component that provides the first level of defense. All organisms of a given species contain the same cellular and molecular components of the innate immune system, which recognize common properties of foreign agents, also referred to as non-self. The adaptive immune system is the highly specific and adaptable component that provides the second level of defense. It recognizes and responds to individual foreign agents in order to provide additional specific protection as needed through a process that

is dependent upon some cellular components of the innate immune system. The adaptive immune system not only varies between organisms, but within the same organisms over time since it reacts to the environment in a specific manner.

The adaptive immune system is regulated by the cooperation between antigen presenting cells and B and T lymphocytes, and is responsible for distinguishing between self and non-self agents, coordinating the immune response, and providing memory of previous responses to efficiently react to reoccurring exposures. The antigen presenting cells bridge the innate and adaptive immunity. These specialized cells take up antigen from pathogens and display markers to the T cells so they can determine what is self and non-self and regulate B cell production of antibodies for the humoral immune response. Lymphocytes provide the attributes of specificity and diversity to the adaptive immune system, which changes with time.

Humoral Immune Response

B cells circulate around the body in an inactivated state while the membrane bound antibodies on their surface perform surveillance of the body for the immune system. The antigen specificity of these antibodies is determined by the amino acid sequence of each of their variable domains, which are derived from the same limited pool of variable domain gene segments (Figure 1.5). The heavy chain variable domain (V_H) is divided into multiple V, D, and J gene segments while the light chain variable domain (V_L) is divided into multiple V and J gene segments. These gene segments are individually assembled in a combinatorial fashion to generate an enormous amount of sequence diversity. This combinatorial assembly is coupled with additional mechanisms that further expand the sequence diversity, which is estimated to be over 10^{10} for humans (56). This process occurs in the bone marrow and is where the antibodies on the surface

of each immature B cell are pre-screened in a highly regulated process to minimize recognition of self antigens and the onset of autoimmunity. B cells that make it through this process are classified as naïve B cells and circulate throughout the body.

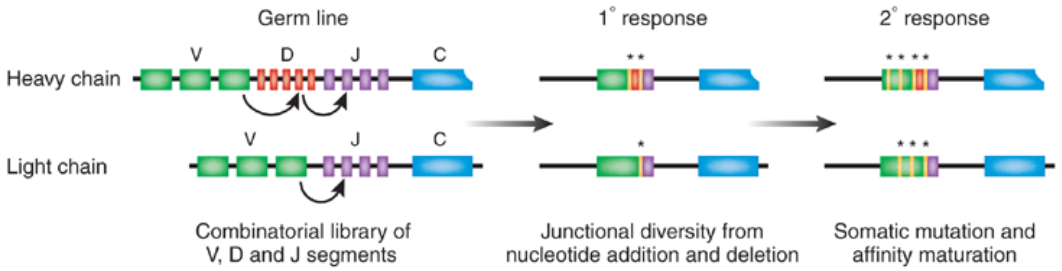

Figure 1.5. Combinatorial assembly of antibody germline gene segments.
Antibody variable domain diversity is obtained by random combinatorial assembly of V, D, and J gene segments, junctional diversity through the random addition and deletion of nucleotides at the joints between the gene segments, and somatic hypermutation mutation of the entire variable domain, which becomes most prevalent during the secondary immune response. Only one heavy chain constant domain is shown. The image is reproduced with permission from *Nature* (95).

The primary immune response begins when a naïve B cell is specifically activated through a process involving the interaction between the membrane bound antibodies on its surface and their antigen. The exact mechanism of this process varies depending upon the antigen encountered, but it is often thymus-dependent and relies upon the presence of a subset of T cells called T helper cells (T_H). Activated B cells migrate toward germinal centers, which are microenvironments located in the lymph nodes and spleen that facilitate B cell proliferation, selection, and differentiation (Figure 1.6). Their antibody variable domain genes are mutated during proliferation through a process called somatic hypermutation, which leads to affinity maturation. This process primarily targets the CDR regions of the V_H and V_L domains and occurs at approximately one mutation per division, a rate one million-fold faster than normal (56). Mutations resulting in antibodies with higher affinities (lower K_D) toward the foreign agent enable those B cells to survive

the antigen selection process by out competing for the limited supply of antigen located in the germinal center, while the other B cells undergo apoptosis and die. Surviving B cells must receive a stimulatory signal from T_H cells before undergoing differentiation into antibody secreting plasma cells and memory B cells. These cell types generate antibodies specific for the current invading foreign agent and dominate the total B cell population, which offers increased protection.

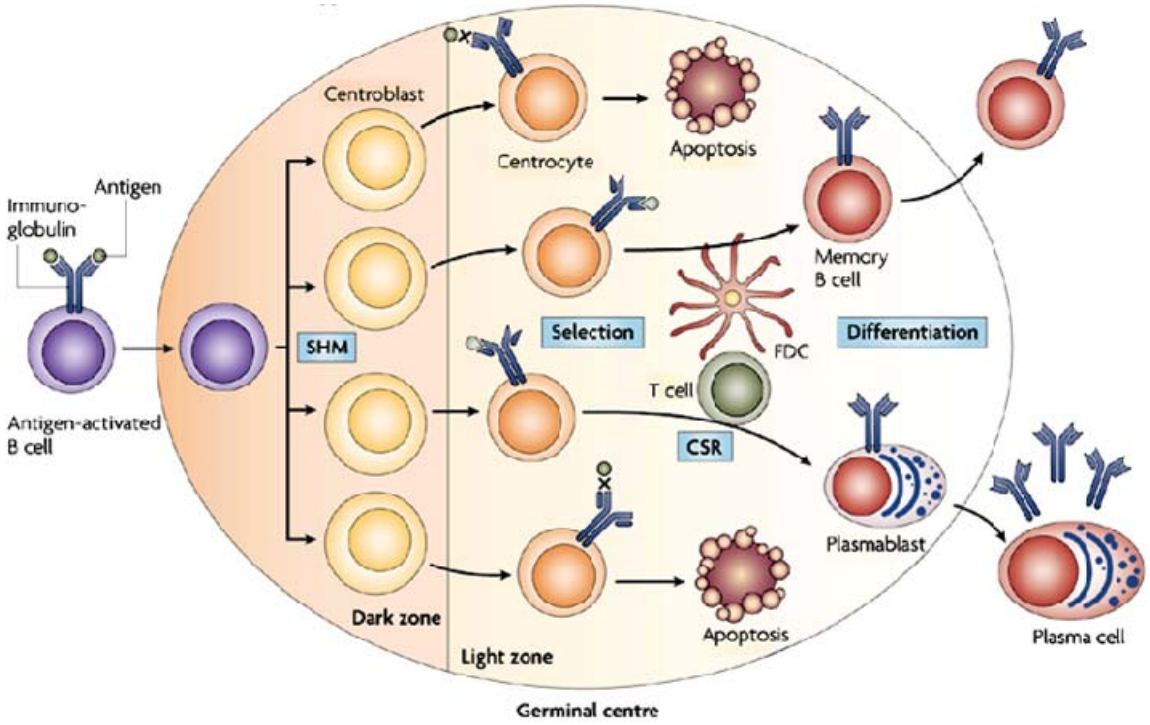

Figure 1.6. B cell proliferation, selection, and differentiation.
The image is reproduced with permission from *Nature* (85).

The plasma cells are responsible for producing soluble antibodies that assist in the immediate elimination of the foreign agent from the body. The maximum antibody concentration of these specific antibodies in the serum, referred to as a serum titer, occurs

one to two weeks following initial agent exposure and is dependent upon the route of exposure (56). Once secreted, the antibodies can bind to the agent and interact with cells of the innate immune system and with the complement system through their Fc region. This leads to various effector functions that facilitate agent removal. Most plasma cells do not have a long life expectancy and undergo apoptosis once the antigen has been eliminated, which typically requires days to weeks (56). However, some plasma cells migrate to the bone marrow where they persist for extended periods of time and continue to secrete antibodies (56, 144).

A memory B cell can last the lifetime of the individual and initiate a secondary immune response. The secondary immune response occurs following repeat exposure to the same foreign agent leading to the activation of memory B cells. As with naïve B cells, memory B cells are activated when antibodies on their surface interact with their specific antigen and this is more efficient in the presence of T_H cells, especially memory T_H cells. Activation of the memory B cells again leads to clonal expansion, but the response is faster, more prolonged, and results in higher antibody titers because the memory B cells are easier to activate and are present in greater quantities compared to naïve B cells (56). Whether or not these memory B cells undergoes subsequent somatic hypermutation in germinal centers to further increases the antibody affinity toward its antigen is a controversial subject (111, 124, 153). The entire process of the immune response results in a heterogeneous population of antibodies circulating in the blood. These antibodies are capable of recognizing, with varying affinities, a variety of epitopes on the foreign agent and help coordinate its removal from the body.

Polyclonal Serum and Passive Immunity

Antibodies produced as part of the humoral immune response can be transferred from the immune individual to a non-immune individual and provide immunity. This process is called "passive immunity" and was first demonstrated in the late 19th century by Emil von Behring and Kitasato Shibasaburo (160). In their studies, they took mice that were immune to diphtheria and extracted the serum fraction of their blood by removing all the cellular components, allowing the remaining plasma to clot, then isolating the fluid fraction. They transferred this serum to guinea-pigs infected with diphtheria which cured them. This therapeutic approach was referred to as "serum therapy" since it was not known that antibodies were responsible for eliminating the infection.

A few years later, Behring teamed up with Paul Ehrlich to produce serum therapy that could be used on humans (160). Ehrlich previously demonstrated the concept of active immunity by building up an animal's tolerance to a toxin by gradually increasing exposure to it. The process is referred to as immunization. They used this approach to immunize dairy cattle and mass produced serum that was successfully used on thousands of humans suffering from diphtheria. Serum therapy has been used to cure other infectious diseases and is still used today for certain indications (12, 25, 117).

It was not long before researchers demonstrated that serum from immune donors could neutralize and precipitate toxins as well as agglutinate bacteria (56). Until the 1930's, it was thought that different substances were responsible for these different activities. However, Arne Tiselius and Elvin Kabat determined the gamma-globulin fraction of serum was responsible for all these activities and called them immunoglobulins, also known as antibodies.

Serum therapy was a revolutionary breakthrough that saved thousands of lives over the course of history, and for its discovery, Behring was awarded the Nobel prize in

1901 (25, 56). Unfortunately, mild to severe complications were often associated with serum therapy, which involved large serum dosages containing various animal proteins, including antibodies, which are immunologically incompatible in humans (56). The humoral immune response generates antibodies specific for the animal proteins resulting in a high quantity of immune complexes. This can lead to symptoms that mimic an allergic reaction and is referred to as serum sickness (56).

Advances in purification techniques have enabled the production of polyclonal antibody preparations from serum with reduced toxicity (117). However, the polyclonal populations of antibodies isolated from different serum preparations results in inconsistent and non-specific biological activities and thus are rarely used for therapy today. These approaches are mainly used to produce research grade polyclonal antibodies for analytical and diagnostic applications (33). They are especially useful reagents when a high level of sensitivity is required since they consist of a heterogeneous population of antibodies that can bind a variety of epitopes on the same antigens simultaneously. The need for the reliable production of identical antibodies with known properties, especially for therapeutic applications, resulted in the development of technologies to produce monoclonal antibodies.

The Hybridoma Technology

In 1948, antibodies found in serum were shown to be produced from plasma B cells (145). Unfortunately, typical B cells are difficult to cultivate and are not suitable for antibody production *in vitro*. However, cancerous B cells known as myelomas are readily cultivated *in vitro* and can lose their ability to produce antibodies. In 1975, Milstein and Kohler created a stable cell line capable of continuous production of a single monoclonal antibody *in vitro* by fusing an antibody producing B cell with a myeloma cell (86),

referred to as a hybridoma. The development of the hybridoma technology marks the beginning of antibody engineering.

In order to generate a hybridoma that produces a monoclonal antibody of desired antigen specificity, a mouse is immunized with the desired antigen and either the peripheral or splenic B cells are isolated (Figure 1.7). The pool of B cells is fused with myeloma cells and various cell-cell fusion products arise including B cell-B cell, myeloma-myeloma, and the desired B cell-myeloma hybrids as well as non-fused cells. These cells are then cultivated under specific conditions that allow only the growth of B cell-myeloma hybrids or hybridomas, each of which, in theory at least, should produce a single antibody protein. The hybridomas are serially diluted to isolate individual cells, and their secreted antibody is tested for binding toward the antigen used for immunization. A commonly used binding assay is an enzyme linked immunosorbant assay (ELISA) since it provides high-throughput parallel screening via multi-well plates. Hybridomas secreting antibodies of interest are collected, and their respective antibodies are expressed for further characterization and production if necessary.

The hybridoma technology is still used today, but has several critical limitations (161). The immunization process required to engage the secondary immune response and generate the highest affinity antibodies *in vivo* is time consuming and difficult to parallelize (56). Further, the affinity of these antibodies is typically in the nanomolar range, but not necessarily in the picomolar range, which is required for many therapeutic antibodies (24, 105). Additionally, mouse antibodies induce an immune response when administered to humans since they are recognized as foreign molecules. This is referred to as the human anti-mouse antibody (HAMA) response. The HAMA response can results in rapid clearance and reduced efficacy of mouse therapeutic antibodies and also increases the risk of allergic reactions (77, 95, 122). In addition, mouse antibodies have

difficulty initiating effector function in humans because of sequence differences in their Fc regions.

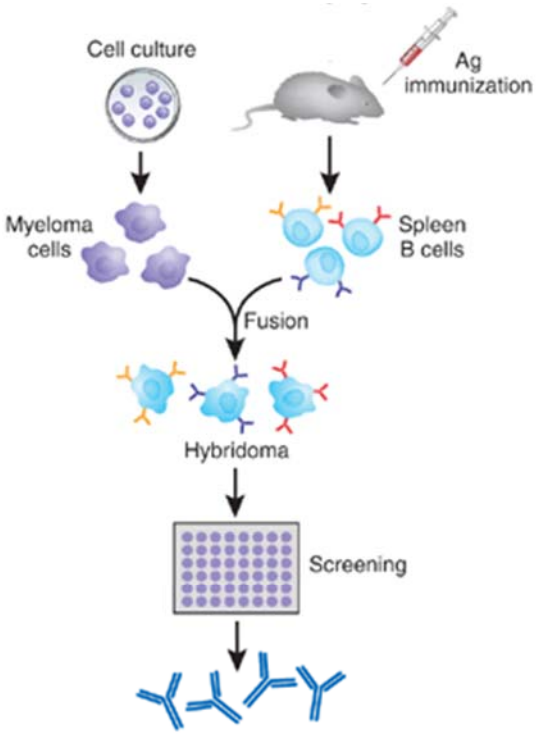

Figure 1.7. The hybrdidoma technology.
The image is reproduced with permission from *Nature* (100).

The use of Human B cells rather than those from mice could in principle be employed to generate human hybridomas. However, generating hybridomas from human B cells is much more difficult than it is from murine cells (41, 161). Even though many of these technical limitations have been overcome, there are obvious ethical reasons that prevent humans from being immunized to produce antibodies (95). Ethical complications can be avoided if the B cells are isolated from individuals who would normally be vaccinated or are naturally responding to an infection or disease, but this approach is only effective for a subset of diseases. Lastly, the majority of therapeutic targets for antibodies are human antigens, and the immune system has evolved to prevent the generation of

antibodies toward them to avoid autoimmunity through a process known as self tolerance (95).

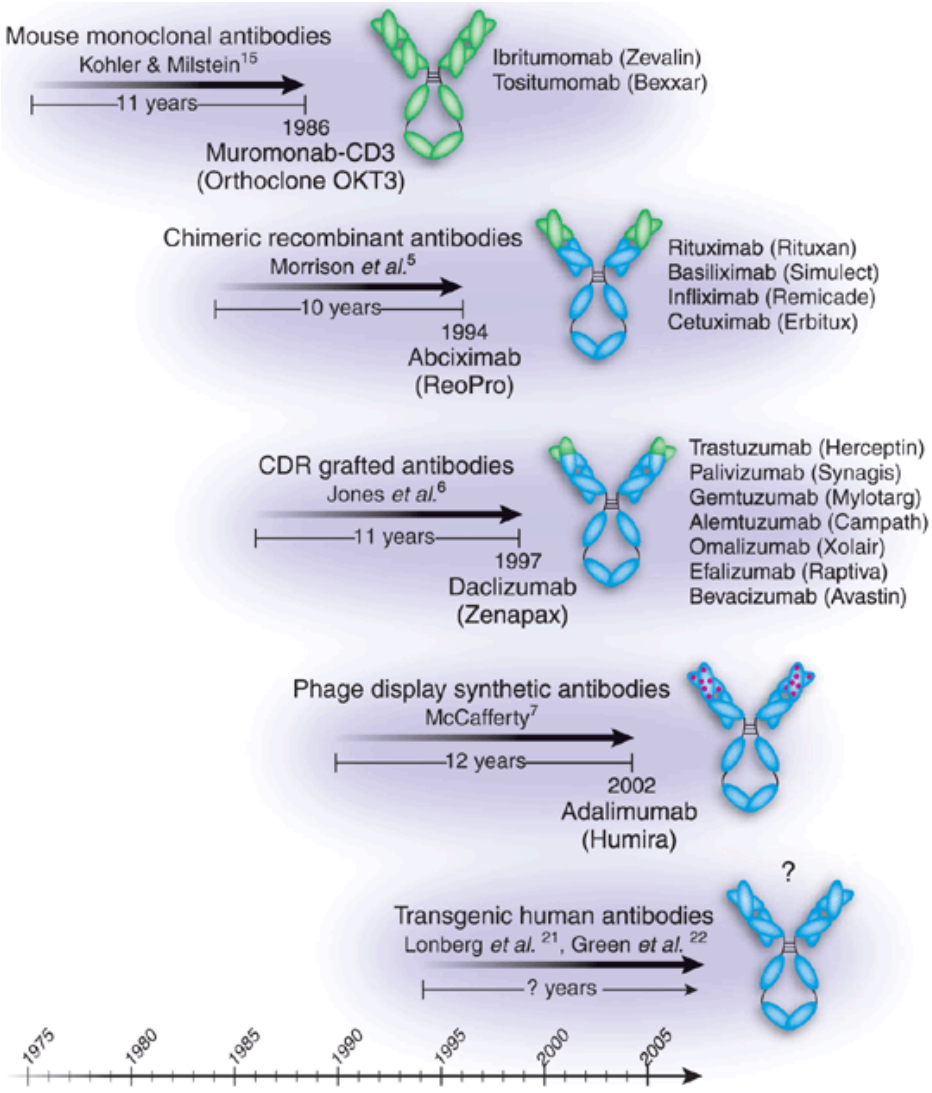

Figure 1.8. The evolution of human antibodies.
Vectibix™ (panitumumab) became the first FDA approved therapeutic antibody generated from a transgenic animal in 2006, but it was not approved at the time this image was previously published. The image is reproduced with permission from *Nature* (95).

Humanization

The risk of immunogenicity associated with therapeutic antibodies derived from mice is reduced by creating chimeric antibodies in which the mouse constant domains are replaced by their human counterparts (122, 129) (Figure 1.8). This approach removes two-thirds of the mouse sequence and simultaneously provides human Fc regions that more effectively engage the human immune system. Although there are several FDA approved chimeric antibodies, some chimeras generate a HAMA response resulting from the remaining mouse variable domains.

The variable domains can be either de-immunized or further humanized through a variety of processes in order to further reduce their immunogenicity (122). Antibodies can be de-immunized by removing potential T-cell epitope sequences identified using bioinformatic techniques (122). However, such methods are unreliable at the moment. The more common approach is humanization by replacing the mouse framework regions with human ones through a process called CDR grafting (Figure 1.9). These approaches can result in a reduction of antibody affinity, which in turn necessitates the reengineering of affinity back into the antibody, a process that is time consuming. Regardless, humanized antibodies can be effective and account for half of the FDA approved antibodies (Table 1).

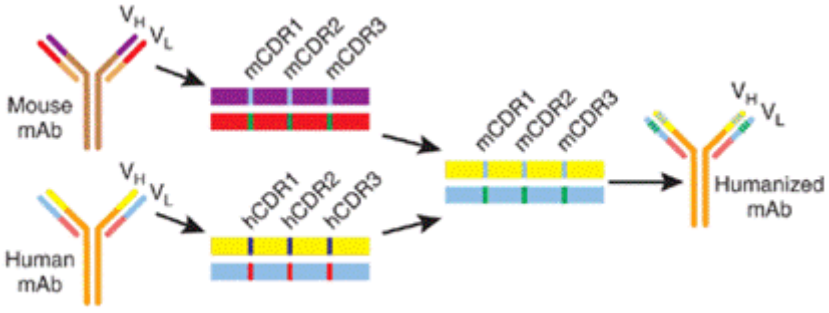

Figure 1.9. Humanization by CDR grafting.
The image is reproduced with permission from *Nature* (100).

Transgenic Mice

The inherent immunogenicity of mouse monoclonal antibodies and the limitations of human hybridomas has led to the engineering of transgenic mice that encode human immunoglobulin genes repertoires instead of their own (95). As a result these mice contain B cells that produce human antibodies. (57, 96). In these mice, the entire mouse heavy chain and kappa light chain genes were removed and most, but not all of the human heavy and kappa light chain genes were introduced in their place (Figure 1.10). Even though only a small fraction of the heavy chain variable domain gene repertoire is encoded by these transgenic mice, they generate antibodies toward a diverse array of antigens (95).

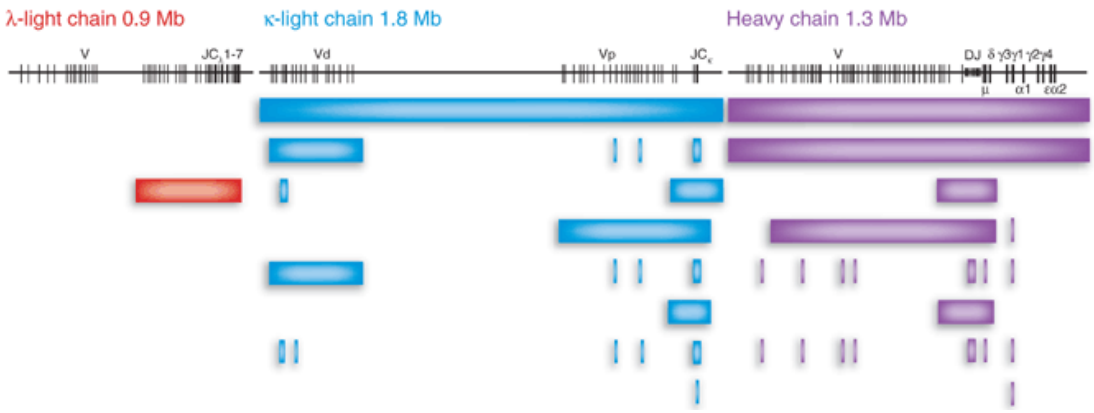

Figure 1.10. Transgenic mice germlines.
The human heavy and light chain immunoglobulin germline gene segments configuration is depicted in the top row. The bars below represent the regions of the human germline that have been introduced into mice for the generation of human antibodies. The image is reproduced with permission from *Nature* (95).

Transgenic mice now exist that contain the gene loci of the entire human heavy and kappa light chains (95). They are capable of generating completely human antibodies with affinities in the low- to sub-nanomolar range (77, 95, 127). The first approved therapeutic antibody generated from a transgenic mouse, Vectibix™ (panitumumab), was

approved in 2006 and many others are in clinical evaluation (77, 95). Although transgenic mice have revolutionized the hybridoma technology by nearly eliminating immunogenicity, they still have similar limitations to hybridomas such as antibody affinity and the ability to generate antibodies toward certain molecules including human proteins that share a high degree of homology with their mouse counterparts.

ANTIBODY DISCOVERY AND ENGINEERING *IN VITRO*

Technologies for the discovery and engineering of antibodies *in vitro* are designed to mimic the *in vivo* generation and selection of antibody diversity accomplished by the immune system in a process known as directed evolution (70, 72). These *in vitro* approaches are more efficient and result in the discovery of a wider array of antibodies compared to hybridomas (72). Further, they circumvent the limitations of the natural immune system and can be used to discover antibodies toward any target including toxins and self antigens. They can also be used to improve a variety of antibody properties including specificity, affinity, stability, avidity, immunogenicity, effector functions, pharmacokinetics, pharmacodymanics, and expression level in heterologous systems for mass production. Regardless of the technology or its application, they all require the generation of sequence diversity and a selection platform for isolation (72).

GENETIC DIVERSITY AND LIBRARY CONSTRUCTION

Genetic diversity of the variable domains is typically created *in vitro* using gene amplification by the polymerase chain reaction (PCR) or by DNA synthesis (158). The resulting gene pools are referred to as a library. Libraries for discovery applications are classified as immune, naïve, or synthetic (Figure 1.11). Immune libraries are cloned from

a donor immunized with a particular antigen, naïve libraries are cloned from a non-immunized donor, and synthetic libraries are rationally designed by randomization of the amino acid positions typically involved in antigen binding as determined from known antibody sequence and structure data (72). The size of the library is critical, as larger libraries allow for greater sequence diversity to be represented, which increases the probability of isolating an antibody with desired properties (70, 75).

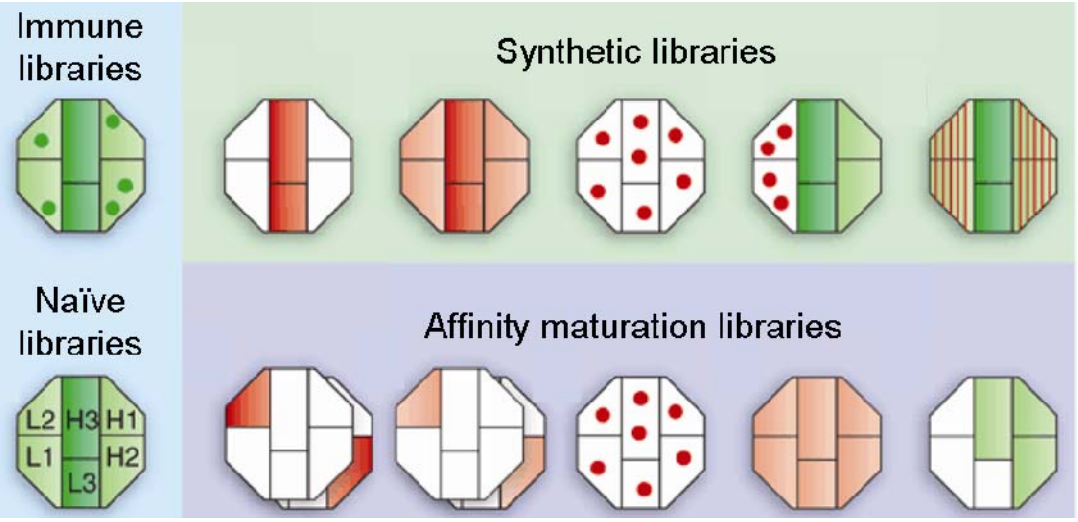

Figure 1.11. Sequence diversity for library construction.
The sequence diversity at the center of the antigen binding site of an antibody is represented by each octagon. Within in each antigen binding site are the six heavy and light chain CDRs which are depicted as different regions. The origin of the CDR sequence is either natural (green) or synthetic (red) with darker shades indicating higher levels of diversity. Dots indicate either mutations from somatic hypermutation (green) or synthetic diversity (red). The image is reproduced with permission from *Nature* (72).

The affinity of antibodies isolated from an immune, naïve, or synthetic library are often sufficient for analytical applications, but too low for a variety of therapeutic applications such as toxin and viral neutralization (19, 105). These antibodies must undergo the process of affinity maturation (Figure 1.11). As with somatic hypermutation *in vivo*, the antibody sequence can be mutated *in vitro* to obtain variants with different

amino acid sequences that confer an increase in affinity. Libraries are constructed by PCR or DNA synthesis using different mutagenesis strategies and are classified as targeted, error-prone, or shuffled (10). Targeted libraries randomize a small number of amino acid residues, frequently located in the complementarity determining regions (CDR), that are likely to interact with the antigen (10). These residues can be precisely determined based on a crystal structure of the antibody-antigen complex or based on general antibody sequence and structure data. Error prone libraries introduce random mutations across the entire gene. They are typically generated *in vitro* by PCR under conditions that randomly introduce mutations at a given rate across the entire gene, but can also be generated *in vivo* using mutator strains of *E. coli* (50, 97). This approach has led to the identification of sites critical for binding that are not structurally obvious and would not have been found from a targeted approach (92). The DNA sequences of several antibodies isolated from either of the previous libraries can be randomly digested then recombined by PCR to create a shuffled library. This approach has generated antibodies with drastically improved properties compared to the individual sequences from which they were derived (113). Finally, all of these strategies can also be used to enhance other antibody properties that have previously been mentioned.

DISPLAY TECHNOLOGIES

In order to efficiently isolate antibodies with desired properties from the enormous gene libraries described above, numerous display technologies have been developed (Figure 1.12) (72). In general, the systems that comprise these different technologies share three steps: a link between genotype and phenotype, application of a selective pressure, and amplification of the selected population (Figure 1.13) (72).

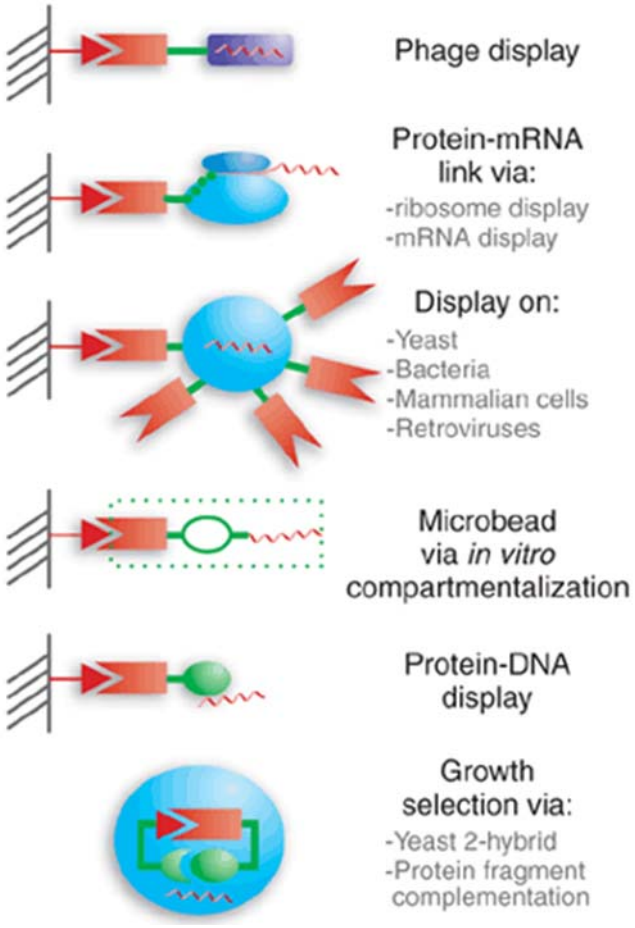

Figure 1.12. *in vitro* display technologies.
The symbols are as follows: surface, black striations; antigen, red arrow; antibody, red rectangle with triangular recess; DNA, wavy red line; phenotype-genotype link, green line; proteins, green rounds shapes; surface, additional blue, green, or purple shapes. The image is reproduced with permission from *Nature* (72).

By applying these steps, the small numbers of antibodies with desired properties are enriched from large libraries containing mostly undesirable antibodies through sequential rounds of screening followed by analysis of monoclonal antibodies produced by individual clones. The three most commonly used technologies are phage, microbial, and ribosome display (72). Phage display on the surface of filamentous bacteriophage is the most established screening system for antibodies as well as other proteins (135, 148).

Microbial display on the surface of bacteria or yeast cells such as *E. coli* and *Saccharomyces cerevisiae*, respectively, have become increasingly popular due to recent advances in flow cytometry (30, 37, 38, 53, 120). There are also several entirely *in vitro* display technologies of which the ribosome display system has been used with the most success (72). Much larger libraries can be constructed using entirely *in vitro* systems since they are not limited by the DNA transformation efficiency of cells.

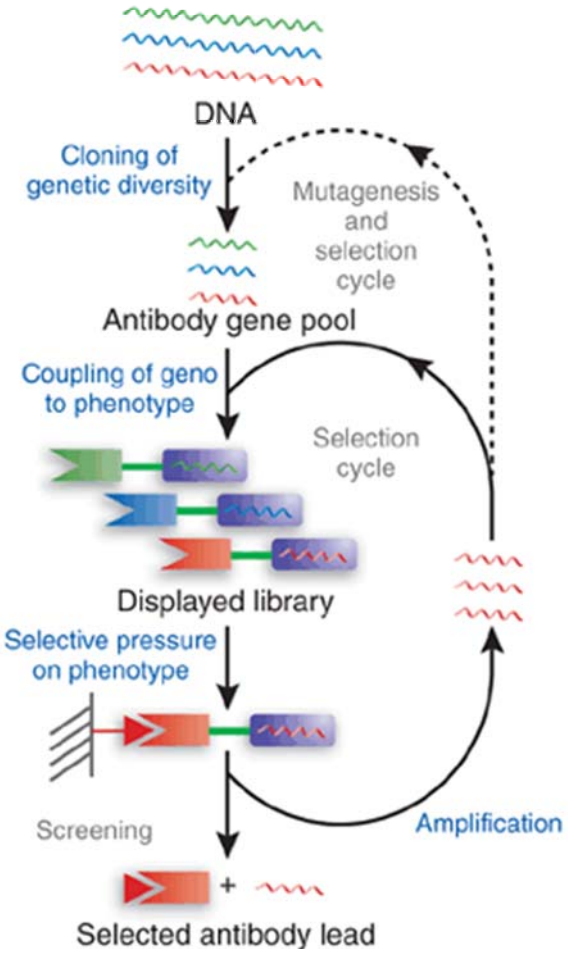

Figure 1.13. *in vitro* selection process.
The symbols are as follows: surface, black striations; antigen, red arrow; antibody, red rectangle with triangular recess; DNA, wavy red line; phenotype-genotype link, green line; proteins, proteins, green rounds shapes; surface, additional blue, green, or purple shapes. The image is reproduced with permission from *Nature* (72).

Phage Display

The first technology used to display a functional antibody binding domain was phage display (109). Phage display is based on encoding the gene of interest in-frame with one of the phage coat proteins and encapsulating the fusion gene within the phage particle. The filamentous bacteriophages M13, fd, and f1 are the most commonly used phage particle (10, 135). They are approximately 1 um long and approximately 10 nm in diameter and are comprised of multiple copies of five different coat proteins which encapsulates the single stranded DNA genome (ssDNA) (Figure 1.14). The phage particles consist of about 3000 copies of the major coat protein (pVIII) which are capped on the ends by approximately 5 copies of each of the minor coat proteins (pIII, pVI, pVII, pIX) (135, 143).

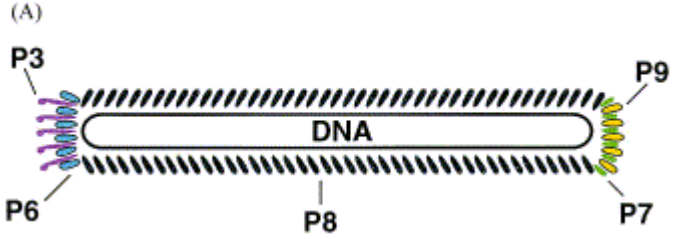

Figure 1.14. Bacteriophage structure and composition.
The image is reproduced with permission from *Biomolecular Engineering* (143).

All of the coat proteins have been used to display recombinant antibody fragments, but pIII remains the most widely used since it is compatible with scFv, Fab and ($F(ab')_2$) display (6, 51, 52, 73, 90, 109, 135). The pIII protein is responsible for bacterial infection and fusions must be carefully made so infectivity can still proceed. They are frequently made at the N-terminus of pIII immediately after the leader peptide, but other variations do exist that also maintain infectivity (19, 87). Polyvalent display on all copies of pIII is achieved by cloning the antibody fragment gene in frame with the pIII gene located in the phage genome (109, 118). The DNA is transformed into *E. coli* and

phage particles displaying the fusion protein are subsequently produced. Phage vectors are difficult to work with since the phage genome is ssDNA, which makes the construction of large libraries difficult (19). The polyvalent display results in avidity effects leading to the isolation of a greater diversity of antibodies, but at the expense of lower affinity antibodies (19). This also makes affinity maturation difficult since a small increase in affinity can not out-compete the avidity effect (19). These issues are circumvented by cloning the antibody fragment gene in frame with the pIII gene using a double stranded DNA (dsDNA) plasmid vector known as a phagemid (109, 118). Phagemids do not contain any other genes from the phage genome, but they do contain the origin of replication and packaging signal from it. *E. coli* is transformed with the phagemid and subsequently infected with helper phage that provides the necessary genes for replication and preferential packaging of the phagemid as ssDNA inside the phage particle. The native pIII encoded by the helper phage genome out competes the non-native antibody-pIII fusion and results in lower levels of fusion display. This display is frequently monovalent and allows the selection of higher affinity antibodies since there is no avidity effect (19).

Phage display has been used to isolate antibodies from immune, naïve, or synthetic libraries and engineer them for improved properties including affinity and stability (72). Antibodies are selected from these libraries through a process called panning (Figure 1.15). Through this process, the target antigen is immobilized on a surface and phage displaying antibodies specific for the antigen are isolated through sequential rounds of adsorption, desorption, and amplification of the phage. Variations of this process exist in order to isolate antibodies with specific properties, but the concept remains the same (10, 71). Humira™ (adalimumab, the first fully human mAb to receive FDA approval, was discovered using phage display (154). Currently, there are at least 16

human mAbs derived from phage display in advanced clinical trials for a wide range of human diseases (81, 119, 129, 154).

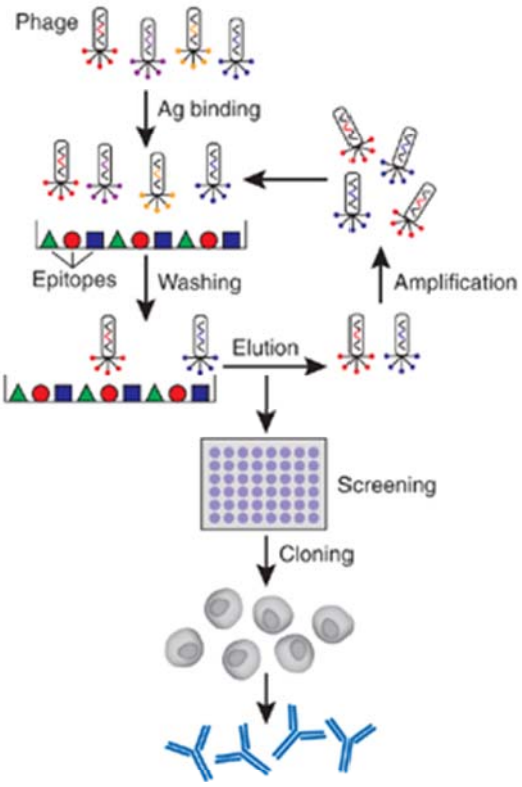

Figure 1.15. Phage panning process.
The image is reproduced with permission from *Nature* (100).

Microbial Display

Antibodies can also be displayed on the surfaces of cells to maintain a link between genotype and phenotype (Figure 1.12). Microbial display on the surface of bacteria or yeast cells, most commonly *E. coli* and *S. cerevisiae,* is typically used because of their faster growth rates, higher transformation efficiencies, and lower production costs compared to mammalian cells. Microbial display has one clear advantage over phage and

ribosome display, namely the ability to utilize fluorescence activated cell sorting (FACS) (38, 63). FACS is a high-throughput screening technique that enables real-time quantitative multi-parameter analysis on a cell by cell basis. Therefore, multiple properties can be monitored simultaneously to specifically isolate antibodies with desired characteristics such as antigen binding and high antibody expression levels.

Flow Cytometry

Flow cytometry is a high-throughput technique used to individually analyze microscopic particles based on their physical and chemical characteristics (Figure 1.16). The most sophisticated flow cytometers are capable of analyzing 10^9 cells/hr and can be used to isolate extremely rare events present at frequencies of less than one in a million (37, 89). In flow cytometry, a narrow, hydrodynamically focused stream of fluid containing the suspended particles in a single file orientation flows through an interrogation chamber in which one or more beams of light, typically lasers, are focused. For each particle, the extent of light scattering and fluorescence emission at different wavelengths are measured by separate detectors to enable multi-parameter analysis. The light scattering determines relative size (FSC) and internal complexity of the particle (SSC) while the fluorescence emissions are used to detect particular properties of the particle. The number of parameters capable of being analyzed simultaneously is dependent upon the number of lasers and detectors with which the flow cytometer is equipped (141).

There are numerous fluorescent molecules available that can be used either independently of or in conjunction with non-fluorescent molecules to determine an overwhelming amount of intracellular and extracellular information about a given cell (103, 141). This includes the presence of surface markers, cell viability, pH, and

membrane potential. Cells can be simultaneously labeled with multiple fluorophores as long as their spectral characteristics are compatible for simultaneous detection. Simultaneous detection of 13 different cellular parameters has been reported (121).

Following labeling of a heterogeneous cell population to identify individual cells with particular characteristics, specialized flow cytometers can be used to individually select these cells through a process known as fluorescence activated cell sorting (FACS) (93, 103). For example, antibodies displayed on the surface of cells can be simultaneously labeled to determine their ability to bind one particular antigen over another and their expression levels (17). Cells displaying antibodies with desired characteristics are diverted into a collection tube by a mechanical or electrical device while the remaining cells are discarded. The collected cells can then be further analyzed.

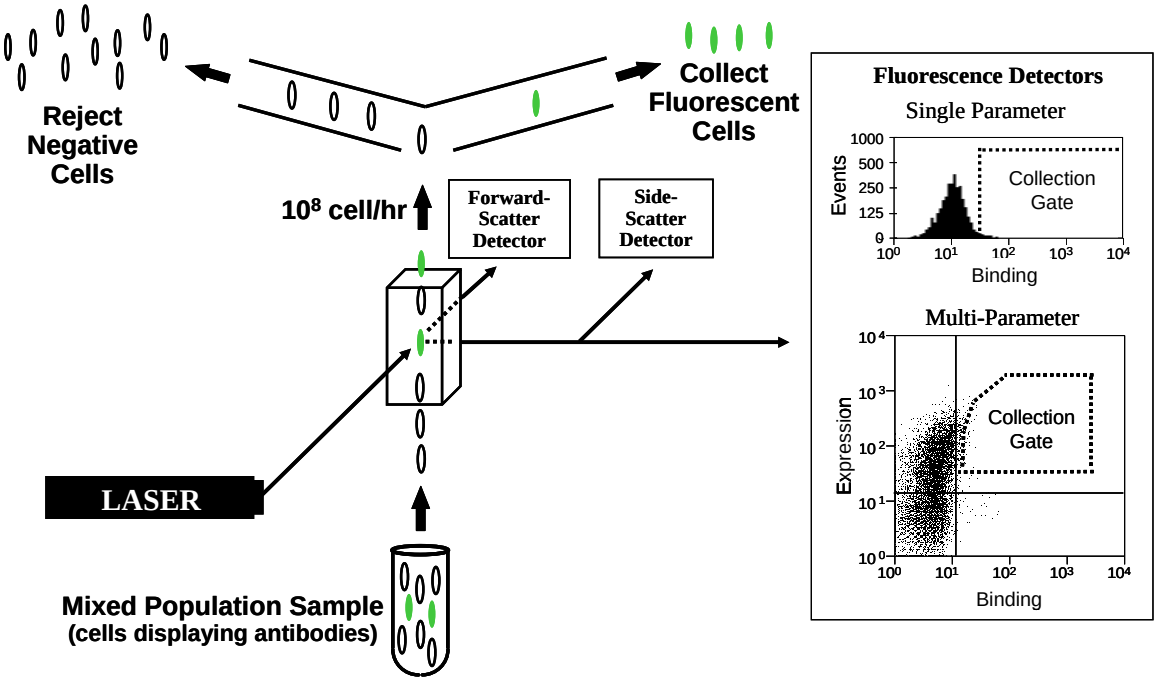

Figure 1.16. Fluorescence activated cell sorting (FACS).

Lpp-OmpA

The display of proteins from the outer membrane seems to be the most obvious choice for a cell surface display system. In 1986, peptides were first displayed on the surface of *E. coli* by inserting them into the external loops of endogenous outer membrane proteins (27, 49). However, inserting large proteins into the external loops often interferes with localization of the fusion protein and therefore unsuccessful display (53). This problem was overcome and the potential of bacterial surface display as a means to isolate antibodies of desired specificity through FACS was demonstrated with the Lpp-OmpA system in 1993 (Figure 1.17) (46).

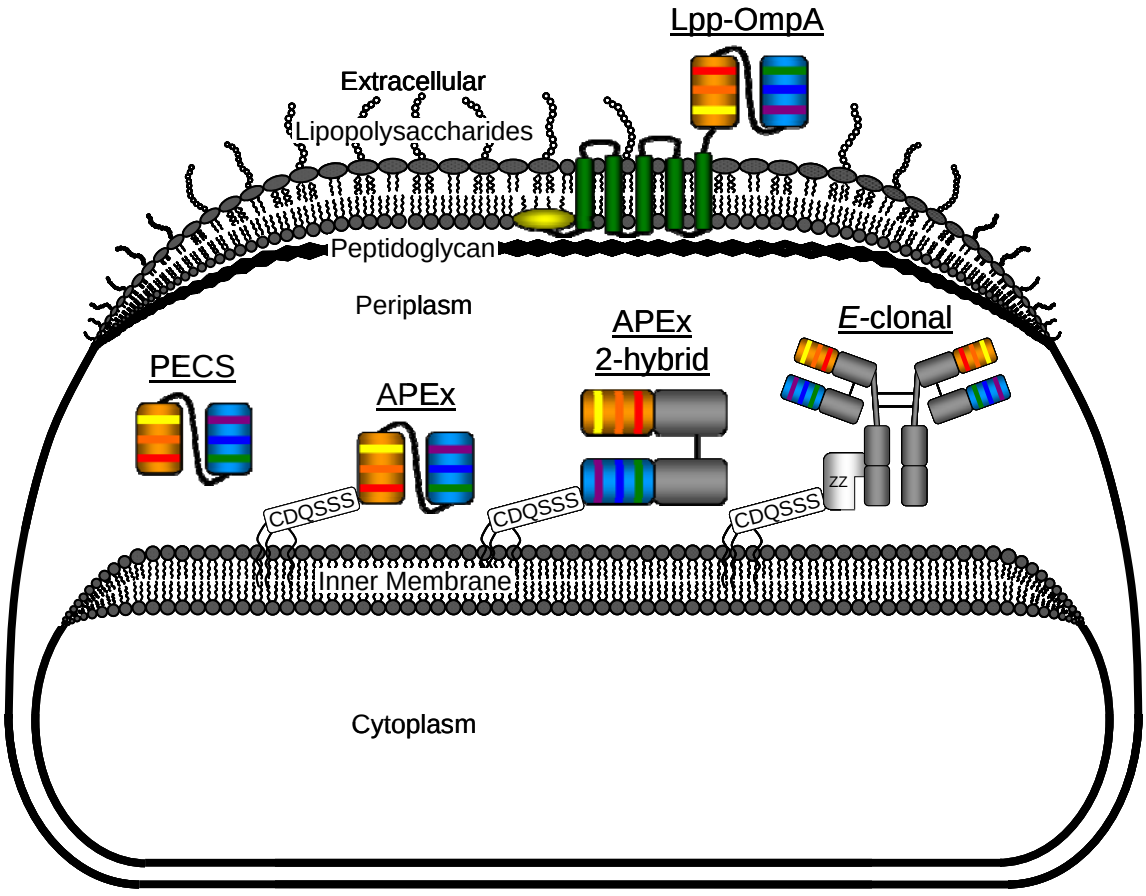

Figure 1.17. *E. coli* antibody display technologies.

The Lpp-OmpA tribrid system was designed based on the specific properties of the *E. coli* major lipoprotein (Lpp) and outer membrane protein A (OmpA) (43). Lpp is an outer membrane lipoprotein localized to the periplasmic face of the outer membrane and is critical for efficient localization of the heterologous protein to the outer membrane (43). OmpA is an outer membrane protein consisting of eight membrane-spanning anti-parallel β-strands forming a β-barrel structure and is responsible for displaying the protein of interest on the surface of the cell (43). Independently, neither system appropriately displays fusions proteins on the bacterial surface, but a combination of the signal sequence and first nine amino acids of Lpp with a truncated form of OmpA enables successful display on the surface of *E. coli* as an Lpp-OmpA fusion (Figure 1.17) (43, 47, 54, 55).

Antibody engineering with the Lpp-OmpA system has been limited to single chain antibody fragments (scFv) directed against low molecular weight antigens such as the hapten digoxigenin. It has been used on multiple occasions to affinity mature a digoxigenin specific antibody and can be used to quantitatively discriminate between mutants that vary in affinity (36, 37). However, most antibodies target higher molecular weight antigens, such as proteins, and there are no reported cases of the display of antibodies specific for larger antigens on the surface of *E. coli* using Lpp-OmpA.

Although protein specific antibodies have not been displayed on *E. coli*, they have been displayed on the surface of the Gram-negative bacteria *Salmonella typhimurium (11)*. OmpA is highly conserved among Enterobacteria and the Lpp-OmpA system is compatible with them (32). The Lpp-OmpA system was used to display an antibody specific for the carcinoembryonic antigen (CEA) on the surface of the *S. typhimurium* and was used for tumor targeting in vivo (11). The utility of the Lpp-OmpA system has been demonstrated for various applications, but future work is needed to determine the

robustness of the system for broader antibody engineering applications (3, 4, 22, 34, 46-48, 82, 134, 142, 151, 155-157).

PECS

In order to display an antibody on the surface of a biological particle, it is typically required to create a fusion between the antibody and a surface protein. This can alter the inherit stability of the antibody. For example, it is frequently observed that scFvs isolated as fusions using phage display do not function when expressed on their own (78). It is rarely beneficial to isolate antibodies that are only stable when expressed as a fusion since the antibody will need to be function on its own for most applications (64). Therefore, it is beneficial to have a display system that does not rely on the creation of an antibody fusion protein and at the same time retains the link between genotype and phenotype.

Periplasmic expression with cytometric screening (PECS) is an innovative fusion-free system that enables the selection of antibody fragments toward low molecular weight targets (Figure 1.17) (29). Through a combination of bacterial strains, growth conditions, and incubation with antigen under high osmotic conditions, scFvs expressed in the periplasm of *E. coli* can be specifically labeled with fluorescently conjugated antigen up to 10 kDa in size then detected by flow cytometry. This process increases the diffusion limitations of the outer membrane by over an order of magnitude while minimally compromising cell viability (29, 132). PECS was used to affinity mature the anti-digoxigenin scFv previously used with the Lpp-OmpA surface display system (28, 36, 37, 39, 46).

A convenient aspect of PECS is its amenability for use with existing phage display libraries. Many phage display vectors contain an amber codon located between

the 3’ end of the scFv gene and the 5’ end of the pIII phage coat protein gene used for displaying the scFv from the phage particle. Incomplete suppression of the amber codon results in early translation termination following scFv synthesis so the fusion partner is not expressed. This leads to soluble scFv in the periplasm of *E. coli* which is then suitable for screening by PECS. A combination of this approach and phage panning was used to isolate anti-digoxigenin specific scFvs from the semi-synthetic Griffin library (29). Interestingly, a high expressing scFv was isolated by PECS that behaved poorly when expressed as a pIII fusion on phage. This result demonstrates how the behavior of a scFv can be affected when expressed as a fusion partner in a display system and why fusion-free approaches may be better suited for antibody engineering.

The PECS system has also been used in a genetic selection to isolate a faster folding scFv variant (132). A library of anti-digoxigenin scFv mutants were expressed in the cytoplasm of an oxidizing strain of *E. coli* to enable proper folding and disulfide bond formation. They were fused a leader peptide specific for the twin arginine translocation (Tat) pathway, which requires proteins to be folded prior to export from the cytoplasm to the periplasm (91). Selection for binding toward digoxigenin using PECS resulted in the isolation of a mutant scFv with the same affinity, but exhibited faster folding, which led to higher export efficiency. This is a great example of how existing systems can be used to isolate antibodies with unique properties.

APEx

An alternative to displaying proteins on the outer membrane of Gram-negative bacteria is to display them on the inner membrane. Anchored Periplasmic Expression (APEx) is a system that anchors proteins to the periplasmic face of the inner membrane of *E. coli* (Figure 1.17) (59). The major advantage of APEx over other *E. coli* display

systems is the displayed antibody can interact with much larger antigens following disruption of the outer membrane and peptidoglycan layer by chemical and enzymatic means (29, 36, 37, 39, 46, 59, 132). APEx has been used for the affinity maturation of two different single chain antibody fragments (scFv) (59, 60).

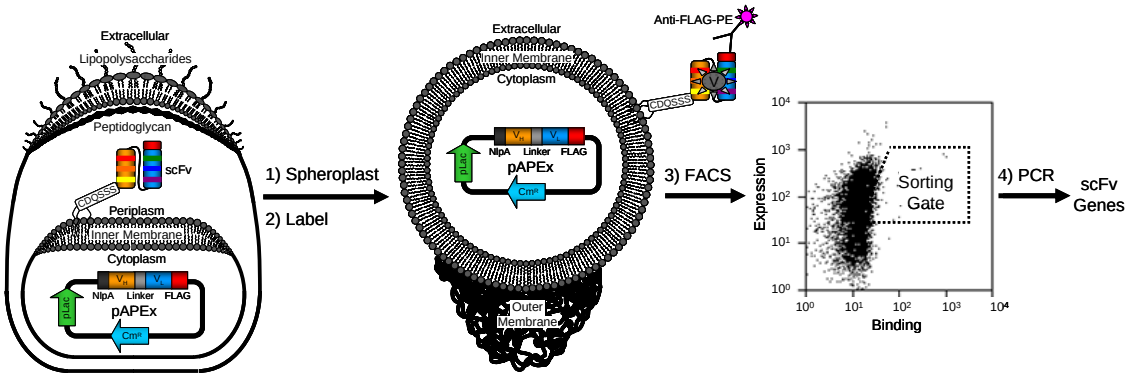

Figure 1.18. APEx antibody display and selection process.
A schematic diagram of anchored periplasmic expression (APEx). Depicted is the original system displaying a scFv antibody fragment reengineered to display a C-terminal epitope peptide sequence (FLAG) to account for simultaneous detection of antigen binding and antibody expression levels.

In APEx, antibody fragments are anchored onto the periplasmic side of the inner membrane via fusion to either a transmembrane domain of an integral membrane protein or to the signal peptide and the first few N-terminal amino acids of an inner membrane lipoprotein, such as new lipoprotein A (NlpA) (59, 79). The latter anchoring strategy is usually preferable because lipoprotein fusions can be expressed at higher levels. However, C-terminal fusions between the antibody and the pIII minor coat protein from M13 bacteriophage enables existing phagemid libraries to be used with the APEx system without the need for DNA manipulations, as is the case with PECS. For the detection and subsequent isolation of antigen specific antibody fragments, the cells are converted to spheroplasts through chemical and enzymatic means in order to disrupt the outer

membrane and peptidoglycan layer, incubated with a fluorescently labeled antigen, and isolated by fluorescence activated cell sorting (FACS) based on high fluorescence (Figure 1.18). Molecules up to 400 kDa in size have been used and hence most soluble proteins are compatible with the system (80).

APEx has been used for the affinity maturation of two different single chain antibody fragments (scFv) as well as to engineer scFvs that fold in the absence of disulfide bonds (59, 60, 140). Variations of APEx have been developed based on having anchored proteins specifically interact with soluble proteins in the periplasm prior to conversion to spheroplasts, which allows the unassociated proteins to diffuse away so only specific interactions are detected (Figure 1.17). This approach has been used to test the interaction between an anchored scFv and soluble peptide antigen fused to GFP, to affinity mature a scFv by simultaneously expressing its antigen in the periplasm, and to engineer a higher expressing Fab by co-expressing an anchored light chain (V_L-C_K) and a soluble heavy chain (V_H-C_{H1}) (59, 80). It has also been used to engineer the first full-length antibody (IgG) display system for the isolation of antibodies from combinatorial libraries expressed in *E. coli*, which is referred to as *E*- clonal (108).

It is important to note that *E. coli* is no longer viable following conversion to spheroplasts. Therefore, the antibody encoding DNA from cells isolated by FACS must be recovered by PCR and re-cloned into the appropriate vector for subsequent rounds of selection or soluble monoclonal antibody screening. This process has the disadvantage of increasing the duration of each round of sorting, but it can also be advantageous (59). For example, the PCR step can be performed under mutagenic conditions to enhance directed evolution and the isolation of higher affinity antibodies.

Yeast Surface Display

Although phage display is the oldest and still dominant antibody display system, yeast surface display is becoming increasingly popular and is the most widely used microbial display system (17, 72). Antibodies are typically displayed on the surface of *S. cerevisiae* by creating an N- or C-terminal fusion to the Aga2p mating adhesion receptor, which naturally forms disulfide bonds with Aga1p and anchors the complex to the cell wall (Figure 1.19) (120). Functional scFvs and Fabs have both been displayed on the surface of yeast, with the latter being accomplished by anchoring the heavy chain which then captures the soluble light chain (120). Antigen binding is simultaneously monitored with antibody expression levels by fluorescent labeling of an epitope peptide located on the C-terminus of the antibody fusion protein (17). This enables antigen binding per antibody to be normalized and cells displaying the highest affinity antibodies can be isolated by FACS. This system has been used to isolate and engineer antibodies toward a wide array of antigens ranging in affinity from micromolar to femtomolar (1).

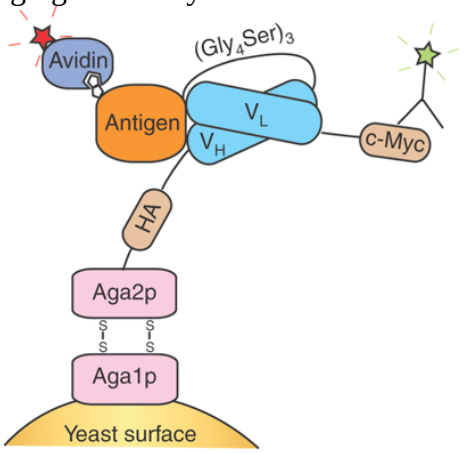

Figure 1.19. Yeast surface display.
Antibody fragment binding toward a biotintylated antigen is detected by fluorescently conjugated avidin. Antibody expression levels are simultaneously detected by a fluorescently conjugated antibody specific for the c-Myc epitope peptide. Appropriate fluorophores are used for detection by flow cytometery. Hemagglutinin (HA) is an alternative marker for surface display detection. The image is reproduced with permission from *Nature* (26).

Ribosome Display

The major drawback to phage display and cell display is the ability to generate large libraries because of limitations in transformation efficiency, the ability of a cell to uptake and maintain exogenous DNA. Ribosome display, however, is an entirely *in vitro* display technology and since library size is independent of transformation efficiency, they can easily exceed 10^{13} different genes (42). The genes are transcribed and translated using cell-free expression systems which contain cell lysates to supply the necessary enzymes and machinery for protein synthesis and are supplemented with additional components such as nucleotides, amino acids, and energy-generating factors (76). Recently, cell-free systems have been reported that use entirely purified components (152).

In ribosome display, a gene pool encoding the desired sequence diversity is generated *in vitro,* typically by PCR, and then the respective proteins are synthesized. In order to maintain the link between the genotype and phenotype, an identical spacer sequence lacking a stop codon is cloned in frame at the 3' end of the antibody gene (Figure 1.20) (164). This allows the antibody to properly fold outside the ribosome tunnel, but prevents the ribosome, mRNA, and antibody fragment complex from being disrupted. This complex is further stabilized by lower temperatures and the addition of magnesium ions, and the displayed antibodies are selected in a process analogous to phage panning (42). The mRNA encoding the isolated antibodies is converted into cDNA by reverse transcription, which is amplified by PCR into DNA so the process can be repeated (10). A major drawback to ribosome display is the conditions for selection cannot interfere with the stability of the ribosome complex. This prevents engineering antibodies toward certain antigens or generating thermally or chemically resistant antibodies.

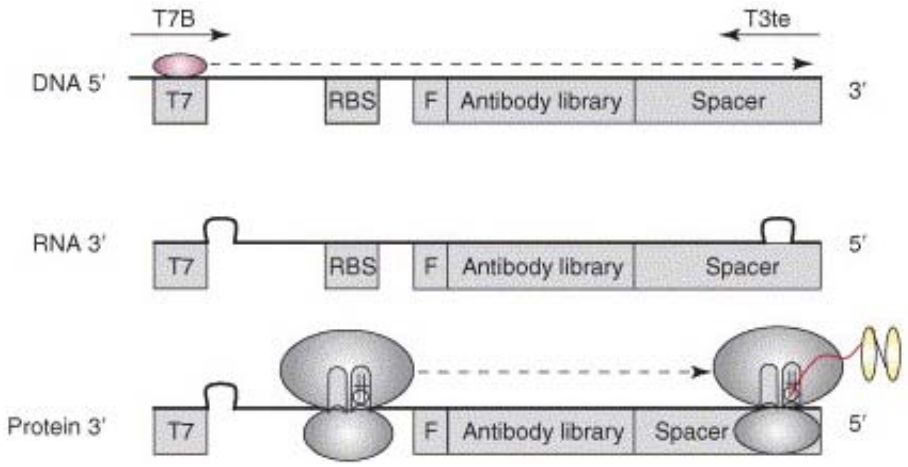

Figure 1.20. Ribosome display.
They symbols are as follows: T7, T7 RNA polymerase promoter; RBS, ribosome binding site; F, FLAG epitope peptide. The image is reproduced with permission from *Drug Discovery Today* (164).

Ribosome and the other *in vitro* systems are well suited for affinity maturation of antibodies because of the inherit directed evolution resulting from *in vitro* recovery and amplification of the DNA sequence (72). This process can be subjected to conditions which add genetic diversity to the recovered antibody genes to further increase their affinity. Ribosome display is becoming increasingly popular for this application and numerous antibodies have been successfully engineered to have higher affinities (72). One such antibody has been optimized using ribosome display and has entered the clinic (42).

Antigen Targets

This dissertation describes the implementation of APEx for the discovery and engineering of antibodies with unique binding properties. It was used to isolate a small panel of antigen specific antibodies specific for the Protective Antigen (PA) component

from *Bacillus anthracis*, the causative agent of anthrax (125). It was also used to affinity mature an antibody specific for the V antigen of *Yersinia pestis*, the etiologic agent of the plague (149). Background information on each of these bacterium and their particular antigens is described below.

Protective antigen (PA) from Bacillus anthracis

The causative agent of anthrax is the spore forming, Gram-negative bacteria *B. anthracis*. It is an attractive biowarfare agent because it has a mortality rate of up to 80% and can penetrate the human body through skin, inhalation, or ingestion (112). Following entry into the body, *B. anthracis* spores germinate into vegetative bacteria that secrete a tripartite exotoxin that is responsible for disease etiology. The protective antigen (PA) component binds to one of two host cell receptors then undergoes proteolytic cleavage by a furin-like protease. It then undergoes a conformational change, which heptamerizes on the cell surface and binds either of the two remaining components, namely LF (lethal toxin) and EF (edema toxin). The complex facilitates entry of LF or EF into the cell through endocytosis (Figure 1.21). Once the toxins reach the cytosol, they begin to catalyze reactions that can ultimately lead to death (125).

Numerous antibodies specific for all three components of the exotoxin have been isolated, but very few have therapeutic properties (20, 92). In order to prevent anthrax intoxication, the antibodies must prevent PA from binding to the cell surface receptors or disrupt toxin assembly (125). For example, affinity matured versions of one particular antibody that is known to prevent the PA receptor interaction from occurring are useful prophylactic and toxin neutralizing therapeutics for *in vivo* anthrax toxin challenges (59, 94, 98, 105). However, single point mutations in PA can drastically reduce the

neutralizing capabilities of these antibodies (138). Therefore, it is critical to isolate additional neutralizing antibodies for anthrax.

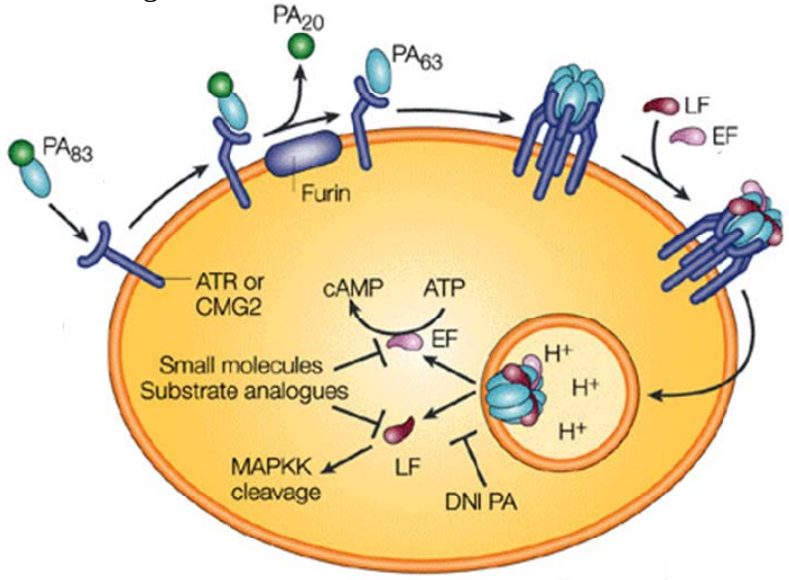

Figure 1.21. Anthrax toxin etiology.
PA_{83} binds to either of two surface receptors (ATR or CMG2) and is cleaved by a furin-like protease to give rise to PA_{63} and PA_{20}. PA_{63} heptamerizes to form a prepore, which induces endocytosis following binding toward lethal factor (LF) or edema factor (EF). Acidification of the endosome LF or EF to enter the cytosol of the host cell resulting a biochemical cascade that can lead to death. The image is reproduced with permission from *Nature* (125).

Virulence (V) antigen from Yersinia pestis

Y. pestis is the etiologic agent of the plague and has been responsible for the pandemic outbreaks occurring throughout the course of history. Today, the most probable cause of an outbreak would be the use of *Y. pestis* as a biological weapon. There are three forms of the plague, namely pneumonic, bubonic and septicemic. Of these, the pneumonic plague is the most dangerous because it highly contagious through person-to-person contact. Antibiotic treatments exist, but the mortality rate associated with pneumonic plague is nearly 100% if treatment is delayed more than 24 hours post-

exposure (165). Even if treatment begins early enough, there are antibiotic resistant strains that render antibiotics unreliable (147).

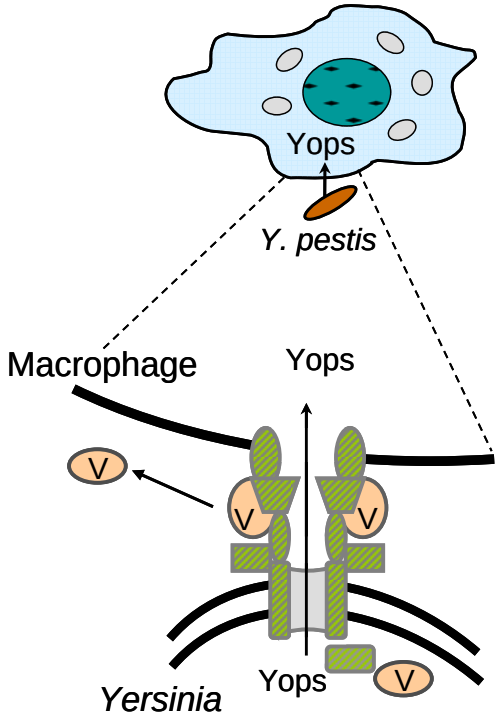

Figure 1.22. Role of V antigen in plague pathogenesis.
The V antigen mediates translocation of effector proteins (Yops) into host macrophages via a type III secretion system. The V antigen also has immunosuppressive functions following release from *Y. pestis*. The image is reproduced with permission from Julie Boyer (18).

Vaccines and antibody therapies are attractive alternatives to antibiotic treatments (18). Plague vaccines are under development, but none are currently available in the US. The most promising vaccines are subunit vaccines based on the F1 capsular protein and the V antigen virulence factor. The V antigen plays a central role in plague pathogenesis (Figure 1.22). It activates a type III secretion system and through this it mediates translocation of the effector proteins known as Yops into macrophages located in the host. It is also released from the bacteria where it has immunosuppressive functions by

increasing levels of the anti-inflammatory cytokine interleukin 10 and decreasing levels of the inflammatory cytokine tumor necrosis factor alpha (147). Passive immunization with monoclonal antibodies (mAb) specific for the F1 capsular protein and the V antigen are attractive alternatives to vaccines and have been shown to be effective against lethal challenges with *Y. pestis* (67-69, 149).

ACKNOWLEDGMENTS

I would like to acknowledge Sai Reddy for critically evaluating this chapter.

Chapter 2.

IgG or scFv Library Screening? A Comparison of Antibodies Isolated by Bacterial Display

INTRODUCTION

Thanks to the development of high throughput screening techniques for the isolation of binding proteins from large libraries, it is now possible to isolate antibodies to virtually any antigen using *in vitro* methodologies. *In vitro* isolation of antibody fragments with desired specificity relies on the screening of large combinatorial libraries using display technologies that link an antibody gene to the respective protein, which is anchored or displayed on the surface of a biological particle such as a prokaryotic or lower eukaryotic cell, virus, or ribosome (2, 8, 106, 122).These methodologies were predicated on expression of heterologous proteins in microorganisms which are easy to genetically manipulate.

Because early attempts to express soluble, full-length IgG in *E. coli* had been unsuccessful (157) *in vitro*, antibody isolation has relied on the use of antigen binding fragments such as the scFv, Fab, $F(ab')_2$, or single V_H or V_L domains, all of which can be expressed in bacteria with relative ease. Fab and scFv fragments usually maintain the binding specificity and affinity of their full-length IgG counterparts. Since they are much smaller than IgG, they display superior tissue biodistribution and rapid blood clearance. Antibody fragments have been fused together with other proteins, such as toxins or Fc domains, to yield molecules with desirable targeting, bioactivity, or biodistribution properties for a variety of therapeutic applications (70). Alternatively, the V_H and V_L

domains can be reformatted as IgGs, expressed in mammalian cells, and used for any therapeutic or other application requiring full-length immunoglobulins.

Our lab has developed technologies for the screening of antibody fragment or, more recently, full-length IgG libraries, by capitalizing on *E. coli* inner membrane display and screening by fluorescence activated cell sorting (FACS). In anchored periplasmic expression (APEx), antibody fragments are anchored onto the periplasmic side of the inner membrane via fusion to either a transmembrane domain of an integral membrane protein or to the signal peptide and the first few N-terminal amino acids of an inner membrane lipoprotein, such as NlpA (59, 79). The latter anchoring strategy is usually preferable because lipoprotein fusions can be expressed at higher levels. For the isolation of antigen specific antibody fragments, the cells are converted to spheroplasts in order to disrupt the outer membrane and peptidoglycan layer, incubated with a fluorescent labeled antigen, and isolated by FACS based on high fluorescence.

For the isolation of IgG, full-length heavy and light chains are expressed from a dicistronic operon and are secreted into the periplasm where they assemble into aglycosylated IgGs that are fully functional for antigen binding (106). The IgG is co-expressed with the ZZ domain from *Staphylococcus aureus* protein A using APEx, which serves to non-covalently capture the antibody molecule onto the inner membrane. Then, the cells are converted to spheroplasts and clones that bind to fluorescently labeled antigen are isolated by FACS, as above. The resulting IgG protein can be expressed directly at the preparative level in *E. coli* and used directly for immunohistochemistry or *in vivo* animal studies. Another potential advantage of IgG library screening is that their higher avidity and stability may result in the isolation of a higher diversity of V_H and V_L domains relative to what could be obtained by screening the same antigen binding site diversity in a monovalent format. Consistent with this hypothesis, it has been shown that

the bivalent display of antibody fragments as $F(ab')_2$ molecules on the surface of filamentous bacteriophage enables the selection of a broader spectrum of antibodies (7, 90).

In this study, we sought to compare and evaluate the antibody binding sites that are isolated when the same library of V_H and V_L domains obtained from an immunized mouse is displayed as either IgGs or scFv fragments. The V_H and V_L genes were constructed by RT-PCR from splenocytes obtained from a mouse immunized with the 83 KDa protective antigen (PA_{83}) from *Bacillus anthracis*, the causative agent of anthrax. Following entry into the body, *B. anthracis* spores germinate into vegetative bacteria that secrete a tripartite exotoxin that is responsible for disease etiology (124). PA_{83} binds to one of two host cell receptors then undergoes proteolytic cleavage, which results in a 63 kDa form (PA_{63}). PA_{63} heptamerizes into a complex that facilitates entry of lethal factor and edema factor into the host cell by endocytosis and can ultimately lead to death. As a result, antibodies toward both PA_{83} and PA_{63} are potential therapeutic and diagnostic reagents (127). IgG and scFv (V_L-V_H and V_H-V_L) immune libraries were screened by APEx using essentially identical conditions. We show that the IgG library resulted in a greater diversity of V_H and V_L domains that conferred a broad range of antigen affinities (K_D=21-440 nM). We show that the isolated variable domains demonstrated format dependent expression levels and affinities following conversion between antibody formats (IgG, V_L-V_H scFv, and V_H-V_L scFv). The results of this study illustrate how libraries of V_H and V_L domains in different formats result in the selection of antibody binding sites exhibiting distinct antigen affinity and expression properties.

RESULTS

Library construction and screening

V_H and V_L genes were generated by RT-PCR from mRNA isolated from splenocytes originating from a mouse that was immunized with *Bacillus anthracis* PA. Overlap extension PCR of the V_H and V_L gene pools was used to construct two scFvs libraries: a V_L-V_H library and a V_H-V_L library. A $(Gly_4Ser)_4$ linker was used to join the variable heavy and variable light domains in both libraries. 1 X 10^7 and 2 X 10^7 transformants were obtained with the V_L-V_H and V_H-V_L libraries, respectively. Analysis of 10 clones from each revealed a high degree of sequence diversity in the variable domains (data not shown).

The two libraries were pooled at a 1:2 ratio (V_L-V_H:V_H-V_L) to account for the difference in the number of independent transformants, the cells were grown in liquid culture, expression of NlpA-scFv protein was induced by adding IPTG, and they were converted to spheroplasts through chemical and enzymatic means (59). A total of 2 X 10^8 spheroplasts (>5-fold library coverage) labeled with 200 nM PA_{63}-FITC were subjected to high-throughput fluorescence activated cell sorting (FACS). Approximately 2% of the cells were collected based on binding to PA as determined by high FITC fluorescence emissions (Figure 2.1). The spheroplasts were immediately resorted as above without additional labeling to maximize the isolation of antibodies specific for PA (59). The scFv genes from the cells collected during the resort were amplified by PCR since the viability of cells undergoing conversion to spheroplasts is low (59). The PCR product of the entire round I gene pool was cloned into pAPEx1 for additional rounds of sorting as follows: (*i*) four additional rounds using decreasing concentrations of PA_{63}-FITC down to 40 nM in an attempt to isolate higher affinity clones; (*ii*) one additional

round using 400 nM PA_{83}-BODIPY in an attempt to isolate antibodies that cross react with both forms of the PA antigen.

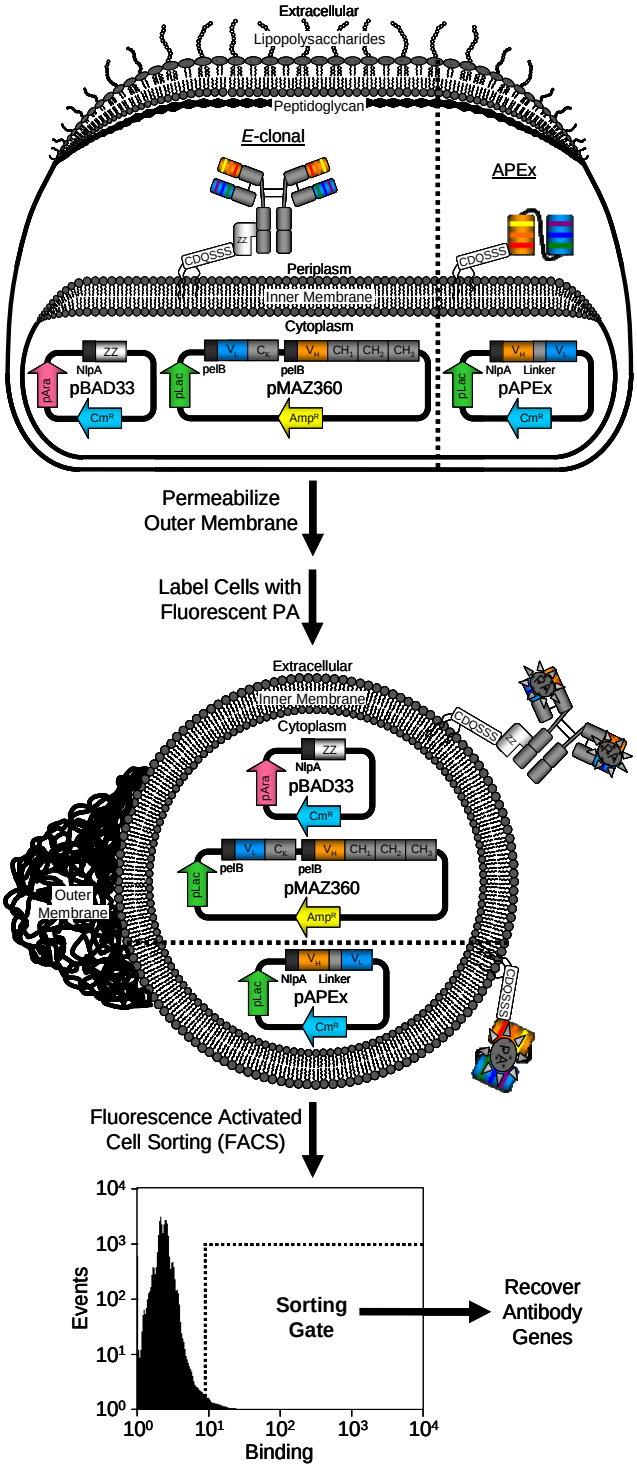

Figure 2.1. Schematic diagram of two APEx display systems. Libraries of either IgG (*E*-clonal) or antibody fragments (APEx) are expressed in the periplasm of *E. coli*. The antibody fragments are expressed from a single plasmid (pAPEx1) as fusions to NlpA(1-6) and are anchored to the periplasmic face of the cytoplasmic membrane. The heavy and light chains of the IgG are expressed as soluble proteins from a single plasmid (pMAZ360-IgG). The IgG antibodies assemble in the periplasm then are captured by the Fc-binding protein ZZ that are expressed from a second plasmid (pBAD33) as fusions to NlpA(1-6). The cells are converted to spheroplatst through chemical and enzymatic degradation of the outer membrane and peptidoglycan layer allowing fluorescently labeled exogenous antigen to interact with the antibodies displayed on the surface of the inner membrane. Spheroplasts containing antibodies specific for the antigen are enriched from the total population by FACS and their antibody genes recovered by PCR. NlpA(1-6), new lipoprotein A (NlpA) leader peptide plus first six amino acids of the mature lipoprotein; CDQSSS, NlpA amino acids 1-6; ZZ, synthetic analogue of the IgG binding B domain of the *Staphylococcus aureus* protein A.

ScFv genes from various rounds of scFv library sorting were directly cloned into pMoPac16 for soluble scAb protein expression then direct binding via ELISA. The scAb format is comprised of a scFv in which the C termini of the variable light chain domain is fused to the human kappa constant domain (HuC_K), resulting in improved expression characteristics in *E. coli* without altering the antibody binding affinity (62). Approximately 400 clones were individually picked and the monoclonal scAbs they encoded for were expressed using 96-well microtiter plates. Lysates were individually analyzed for binding toward PA_{83} via ELISA. Of all the clones tested, only 2 showed significant binding (>5-fold above background) (106). DNA sequencing revealed that one of the isolated anti-PA scFvs, B12, was oriented V_L-V_H and the other, C9, was oriented V_H-V_L. Further analysis indicated that these two V_H and V_L domains originated from different germline genes (Table 2.1).

Table 2.1. Variable domain germline gene sequencesa

Antibody	Heavy Chain	Antibody	Light Chain
H2*b*, B12*c*	J558.18	H2*b*, C3*b*	ce9
D1*b*, F10*b*	VHSM7.a4.108	B2*b*, D1*b*, F10*b*	19-23
C3*b*, C9*d*	J558.32	C9*d*	23-39
B2*b*	VHSM7.a3.93	B12I	bb1

[a]V gene segment determined using IgBlast from NCBI

[b]Isolated as an IgG

[c]Isolated as a VL-VH scFv

[d] Isolated as a VH-VL scFv

Five unique anti-PA clones (B2, C3, D1, H2, and F10) were previously isolated as full-length IgG antibodies from a combinatorial library constructed from the same cDNA and selected by FACS (106). Within this group, there were four different V_H and two different V_L germline genes (Table 2.1). Both of these V_L germlines were different from those of the scFvs, but two of V_H germlines were identical. The V_H domains of C3 and C9 only differed in 2 amino acids, but those of H2 and B12 differed by 13 amino acids of which 6 were in CDRs (Figure 2.2). In total, four different V_H and four different V_L germlines were represented among the seven anti-PA antibodies.

Variable Heavy Chain (V_H)

	FW 1	CDR 1	FW 2	CDR 2
H2	EVKLQQSGPELVKPGASVKISCKGSG	YAISSSWMN	WVKQRPGQGPEWIG	RIYPGDGDTNYNGKFKG
F10	..Q.....A...RS.....L..TA..	FN.KDYY.H	......E..L....	W.D.EN...E.AP..Q.
C3	Q.Q.K...A.........L...A..	.TFT.YDI.	..R...E..L....	W.F....S.K..E....
D1	..Q.VE..A...RS.....L..TA..	FN.KDYY.H	......E..L....	W.D.EN...E.AP..Q.
B2	..Q.....A.........L..TA..	FN.KDTY.H	......E..L....	..D.EN.N.K.DP..Q.
C9	Q.Q.....A.........L..RA..	.TFT.YDI.	..R...E..L....	W.F....S.K..E....
B12	Q.Q.........R......T...A..	.TF......	.........L....	.M.....E.........

	FW 3	CDR 3	FW 4	
H2	KATLTADKSSSTAYMQLSSLTSVDSAVYFCAR	GGLPYAVDY	WGQGTSVTVSS	118
F10	...MS..T..N...L.......E.T...Y.NA	.TPFEGLRRADY	.....TL....	121
C3	.....T...........R...E.....	...YFDY	.....TL....	116
D1	...M...T..N...L.......E.T...Y.NA	.TPFEGLRRADY	.....TL....	121
B2	...I...T..N...L.......E.T...Y...	FLITTGYFDY	.....TL....	119
C9	.....T...........R...E.....	...YFDY	.....TL....	116
B12	....	..I...M..	.S.....	118

Variable Light Chain (V_L)

	FW 1	CDR 1	FW 2	CDR 2
H2	DIQMTQSPSSLSASVGDRVTVTC	RASQGIRNYLN	WYQQKPGKAPKFLIY	YTSRLLP
F10	..V....HKFM.T......SI..	K...DVGTAVA	.......QS..L...	WA.TRHT
C3	.....	.....	.....	.....
D1	..V....HKFM.T......SI..	K...DVGTAVA	.......QS.RL...	WA.TRHT
B2	..VL...HKFM.T......SI..	K...DVGTAVA	.......QS..L...	WA.TRHT
C9	..V.....AT..VTP....SLS.	....S.SD..H	.....SHES.RL..K	.A.QSIS
B12	..V...T.L..PV.L..QASIS.	.S..SLVHSNGNTYLH	..L....QS..L...	KV.NRFS

	FW 3	CDR 3	FW 4
H2	GVPSRFSGSGSGTDYTLTINSLEQEDIATYYC	QQGNTPPWT	FGQGTKVEIKR
F10	...D..T.......F....SNVQS..L.D.F.	..YSSY.L.	..A...L.LN.
C3	.....	.....	.....
D1	...D..T.......F....TNVQS..L.D.F.	..YSSY.Y.	..G...L....
B2	...D..T.......F....SNVQS..L.D.F.	..YSSY.L.	..A...L....
C9	.I.........S.F..S...V.P..VGV...	.N.YSF.R.	..G...L....
B12	...D.........L..K.SRV.A..LGV.F.	S.STHV..A	..G...L....

Figure 2.2. Amino acid sequence analysis of the antibody variable domains.
Anti-PA antibodies isolated using APEx or *E*-clonal systems. Frameworks (FW) and complementarity determining regions (CDR) based on Kabat numbering (102).

Variable domain format comparison

The anti-PA IgG variable domain genes were converted to both scFv orientations (V_H-V_L and V_L-V_H) and cloned into pMoPac16 for scAb protein expression. Similarly, the anti-PA scFv variable domain genes were converted to the scFv orientation opposite to that of which they were isolated as well as to IgG format and cloned into the appropriate vectors for scAb and IgG protein expression (see Figure 2.3A). The relative expression level of the 21 proteins encoded by these 21 antibody constructs was determined by Western blot analysis (Figure 2.3B and 2.3C).

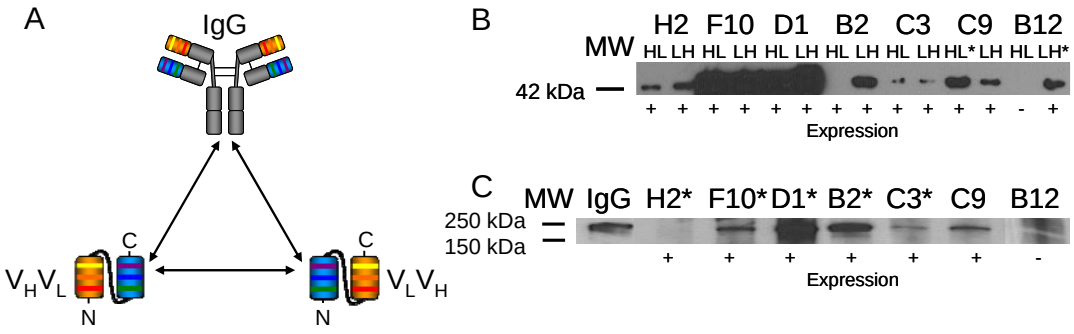

Figure 2.3. Variable domains format dependent expression levels.
Format dependent expression levels of antibodies as determined by Western blot analysis. (A) Schematic diagram depicting the conversion of the isolated antibodies from one format to another. Western blot analysis of the antibodies expressed as (B) scAbs and (C) IgGs. Some antibodies were (+) and others were not (-) able to be purified from large scale cultures. *format of the antibody as it was originally isolated. N, N-terminus; C, C-terminus; HL, V_H-V_L; LH, V_L-V_H; MW, molecular weight; IgG, 10 ng of IgG isolated from human serum

The relative expression level of the scAbs varied from less than 10 ng/L (B12 V_H-V_L and B2 V_H-V_L) to over 1 mg/L (F10 and D1) and was dependent on the orientation of the variable domains for each of the seven antigen binding sites. As expected, the expression of both B12 and C9 was detectable in the scFv orientation they were isolated in. However, the expression level of B12 was undetectable and C9 was expressed

significantly lower when the orientations of their variable domains were switched. Even though B12 and B2 were both undetectable as V_H-V_L scAbs, B2 could be expressed to purifiable quantities from two liters of culture volume while B12 was not. The highest expressing scAbs were originally isolated as IgGs (F10 and D1), but the remaining IgGs typically expressed poorly as scAbs regardless of their variable domain orientations.

As with the scAbs, the relative expression levels of the IgGs was highly variable. Five of the seven expressed fully assembled IgG (see Figure 2.3C). One of these five is C9, which was originally isolated as a scFv. Even if the antibodies originated from same the germline gene sequences for both variable domains, their relative protein expression levels were still format dependent. For example, both D1 and F10 share the same V_H and V_L germline genes, the proteins they encode for are only different by 9 amino acids in total, they both express very well as scAbs in both orientations, but only D1 expresses very well as an IgG.

Monomeric scAb and full-length IgG proteins were expressed and purified from up to two liters of culture volume in order to obtain enough protein for antigen binding studies. As was previously stated, B12 V_H-V_L scAb and IgG proteins could not be purified following multiple attempts and therefore binding studies could not be performed with them. Detailed analysis of the binding kinetics toward both PA_{83} and PA_{63} using surface Plasmon Resonance (SPR) was performed for all clones that could be expressed. The SPR results for each antibody in the format in which they were originally isolated are shown (Table 2.2). C9 was isolated as a V_H-V_L scFv and exhibited the highest affinity at 6 nM. B2 was isolated as an IgG and exhibited the lowest affinity at 440 nM (106).

Table 2.2. Binding kinetics of isolated antibodies determined by SPR

Antibody	Isolated Format	K_a ($M^{-1}s^{-1}$)	k_d (s^{-1})	K_D (nM)
H2[b]	IgG	1.3 X 10^6	2.7 X 10^{-2}	21
F10[a]	IgG	4.9 X 10^5	1.5 X 10^{-2}	31
C3[b]	IgG	6.8 X 10^5	3.2 X 10^{-2}	47
D1[a]	IgG	3.5 X 10^5	1.9 X 10^{-2}	55
B2[a]	IgG	3.2 X 10^4	1.4 X 10^{-2}	440
C9[b]	V_HV_L	1.5 X 10^5	9.0 X 10^{-4}	6
B12[a,b]	V_LV_H	9.1 X 10^4	4.9 X 10^{-3}	50

[a]Affinity toward PA_{63}

[b]Affinity toward PA_{83}

Some clones could not be analyzed by SPR due to a combination of low affinities and low protein yields following expression and purification. Therefore, the apparent K_D of each antibody toward both PA_{83} and PA_{63} were determined by ELISA half-maximal binding (Figure 2.4). Antibodies that exhibited very poor binding did not reach saturation in the ELISA assays even at the highest concentration used (4 μM) (Figure 2.5B). For these antibodies, the K_D values were calculated using a non-linear optimization approach based on the ELISA data and equilibrium kinetics (Figure 2.5C) (26). The validity of this approach was proven by obtaining similar K_D values to those that were obtainable by SPR (Figure 2.5).

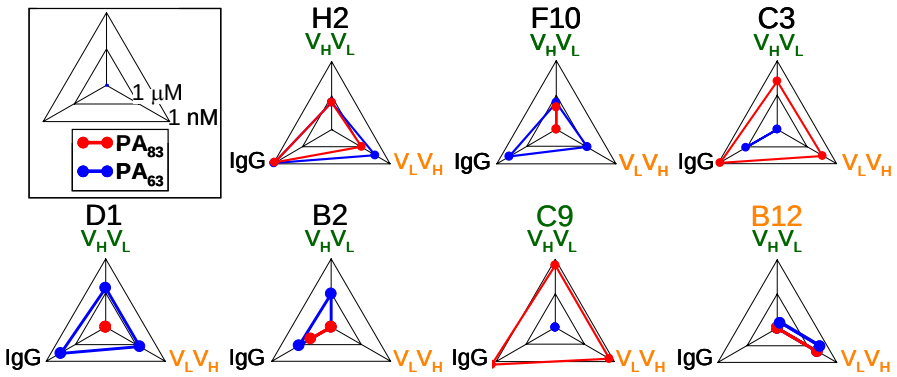

Figure 2.4. Variable domains format dependent specificity and affinity.
Radar plots indicating the affinities of each antibody as determined by ELISA. Each of the three axes represents a different antibody format. Dots on each axis indicate the K_D against PA_{83} (red) or PA_{63} (blue). The outer most, middle and center vertexes indicate K_Ds of 1 nM, 1 μM and 1 mM or less, respectively. represented by each octagon.

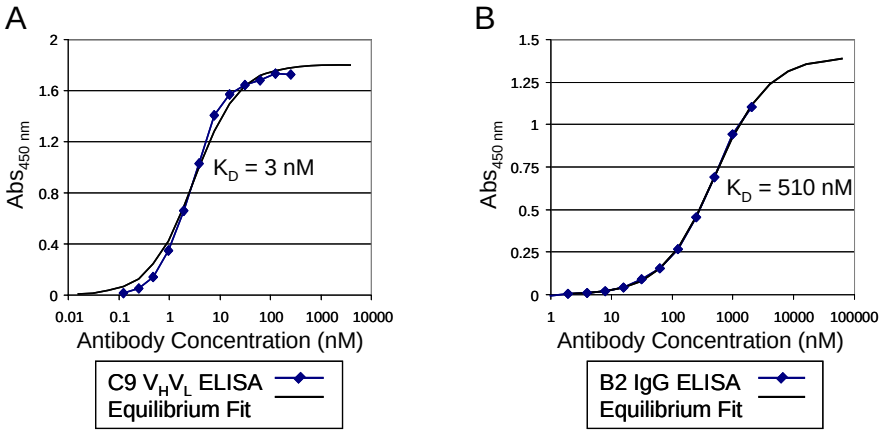

Figure 2.5. Antibody apparent affinity determination by ELISA.
Examples of (A) complete and (B) incomplete ELISA data generated for two different antibodies and used to calculate the K_Ds by a non-linear optimization approach. ELISA data was generated from the average of duplicate runs. The non-linear optimization approach was previously used to determine the affinities of yeast surface displayed antibody fragments by flow cytometry (26). (C) Equilibrium equation that the ELISA data should fit (26). (D) Comparison of K_Ds determined by ELISA and SPR for two different antibody formats. ELISA K_Ds were generated from the data in (A) and (B).

The affinity and specificity results determined by ELISA and SPR are summarized as Venn diagrams for both PA_{83} and PA_{63} (Figure 2.6). The affinities of the variable domains in different formats for either PA_{83} or PA_{63} were considered equivalent if they were within 5-fold of each other. Overall, we observed a high degree of variation in the binding behavior of these seven antigen binding sites when expressed as different antibody formats. Only one of the antibodies (C9) binds to a given antigen (PA_{83}) with the same affinity independent of the format. Interestingly, the V_H domains of C3 and C9 only differed in 2 amino acids. However, the V_L domains of these antibodies were derived from different germline sequences and this might have affected their expression properties and possibly the affinity. Expression levels did not correlate with affinities either. For example, F10 expresses very well in both scAb formats, but the affinities are over 10- and 100-fold lower than the IgG format. However, B2 V_H-V_L was amongst the worst expressing scAbs, but its affinity was within 2-fold of when it was expressed as an IgG

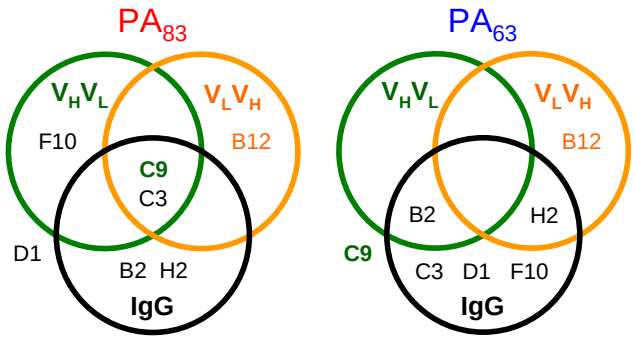

Figure 2.6. Summary of antibody specificity and affinity.
Venn diagrams summarizing specificity and affinity of the anti-PA antibodies in different variable domain formats as determined by SPR and ELISA. Each circle represents a different antibody format as follows: V_H-V_L (green), V_L-V_H (yellow) and IgG (black). The antibody is located in overlapping regions of the circles if the K_D of the formats are within 5-fold of each other. Antibodies that do not bind a particular antigen are located outside all circles.

DISCUSSION

The ability to rapidly produce antibodies has been accelerated by the invention of *in vitro* display systems including phage, ribosome, and microbial display (72). As a result of the necessity to maintain a link between genotype and phenotype and the complexity of expressing full-length antibodies outside of mammalian cell culture, all of these systems have relied on the display of recombinant antibody fragments. However, our lab recently developed a system for the display and selection of full-length IgG antibodies from combinatorial libraries expressed in *E. coli* (106). As a result, it is now possible to display and select recombinant antigen binding sites expressed in a variety of different formats. The present study sought to examine the limitations and relative merits of using different antibody formats in library screening experiments.

The diversity of antibody binding sites obtained when the same library of V_H and V_L domains from an immunized animal is screened as either IgG or scFv molecules is compared. The two libraries were screened by *E. coli* anchored periplasmic expression (APEx) using similar cell labeling and fluorescence activated cell sorting (FACS) conditions. A total of seven different antibodies specific for the protective antigen component of *B. anthracis* were isolated and were comprised of four different V_H and four different V_L germlines genes. IgG display accounted for 6 of these germlines which exhibited a wide range of (monovalent) affinities, although, a biding site with a slightly higher affinity (K_D=6 nM) was isolated from the scFv library.

Each pair of antibody variable domains comprising the seven anti-PA was expressed as scFv in two different orientations (V_H-V_L and V_L-V_H) as well as IgG molecules. Protein expression levels in *E. coli* and binding activity were evaluated. To maximize the expression and stability properties of the scFvs, they were expressed as scAbs since the addition of the human kappa constant is known to enhance these

properties of scFvs (62, 105). This analysis revealed that not only can converting the variable domains between the IgG and antibody fragment format adversely affect expression and antigen binding, but so can the orientation of the variable domains within an antibody fragment. Although scFvs are often unstable and can have reduced affinities compared to their Fab and IgG counterparts (52, 62, 105), the orientation of the variable domains compared to the linker is an approach to retain affinity upon conversion to the scFv, or in this case, the more stable scAb format.

It was surprising that screening two different immune libraries generated from identical cDNA and each containing at least 10^7 members resulted in the isolation of different antibodies. Multiple attempts at screening the scFv library only resulted in the isolation of two different antibody clones. In contrast, a single attempt at screening the IgG library resulted in five unique antibodies. One possible explanation for the lower success rate of the scFv library screen is the inability of many variable domains to be expressed and maintain affinity in this format. It was shown that several pairs of variable domains isolated as IgGs displayed substantially reduced affinity when expressed as scAbs, and hence they were not recovered from the scFv library. Additionally, the variable domains from one of the two isolated scFvs did not express or function as an IgG,

Our results indicate that the antibody format used during *in vitro* selection effects which antibody variable domains will be isolated during screening. In general, the full-length IgG antibody was the preferred variable domain format to isolate antibodies from immune libraries expressed in *E. coli*. This is likely the result of the increased stability of the IgG compared to linker linked antibody fragments (52, 106). However, antibodies can also be isolated that only express and function as an antibody fragment and the orientation of the fragment can drastically impact both expression and binding properties.

Based on the unpredictable variation of antibody properties following variable domain format conversion, it is recommended to choose a library format based on the final application of the antibody. If effector function will be required as is typical with most cancer therapeutics, formats that best represent the IgG structure (i.e. Fab, Fab_2, IgG) should be utilized during the discovery process. If enhanced biodistribution and blood clearance properties are required as is for imaging applications, smaller formats should be used (i.e. V_H, V_L, scFv).

MATERIALS AND METHODS

Bacterial strains and plasmid vectors

Escherichia coli Jude-1 cells [DH10B F'::Tn10(Tet^r)] were used for all experiments. Plasmids pAPEx1 was used for *E. coli* display of soluble single chain variable fragment antibodies (scFv) (59). Plasmids pMoPac16 and pMAZ360-IgG were used for soluble single chain antibody fragment (scAb) expression and IgG expression, respectively (106).

Antibody fragment library construction

Mice immunization with the protective antigen (PA_{83}) component from *Bacillus anthracis* in complete Freud's adjuvant and the isolation of V_H and V_L genes were performed using established procedures (106). The V_H and V_L genes were fused by overlap extension PCR to give rise to either V_L-$(Gly_4Ser)_4$-V_H scFv (V_L-V_H) according to published protocols or to V_H-$(Gly_4Ser)_4$-V_L scFv (V_H-V_L). The individual scFv gene pools, V_H-V_L and V_L-V_H, were separately cloned into pAPEx1 via the non-compatible SfiI sites, and the ligation products were transformed into electrocompetent *E. coli* Jude-1

(59). Cells were cultured on agar plates containing LB medium supplemented with 2% (wt/vol) glucose (2% glc) and 30 μg/ml chloramphenicol (Cm30) and grown overnight at 25 ºC. Frozen cell stocks were prepared by transferring the cells to LB medium supplemented with 2% glc and 15% glycerol to A_{600} ~10 then stored at -80 ºC.

Isolation of anti-PA antibodies

Purified PA_{83}, kindly provided by Stephen Leppla (National Institute of Health, Bethesda, MD), was conjugated to BODIPY® using 6-((4,4-difluoro-5,7-dimethyl-4-bora-3a,4a-diaza-s-indacene-3-propionyl)amino)hexanoic acid succinimidyl ester (Invitrogen, Carlsbad, CA) at a molar ratio of 1:8 following the manufacturer's protocol. Free BODIPY FL-X SE was removed using a NAP-10 gel filtration column following the manufacturer's protocol (GE Healthcare, Uppsala, Sweden). The extent of conjugation was determined based on the ratio of A_{280} and A_{504} measured using a NanoDrop™ 1000 and the appropriate extinction coefficients and correction factors as recommended by the manufacturer (Invitrogen, Carlsbad, CA). PA_{83} extinction coefficient was calculated using Protein Calculator (http://www.scripps.edu/~cdputnam/protcalc.html, Putnam Lab at The Scripps Research Institute, La Jolla, CA).

The V_H-V_L and V_L-V_H scFv library frozen cell stocks were thawed on ice, combined in proportion to the number of individual transformants, subcultured to A_{600} 0.1 in TB medium supplemented with 2% glc and Cm30, grown to A_{600} ~0.8-1.2 at 37ºC, cooled for 30 min to 25 ºC, and protein expression was induced with the addition of 1mM Isopropyl-β-d-thiogalactopyranoside (IPTG). After 4h induction at 25 ºC, 1 ml of cells at A_{600} 8.0 were converted to spheroplasts using Tris/Sucrose/EDTA/lysozyme as described (59, 107). The spheroplasted cells were labeled with 200 nM PA_{63}-FITC (List Biological Laboratories, Campbell, CA) in phosphate buffered saline (PBS) for 1 h at 25 ºC. Labeled

spheroplasts were washed with PBS and analyzed on a MoFlo (Dako, Glostrup, Denmark) droplet deflection flow cytometer by exciting with a 488-nm laser and measuring the fluorescence emission spectrum of FITC with a 530/40 band-pass filter. The library population was gated on the spheroplast population as determined by the forward scatter (FSC) and side scatter (SSC) parameters (106), and the most fluorescent 1-2% of the population based on the FITC emission spectra was collected (59, 106). The collected spheroplasts were immediately resorted, and the scFv genes in the resort solution were by amplified by PCR using primers BRH06 (5'-GCGGATAACAATTTCACACAGG-3') and AHX89 (5'-CGCAGTAGCGGTAAACGGC-3') (59). The amplified DNA was cloned into pAPEx1 via the non-compatible SfiI restriction sites, and the ligation mixture was transformed into electrocompetent *E. coli* Jude-1. At least 10-fold excess of colonies relative to the number of events in the resort were obtained. Colonies were scraped from the agar plates into liquid media and subjected to additional rounds of sorting as follows: (*i*) four additional rounds using decreasing concentrations of PA_{63}-FITC down to 40 nM; (*ii*) one additional round using 400 nM PA_{83}-BODIPY.

The scFv genes from each round of sorting were subcloned into pMoPac16, and the ligation products were transformed into *E. coli* Jude-1 for expression of soluble scAb proteins (59). Briefly, approximately 200 individual colonies from both final rounds were picked and cultured at 30 ºC in round bottom 96-well microtiter plates containing 200 µl of TB medium supplemented with 2% glc and 200 µg/ml ampicillin (Amp200). After overnight growth, 4 µl aliquots were transferred to a master microtiter plate containing 156 µl TB medium supplemented with 2% glc and Amp200, cultured for 8 h at 30 ºC, and stored at 4 ºC for up to two weeks. The remaining cells were pelleted by centrifugation and resuspended in 200 µl of TB medium supplemented with Amp200 and

1 mM IPTG to induce protein expression. After 4 h of incubation at 25 ºC, cells were pelleted by centrifugation and lysed by either sonication in 200 µl PBS or by incubation in 200 µl lysis buffer (BugBuster™ HT Protein Extraction Reagent (Novagen, Madison, WI) diluted 1:4 in PBS) (107) for 30 min at 25 ºC, and finally, the insoluble fractions were removed by centrifugation. Clarified lysates were individually analyzed for binding toward PA_{83} using enzyme-linked immunosorbent assay (ELISA) as described (106, 107). ScAb immunocomplexes were detected using an anti-polyhistidine (anti-His) peroxidase (HRP) conjugate (Sigma-Aldrich, St. Louis, MO) applied at a 1:2,500. The screening of the V_H and V_L gene pool in the IgG format has been describe (106). Antibody variable domain germlines were determined using IGBlast (http://www.ncbi.nlm.nih.gov/igblast/, National Center for Biotechnology Information, Bethesda, MD).

Variable domain format conversion

The isolated scFv (B12, C9) and full-length anti-PA antibody (B2, C3, D1, F10, H2) variable domain genes were converted to V_H-V_L, V_L-V_H, and IgG formats. Briefly, genes encoding the variable domains in pMoPac16 and pMAZ360-IgG plasmid DNA were amplified by PCR using variable domain specific primers, combined by overlap extension PCR, and cloned into pMoPac16 via the non-compatible Sfi sites, Likewise, genes encoding variable domains in pMoPac16 were amplified by PCR and sequentially cloned into pMAZ360-IgG via NheI/HindIII and NcoI/NotI restriction sites.

Protein expression and purification

Monomeric scAb and full-length IgG proteins were expressed and purified according to published procedures (59, 64, 106, 107). For scAb protein expression, *E. coli* Jude-1 containing pMoPac16 derivatives encoding the desired scAb genes were cultured in 2 ml of TB medium supplemented with 2% glc and Amp200 for 8 h at 30 ºC then used to inoculate of 500 ml of TB supplemented with 2% glc and Amp200. After overnight growth at 30 ºC, cells were pelleted by centrifugation and resuspended in 500 ml of TB medium supplemented with Amp200 and 1 mM IPTG to induce protein expression. After 4 h of incubation at 25 ºC, cells were pelleted by centrifugation, and the periplasmic fraction from the cell pellet was isolated by osmotic shock according to published procedures (64). ScAb proteins were purified from the shockate by immobilized metal affinity chromatography (IMAC) using Ni-NTA Agarose based on the manufacturer's protocol (Qiagen, Hilden, Germany), and monomeric scAbs were further isolated by size-exclusion FPLC (SEC) on a Superdex^{TM} 200 column (GE Healthcare, Uppsala, Sweden) using PBS or HBS-P (GE Healthcare, Uppsala, Sweden) as the elution buffer.

For IgG protein expression, *E. coli* Jude-1 containing pMAZ360-IgG derivatives encoding the desired IgG genes were cultured in 10 ml of LB medium supplemented with 2% glc and Amp200 overnight at 30 ºC. Overnight cultures were subcultured to A_{600} 0.2 in 500 ml of TB medium supplemented with 2% glc and Amp100, grown to A_{600} ~0.8-1.2 at 30 ºC, cells were pelleted by centrifugation and resuspended in 500 ml of TB medium supplemented with Amp100 and 1 mM IPTG to induce protein expression. After 16 h of incubation at 25 ºC, cells were pelleted by centrifugation, resupsended in 50 ml lysis buffer for 2 h at 25 ºC, and the insoluble fraction was removed by centrifugation. IgG proteins were purified from the clarified lysate by Protein A chromatography (Pierce,

Rockford, IL) according to published procedures (107). IgG proteins were concentrated on an Amicon® Ultra 10K MWCO (Millipore, Billerica, MA) according to the manufacturer's protocol using PBS or HBS-EP buffer. All proteins were quantified based on the A_{280} measured using a NanoDrop^{TM} 1000. Purity was determined by SDS-PAGE using either a 4-20% or 12% gel (NuSep, Lawrenceville, GA) stained with GelCode Blue (Thermo Fisher Scientific, Rockford, IL) for scAb and IgG proteins, respectively. All antibodies used in this work were at least 80% pure.

Western blot analysis

The scAb and IgG proteins were expressed essentially as described above. For scAb protein expression, 1 ml of TB medium supplemented with 2% glc and Amp200 was inoculated with individual colonies of *E. coli* Jude-1 containing pMoPac16 derivatives encoding the desired scAb genes and grown at 30 ºC. Overnight cultures were subcultured 1:20 in 1 ml of TB medium supplemented with 2% glc and Amp200 for 2 h at 30 °C, cells were pelleted by centrifugation and resuspended in TB medium supplemented with Amp200 and 1 mM IPTG to induce protein expression. After 4 h of incubation at 25ºC, total protein from an equivalent amount of cells based on A_{600} were resolved under reducing conditions by SDS-PAGE on a 4-20% gel and analyzed by Western blot with a 1:10,000 dilution of anti-His HRP conjugate as described (131).

For full-length IgG protein expression, 1 ml of LB medium supplemented with 2% glc and Amp100 was inoculated with individual colonies of *E. coli* Jude-1 containing pMAZ360-IgG derivatives encoding the desired IgG genes and grown at 30 ºC. Overnight cultures were subculture to 1:20 in 1 ml of TB medium supplemented with 2% glc and Amp100, grown to A_{600} ~0.8-1.2 at 30 ºC, cells were pelleted by centrifugation and resuspended in 1 ml of TB medium supplemented with Amp100 and 1 mM IPTG to

induce protein expression. After 16 h of incubation at 25ºC, total protein from an equivalent amount of cells based on A_{600} were resolved under non-reducing conditions by SDS-PAGE on a 12% gel and analyzed by Western blot with a 1:7,500 dilution of goat anti-human heavy and light chain IgG (anti-IgG) polyclonal serum peroxidase (HRP) conjugate (Jackson ImmunoResearch Laboratories, West Grove, PA) as described (106).

Surface Plasmon resonance (SPR)

The antigen binding kinetics of purified monomeric scAbs were determined as described (59). Briefly, approximately 400 response units (RU) of PA_{83} or PA_{63} were coupled to a CM5 chip (GE Healthcare, Uppsala, Sweden) by using 1-ethyl-3-(3-dimethylaminopropyl) carbodiimide/*N*-hydroxy succinimide (EDC/NHS) chemistry. BSA was similarly coupled to the chip and used for in-line subtraction. Samples were injected for 1 min and dissociation was monitored for 5 min at 100 μl/min in HBS-P. The surface was regenerated with a pulse of 4 M $MgCl_2$. Several 2-fold dilutions of each antibody beginning at an appropriate concentration were performed in duplicate, double referenced with a blank, and k_{on} and k_{off} determined using BIAevaluation software (GE Healthcare, Uppsala, Sweden) (115).

The antigen binding kinetics of purified IgGs were determined as described (106). Briefly, approximately 10,000 RU of goat anti-human IgG1 Fcγ fragment specific (anti-Fc) (Jackson ImmunoResearch Laboratories, West Grove, PA) were coupled to a CM5 chip by using EDC/NHS chemistry. ~3 μg/ml of purified IgG in HBS-P was injected at 5 μl/min to achieve ~100 RU of captured IgG, stabilized with buffer for 5 min at 50 μl/min, and PA_{83} or PA_{63} was injected for 1 min and dissociation monitored for 5 min at 50 μl/min. The surface was regenerated with a pulse of 100 mM H_3PO_4. Several 2-fold dilutions of PA_{83} or PA_{63} beginning at 200 nM were performed in duplicate, double

referenced with a blank, and k_{on} and k_{off} were determined using BIAevaluation software (115). The antigen binding kinetics of purified IgG were also determined by directing binding as described above for monomeric scAbs.

ELISA

Apparent antibody affinity (K_D) was determined by ELISA half-maximal binding. Briefly, Costar® high binding 96-well EIA/RIA plates were coated overnight at 4º C with 50 µl of 5 µg/ml PA_{83}, PA_{63}, or transferrin in PBS. The plates were washed with PBS then blocked with PBS supplemented with 2% milk (MPBS). Ten 2-fold dilutions of purified monomeric antibody (either scAb or IgG) in MPBS were performed in duplicate starting at up to 4 µM in concentration and incubated at room temperature for 2 h. The plates were washed with PBS and PBST. ScAb immunocomplexes were detected as described above. IgG immunocomplexes were detected using an anti-IgG HRP conjugate as described (106, 107). The plates were washed, developed, and the A_{450} was measured. The A_{450} for duplicate runs was averaged, and the specific A_{450} ($A_{specific}$) for each antibody concentration was determined by subtracting the background. An apparent K_D for each antibody toward either PA_{83} or PA_{63} was determined from the plot of $A_{specific}$ as a function of antibody concentration ([Ab]) using a modified version of the non-linear optimization approach described (26). The Solver tool in Microsoft Excel™ (Microsoft, Redmond, WA) was used to calculate the K_D by varying K_D, A_{range}, and A_{min} to minimize the summation of following equation calculated for each [Ab]: $(A_{specific} - A_{tot})^2$.

ACKNOWLEDGEMENTS

I would like to acknowledge Yariv Mazor, Sean Carroll, and Clinton Leysath for their contributions, in varying capacities, to the work presented in this chapter.

Chapter 3.

Optimization of Library Screening by APEx

INTRODUCTION

Anchored periplasmic expression (APEx) is a protein display technology that has been used successfully for antibody engineering in vitro (59). In APEx, antibody fragments are anchored onto the periplasmic side of the inner membrane via fusion to either a transmembrane domain of an integral membrane protein or to the signal peptide and the first few N-terminal amino acids of an inner membrane lipoprotein, such as NlpA (59, 79). The latter anchoring strategy is usually preferable because lipoprotein fusions can be expressed at higher levels. For the detection and subsequent isolation of antigen specific antibody fragments, the cells are converted to spheroplasts in order to disrupt the outer membrane and peptidoglycan layer, incubated with a fluorescently labeled antigen, and isolated by fluorescence activated cell sorting (FACS) based on high fluorescence. APEx was effectively used to increase the affinities of two single chain variable fragment antibodies derived from hybridomas. The affinity of one of these antibodies was increased from 4300 to 35 pM, and this increase was essential for therapeutic potency in animal models of the disease (98, 105). Additionally, APEx was used to increase the affinity of two other antibodies by at least 100-fold giving rise to scFvs exhibiting equilibrium dissociation constants in the range of 45-100 pM (Chapter 2 and M. Rani, T.V.B., G.G., and B.I. unpublished data).

In this work, I used APEx for the screening of mouse immune libraries. Three antigens were used to immunize mice: the protective antigen (PA) from Bacillus

anthracis, human soluble tumor necrosis factor receptor I (TNF-RI), and human soluble tumor necrosis factor receptor II (TNF-RII). The serum titers from the respective mice indicated a significant immune response to these antigens. The VH and VL genes were amplified by RT-PCR from splenocytes and scFv combinatorial libraries were displayed using APEx. However, following several rounds of sorting, only two antibodies for the Bacillus anthracis protective antigen (PA) and none for either TNF-RI or TNF-RII were isolated (Chapter 2; data not shown).

The limited success of these studies contrasts the very successful application of APEx for antibody affinity maturation discussed above. Here I undertook extensive studies to optimize the efficiency of library screening by APEx. One of the issues encountered during the screening of immune libraries was the selection of the correct population of spheroplasts to be collected by the flow cytometer during FACS. In flow cytometry, the forward and side scatter (FSC and SSC respectively) of the laser beam are roughly proportional to the relative size and internal complexity of individual cells in a population. The FSC and SSC signals of a population of intact E. coli normally have a narrow distribution. However, following spheroplasting, i.e. the chemical removal of the cell's outer membrane and cell wall, the FSC and SSC signals become more complex. Thus distinguishing the cells to be interrogated for their fluorescence properties becomes more difficult. In the immune library screens mentioned above, simultaneous labeling for both antigen binding and inner membrane integrity, which has been shown to increase the isolation efficiency of antigen specific antibodies, was also an ineffective approach (38, 59). Further, antibodies from immune libraries will have lower affinities compared to antibodies isolated during affinity maturation. Lower affinity leads to cells with lower fluorescence which is more difficult to distinguish from cells displaying antibodies without the desired antigen specificity.

In this chapter I introduced several modifications to the APEx methodology: First, the APEx expression system was reengineered by incorporating a C-terminal epitope peptide that allows for the detection of the absolute amount of antibody protein displayed on a cell. In this manner both the amount of protein and antigen binding can be determined simultaneously by 2-color flow cytometry. Second, this system was used examine the effects of converting E. coli to spheroplasts and led to the development of optimal FACS settings. The combination of simultaneous detection of antibody expression levels and binding coupled with optimized FACS settings was shown to enable the isolation of antigen specific antibodies in a more efficient manner. Third, additional strategies for protein display in E. coli were discovered (106). Specifically, soluble proteins expressed in the periplasm of E. coli were found to be retained following conversion to spherplasts. The degree to which soluble proteins were retained by spheroplasts was roughly proportional to their molecular weight. The lack of an anchoring motif resulted in a slight decrease in fluorescence, but nonetheless the cell fluorescence was significantly higher than background.

RESULTS

Spheroplast Heterogeneity

The chemical and enzymatic treatment used to create E. coli spheroplasts results in a more heterogeneous population compared to untreated cells. These morphological differences in turn result in an altered FSC and SSC signals relative to untreated E. coli cells (Figure 3.1). Spheroplasted cells expressing the 26.10 scFv with and without a C-

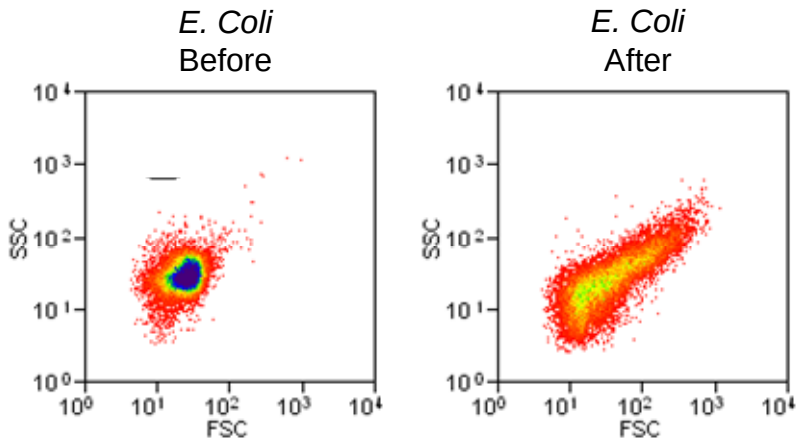

Figure 3.1. Comparison of.*E. coli* and *E. coli* spheroplasts by flow cytometry. FSC vs. SSC signals of an *E. coli* population before and after treatment with Tris-Sucrose, EDTA, Lysozyme, and $MgCl_2$.

terminal FLAG epitope FLAG epitope peptide were fluorescently labeled with anti-FLAG-PE (59). The fluorescence emission intensity of fluorescently labeled spheroplasts shows a broad distribution as determined by flow cytometry (Figure 3.2). The fluorescent signal of both the control cells and the cells expressing an antibody fused with a C-terminal FLAG peptide increased with cell size as determined by the FSC and SSC signals. The increase of the fluorescence signal with cell size was more pronounced for cells expressing the scFv-FLAG fusion.

Spheroplasts expressing scFv either with or without the FLAG peptide and labeled with anti-FLAG-PE were imaged using an inverted fluorescence microscope under brightfield and fluorescence emission (Figure 3.3). Brightfield microscopy confirmed that the spheroplast treatment resulted in the convertion of more than 90% of the E. coli into spherical cells, as a result of the degradation of the cell wall and the solubilization of the outer membrane (14). In addition, however, large aggregates comprising of many tens of spheroplasted cells were also observed. Following labeling with anti-FLAG antibodies conjugated to the fluorescent protein Phycoerythrin (anti-

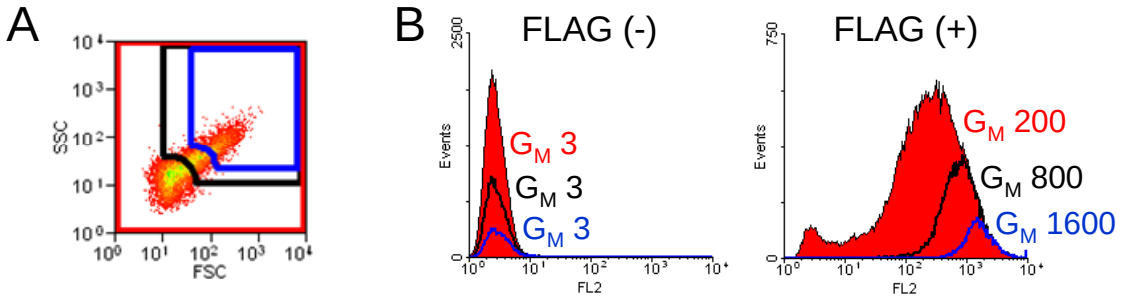

Figure 3.2. Flow cytometry gating effects on fluorescent signals.
Two monoclonal populations of spheroplasts displaying a scFv either with or without a C-terminal FLAG epitope peptide using APEx were fluorescently labeled with 5 mg/ml anti-FLAG-PE. Each population was analyzed by flow cytometry based on FSC, SSC, and PE emission signals. (A) Three gates were created based on FSC vs. SSC signal. (B) The PE emission distribution of each monoclonal population based on the gates in (A) are depicted on separate histograms. The geometric mean (G_M) of the gated population is indicated. , FLAG(-), scFv without FLAG peptide; , FLAG(+), scFv with FLAG peptide.

FLAG-PE), only spheroplasts expressing scFv-FLAG became fluorescent (Figure 3.3). The intensity of the fluorescence emission correlated with the size of the cell aggregates. High fluorescent aggregates represent an artifact in sorting experiment because the fluorescence intensity does not arise from better binding of the label on a per cell basis but instead it is the consequence of the large number of ligands in the aggregate. In other words the aggregates fluoresce intensely even if their constituent cells express proteins that bind weakly to the probe. As a result, the isolation of highly fluorescent events comprised of aggregates fails to give rise to useful antibodies. Note that in the field of view shown in Figure 3.3 labeled FLAG(+), one spheroplast was found not to be fluorescent and was highlighted in white. Such non-fluorescent cells can arise either from the loss of the plasmid that encodes the scFv-FLAG protein or from incomplete disruption of the cell wall and outer membrane which in turn could prevent the binding of anti-FLAG-PE to its cellular target.

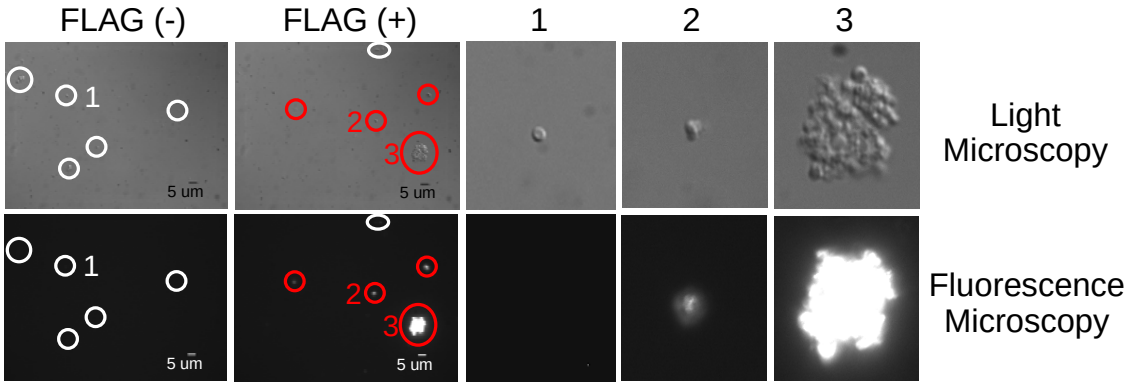

Figure 3.3. Microscopy images correlate "spheroplast" size and fluorescence. Two monoclonal populations of spheroplasts displaying a scFv either with or without a C-terminal FLAG epitope peptide using APEx were fluorescently labeled with 5 mg/ml anti-FLAG-PE and imaged under visible light and with fluorescence emission (>590 nm). Red circles indicate fluorescent objects and white circles indicate non-fluorescent "spheroplasts". The three "spheroplasts" labeled 1, 2, and 3 were digital magnified to the same degree. FLAG(-), scFv without FLAG peptide; FLAG(+), scFv with FLAG peptide.

Optimized Gates for FACS

A FACS enrichment experiment was designed to determine the optimum FSC and SSC signals that enable the recovery of individual spheroplasts displaying antibodies with desired binding properties as determined by fluorescence emission. The ability to isolate spheroplasts displaying a single domain antibody (dAb) from spheroplasts displaying a scFv with different binding specificities was easily determined by PCR analysis of the population isolated by FACS since the size of the genes encoding these antibodies are different. A gene encoding a TNF-RI specific dAb fused to a C-terminal FLAG peptide was constructed. The dAb gene was also fused to the leader peptide and first 6 amino acids of NlpA for display on the inner membrane of E. coli. Cells expressing this molecules were designated dAb(+). dAb(+) cells were converted to spheroplasts and mixed with control spheroplasts displaying an unrelated antibody,

namely the anti-digoxigenin 26.10 scFv either with or without a C-terminal FLAG peptide (scFv(+) and scFv(-), respectively). 1:1 mixtures of dAb(+) with scFv(-) or scFv(+) and also unmixed dAb(+), scFv(-), and scFv (+) spheroplasts were labeled with TNF-RIexpressed andpurified from insect cells and conjugated to the fluorescent dye BODIPY. Additionally the spheroplasts were labeled with anti-FLAG-PE (Figure 3.4).

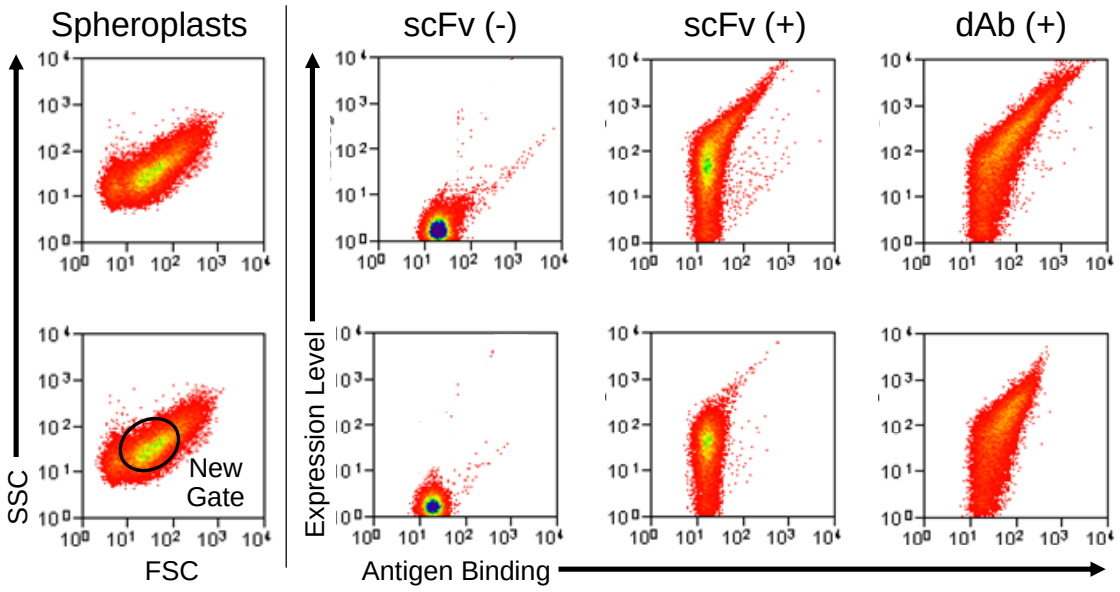

Figure 3.4. Optimized FACS gate for APEx.
FSC vs. SSC flow cytometry signal of *E. coli* spheroplasts. The New gate for FACS is depicted. Spheroplasts displaying various antibody fragments using APEx were fluorescently labeled with 5 µg/ml anti-FLAG-PE and 2.5 µM TNF-RI-BODIPY and the fluorescence emission distribution of PE (Expression Level) and BODIPY (Antigen Binding) for the total population (top row) or gated population (bottom row) are shown. scFv(-), anti-digoxigenin scFv; scFv(+), anti-digoxigenin scFv with C-terminal FLAG peptide; dAb(+) anti-TNF-RI dAb with C-terminal FLAG peptide.

The FSC vs. SSC dot plot data were gated to either account for the total cell population (total) or to exclude the large intensely fluorescent aggregates, which as described above are undesirable for library screening purposes. The latter gate that excludes aggregates was termed “New gate” in Figure 3.4. The dAb(+):scFv(-) and dAb(+):scFv(+) mixtures

were sorted either by using the total or the New gate settings and events displaying high PE and BODIPY fluorescence were collected (Figure 3.5). Analysis of the resulting population revealed that the fraction of the desired dAb(+) clones after sorting of the dAb(+):scFv(-) mixture was increased from 50% to 90% using the "new gate" compared to 70% using the "total" gate. Similarly, after sorting of the dAb(+):scFv(+) mixture the "New gate" resulted in 80% dAb(+) clones compared to 60% without.

Retention of Higher Molecular Weight Antibodies by Spheroplasts

In the studies described so far in this work, libraries of IgG antibodies or antibody fragments had been tethered onto the E. coli inner membrane to prevent their release from spheroplasts after the outer membrane had been disrupted. It was noticed, however, that in many instances, cells expressing antibody fragments in a soluble form within the periplasmic space could also be stained by fluorescent ligands following spheroplasting. These observations indicated that under certain conditions soluble periplasmic proteins are retained by spheroplasts via an unknown mechanism. Experiments were carried out to investigate whether the retention of

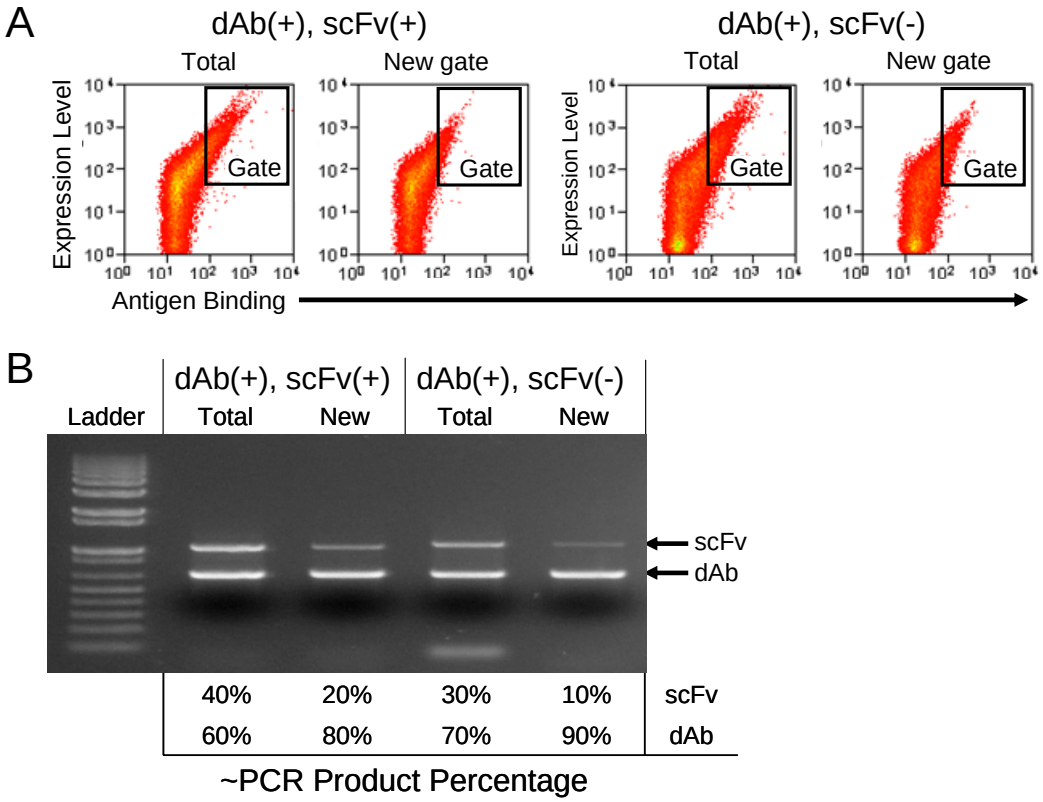

Figure 3.5. FACS enrichment experiment.
Equally mixed populations of spheroplasts displaying different antibody fragments using APEx were fluorescently labeled with 5 μg/ml anti-FLAG-PE and 2.5 μM TNF-RI-BODIPY. (A) The fluorescence emission distribution of PE (Expression Level) and BODIPY (Antigen Binding) for the total population (total) or gated population (New gate) of each sample are shown. (B) PCR recovery of antibody genes following one round of FACS. The brightest events in terms of PE and BODIPY fluorescence emission from the total or New gate FSC vs. SSC population were collected using the depicted gate in order to isolate the anti-TNF-RI dAb. The antibody genes from the collected spheroplasts were amplified by PCR using identical primers, separated on an agarose gel, imaged under UV light, and the PCR product percentages were determined using densitometry analysis. scFv(-), anti-digoxigenin scFv; scFv(+), anti-digoxigenin scFv with C-terminal FLAG peptide; dAb(+) anti-TNF-RI dAb with C-terminal FLAG peptide.

soluble periplasmic ligand binding proteins following spheroplasting is dependent on the molecular weight of the polypeptide. Plasmids were constructed for E. coli periplasmic expression of the anti-PA antibody M18.1 in different recombinant antibody formats

having varying molecular weights (Table 3.1 and 3.2). Additionally, plasmids were constructed for scFv and IgG anchoring to the periplasmic face of the inner membrane. scFv anchoring was accomplished by creating either N- or C-terminal fusions to the E. coli new lipoprotein A (NlpA) or to the M13 bacteriophage gene III protein (g3p), respectively (59). IgG anchoring was accomplished by non-covalent binding to an NlpA-ZZ domain fusion (106). The ZZ domain is a synthetic analogue of the IgG binding domain of Staphylococcus aureus Protein A. The inner membrane tethered NlpA-ZZ non-covalently captures the solubly expressed IgG antibody which becomes associated with the inner membrane. In this system, the IgG is expressed under control of the lac promoter whereas the NlpA-ZZ is expressed under control of the arabinose-dependent BAD promoter (106). Cells were converted to spheroplasts, fluorescently labeled with

Table 3.1. Plasmids used in this study

Plasmid	Purpose	Relevant characteristics	Source
pMoPac12	scFv expression	Amp^r, *lac* promoter, pelB leader, *skp* gene	(65)
pMoPac16	scAb expression	*HuC* gene in pMoPac12	(65)
pAPEx1	scFv N-terminal anchoring	Cm^r, *lac* promoter, NlpA leader and amino acids 1-6	(59)
pFLAG-APEx	scFv N-terminal anchoring & C-terminal FLAG	C-terminal FLAG peptide in pAPEx1	This study
pAK200	scFv C-terminal anchoring	Cm^r, *lac* promoter, truncated gene III protein (g3p)amino acids 250-406	(87)
pMAZ360-IgG	IgG expression	Amp^r, *lac* promoter, pelB leaders	(106)
pBAD33-NlpA-ZZ	ZZ domain N-terminal anchoring	Cm^r, BAD promoter, NlpA leader and amino acids 1-6	(106)

Table 3.2. Molecular weights of recombinant antibody formats

Format	Approximate Molecular Weight (kDa)
scFv	30
scAb	45
IgG	150

PA-FITC, and analyzed by flow cytometry. Spheroplasts containing the anti-digoxigenin 26.10 scFv as an NlpA fusion were used as a negative control for antigen binding. Cells expressing any of the anti-PA antibody fragments in a soluble form, including the smaller scFv exhibited at least 3-fold higher fluorescence compared the control as determined by the geometric means of the populations (Figure 3.6). The N-terminal scFv fusion (NlpA-scFv) resulted in a more uniform and enhanced fluorescence distribution compared to the C-terminal fusion (scFv-g3p), which is consistent with previous accounts (59). The highest fluorescence was obtained for NlpA-scFv and anchored IgG (IgG + NlpA-ZZ). IgG expression without the anchoring ZZ domain resulted in a 60% fluorescence reduction, which was nonetheless still 10-fold higher than that of the control. Soluble scFv expression resulted in a 7-fold lower fluorescence relative to the NlpA anchored version. Expression of the larger scAb fragment (45 kDa vs 30 Kda for scFvs) resulted in a 2-fold lower fluorescence relative to the NlpA anchored scFv.

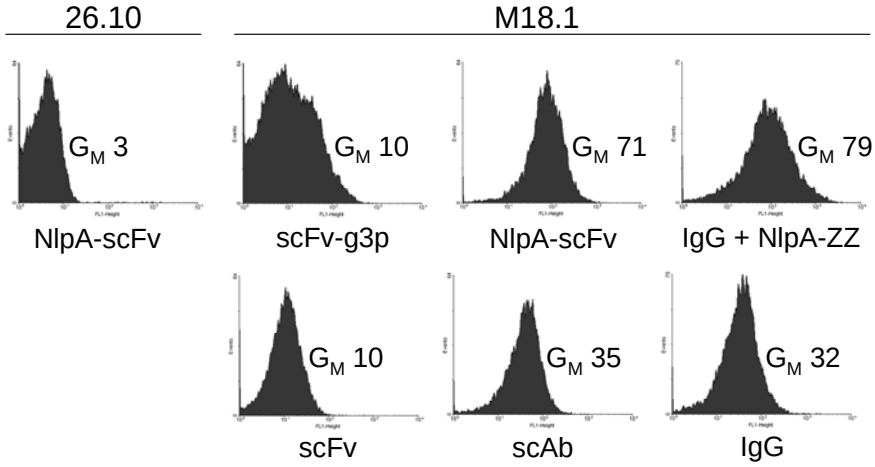

Figure 3.6. Effect of antibody molecular weight and anchoring approaches.
Spheroplasts displaying antibodies with different antigen specificities, in different formats, with or without inner membrane anchoring were fluorescently labeled with PA_{63}-FITC. The spheroplast populations were gated based on FSC vs. SSC and the resulting FITC fluorescence emission distribution and geometric mean (G_M) are shown. 26.10, anti-digoxigenin antibody; M18.1, anti-PA antibody.

DISCUSSION

In the standard APEx sorting protocol, the spheroplasts are fluorescently labeled for both antigen binding and inner membrane integrity (59). Monitoring inner membrane integrity with stains such as propidium iodide, a membrane impermeable molecule that only fluoresces when it intercalates with nucleic acids, has been shown to minimize the isolation of cells displaying antibodies that non-specifically bind to the fluorescently labeled antigen (38). This is accomplished by selecting cells based on high fluorescence emission for antigen binding and low emission for propidium iodide. However, when labeling antibodies displayed using APEx in this manner, the fluorescent signals for antigen binding and inner-membrane integrity increase relative to each other so the benefit of monitoring inner membrane integrity with APEx is questionable (59).

The fusion of a C-terminal FLAG epitope peptide to antibody fragments enables the detection of antibody expression levels (17). Thus, antigen binding per antibody can be normalized and cells displaying the highest affinity antibodies may be isolated by FACS. We showed that the incorporation of the FLAG peptide and labeling with anti-FLAG-PE resulted in a highly fluorescent population as compared to a population without the FLAG peptide (Figure 3.2). As is typically seen when fluorescently labeling spheroplasts displaying antibodies using APEx, the fluorescence intensity of each population increased with increasing FSC vs. SSC signals. This correlation between fluorescence and size was analyzed by brightfield and fluorescence microscopy (Figure 3.3). Although the majority of the population was individual spheroplasts that are approximately the same size as normal E. coli (data not shown), large aggregates were also observed. These aggregates were found to be highly fluorescent and their formation correlates with the highly fluorescent signals seen in dot plot regions of high FSC vs. SSC (Figure 3.2). In an antibody library there are very few cells displaying antigen

specific antibodies. By contrast, aggregates comprised of both intact and partially lysed spheroplasts display high non-specific labeling (data not shown). As a result, the sorting of fluorescent aggregates gives rise to clones that display low affinity or highly unspecific antibodies, while desired clones that exist as individual spheroplasts, and thus exhibit lower fluorescence, are overlooked. The design of an improved gating strategy restricting the FSC vs. SSC signals resulted in a higher enrichment efficiency of cells displaying antigen specific antibodies (Figure 3.5). This approach was used to isolate high affinity antibody variants specific for the V antigen of Yersinia pestis (Chapter 4).

In most protein display technologies, the antibody is displayed by creating a fusion between the antibody and a protein on the surface of the biological particle, such as a cell or bacteriphage. Antibodies expressed in the context of a fusion partner can be more stable and express better compared to their expression as unfused molecules. For example, it has been observed that scFvs isolated as fusions using phage display do not function when expressed on their own (78). It is undesirable to isolate antibodies with this characteristic since the antibody will eventually need to be expressed as a soluble protein for practical applications. Further, it is difficult to display complex proteins that contain multiple polypeptides as fusions. For example, creating a fusion with either the full-length light or heavy chain of an antibody would likely inhibit all four chains to assembly into a functional IgG since two identical chains would be anchored by different proteins, thus a spatial separation would prevent their assembly. In this study, it was shown that 150 kDa full-length IgG antibodies expressed as soluble proteins in the periplasm of E. coli are retained by spheroplasts and can be detected by flow cytometry following specific labeling with fluorescently labeled antigen (Figure 3.6). Additional experiments with a ~30 kDa scFv and a ~45 kDa scAb antibody fragment also demonstrated that expression of these proteins in soluble form in the periplasm results in

specific labeling following conversion of E. coli to spheroplasts. This finding was surprising since the disruption of the bacterial outer membrane results in the release of the contents of the periplasm into the surrounding environment, a phenomenon that has been extensively documented for over 40 years and exploited for the purification of periplasmic proteins (66, 88). The mechanism that underlies this observation is not clear. Two possible explanations are: (i) a portion of the "solubly" expressed polypeptide is not processed by the signal peptidase and thus retains the signal peptide which is an N-terminal hydrophobic sequence that directs export across the membrane. The signal sequence forms a transmembrane α-helix which then serves to anchor the polypeptide in the membrane. Such inhibition of signal peptide processing may be occurring because the antibody fragment is overexpressed and the large amount of protein may result in saturation of the signal peptidase. (ii) The antibody fragment is present in a fully soluble form in the periplasm but it is localized in a cell envelope compartment that is enmeshed in cell wall fragments. Such cell wall remnants have been observed in electron micrographs of spheroplasted cells (14). Regardless of the precise mechanism, the data presented here indicates that the retention of solubly expressed proteins by spheroplasts is dependent on the molecular weight.

A significant advantage of this fusion-free antibody engineering approach compared to its predecessors is its compatibility with higher molecular weight antigens, which is typical of most therapeutic antibodies (24). A previously described fusion-free system referred to as periplasmic expression with cytometric screening (PECS) was successfully used to isolate and engineer antibody fragments with desired specificity. However, it was only compatible with antigens less than 10 kDa in size, which is relatively small for a protein (29) In this study, the antigen used is a 63 kDa protein and additional studies have demonstrated specific binding with antigens up to 150 kDa (data

not shown). Although this study did not include a library screening experiment, experimental evidence suggests that it is feasible. For example, even though spheroplasts expressing soluble antibody fragments having a lower molecular weight exhibit a more marked decrease in fluorescence signal relative to the corresponding anchored protein construct, the fluorescence signal is still several fold higher than controls, and thus sufficient for library screening experiments. Therefore, this fusion-free approach can be used to engineering a variety of binding proteins toward a wide range of antigens as long as the binding proteins can be functionally expressed in the periplasm of E. coli.

MATERIALS AND METHODS

Bacterial strains and plasmid vectors

Escherichia coli Jude-1 [DH10B F'::Tn10(Tetr)] was used for all experiments. All plasmids used in this study are summarized in Table 3.1. Plasmid pMoPac12, pMoPac16, and pMAZ360-IgG were used for soluble single chain variable fragment (scFv), single chain antibody fragment (scAb), and full-length antibody (IgG) expression, respectively, and have been described (65, 106). Plasmid pBAD33-NlpA-ZZ was used to display an IgG binding domain (106). Plasmids pAPEx1 and pAK200 were used for N-terminal and C-terminal display of scFv, respectively (59). pFLAG-APEx was constructed by replacing the polyhistidine and c-myc sequences in pAPEx1 via BamHI and NotI restriction sites with the FLAG epitope peptide sequence amplified by PCR using primers TVB100 (5'-GTCGCTGCGGCCGCAGATTACAAAGACGACGATGACAAGTAGTGATATCGCAAGCTTGACC-3') and TVB101 (5'-CAGCGAGGATCCGTGACGCAGTAGCGGTAAACGGC-3'). A single domain

antibody (dAb) specific for TNF-RI (TAR2H-10 Sequence ID No. 31; Domantis, Cambridge, UK) was assembled by PCR according to established protocols (74). The dAb was cloned into pFLAG-APEx via the non-compatible SfiI restriction sites, and the ligation product was transformed into chemically competent E. coli Jude-1.

Fluorescence Microscopy

The anti-digoxigenin 26.10 scFv gene (59) was cloned into pAPEx1 and pFLAG-APEx via the non-compatible SfiI restriction sites, and the ligation products were transformed into chemically competent E. coli Jude-1 cells. Cells were cultured at 30 ºC in 2 ml of Terrific Broth (TB) medium (Becton Dickinson Difco™, Sparks, MD) supplemented with 2% (w/v) glucose (2% glc) and 30 □g/ml chloramphenicol (Cm30). After overnight growth, cells were subcultured to A600 0.1 in 2 ml TB medium supplemented with 2% glc and Cm30 at 37 ºC, grown to A600 ~0.8-1.2, cooled for 30 min to 25 ºC, and protein expression was induced with the addition of 1mM IPTG. After 4h of incubation at 25 ºC, 1 ml of cells at A600=8.0 were converted to spheroplasts using Tris/Sucrose/EDTA/lysozyme as previously described (59, 107). The spheroplasted cells were labeled with 5 □g/ml PhycoLink® anti-Flag® R-Phycoerythrin (anti-Flag PE) (Prozyme, San Leandro, CA) in PBS for 30 min at 25 ºC, then washed with PBS. Spheroplasts were imaged with a Leica DM IRBE inverted fluorescence microscope (Leica Microsystems, Wetzlar, Germany) equipped with a Leica DFC350 FX fluorescence camera.

Fluorescence Activated Cell Sorting

Tumor necrosis factor receptor I (TNF-RI) kindly provided by M. Rani (The University of Texas at Austin) was conjugated to BODIPYTM using 6-((4,4-difluoro-5,7-dimethyl-4-bora-3a,4a-diaza-s-indacene-3-propionyl)amino)hexanoic acid succinimidyl ester (Invitrogen, Carlsbad, CA) at a molar ratio of 1:10 following the manufacturer's protocol. Free BODIPY FL-X SE was removed using a NAP-10 gel filtration column following the manufacturer's protocol (GE Healthcare, Uppsala, Sweden). The extent of conjugation was determined based on the ratio of A280 and A504 measured using a NanoDropTM 1000 and the appropriate extinction coefficients and correction factors as recommended by the manufacturer (Invitrogen, Carlsbad, CA; http://www.scripps.edu/~cdputnam/protcalc.html, Putnam Lab at The Scripps Research Institute, La Jolla, CA). E. coli Jude-1 containing pAPEx1 encoding 26.10 scFv (scFv(-)), pFLAG-APEx encoding 26.10 scFv (scFv(+)), and pFLAG-APEx encoding the dAb (dAb(+)) were grown, protein expression induced, and converted to spheroplasts as described above. An equal number scFv(-) and dAb(+) spheroplasts were combined as were scFv(+) and dAb(+) spheroplasts. All the combined and individual spheroplast populations were fluorescently labeled for antigen binding and antibody expression levels. Briefly, spheroplasted cells were first labeled with 5 □g/ml PhycoLink® anti-Flag® R-Phycoerythrin (anti-Flag PE) (Prozyme, San Leandro, CA) in PBS for 30 min at 25 ºC. The spheroplasts were washed with PBS, labeled with 2.5 □M TNF-RI conjugated to BODIPY (RI-BODIPY) in PBS for 1 h at 25 ºC. The spheroplasts were washed with PBS and analyzed on a MoFlo (Dako, Glostrup, Denmark) droplet deflection flow cytometer by exciting with a 488-nm laser and measuring the fluorescence emission spectrum of BODIPY and PE with 530/40 and 570/40 band-pass filters, respectively. Fluorescence compensation was performed as previously described (107). The

spheroplast populations were gated by the forward scatter (FSC) and side scatter (SSC) parameters, and 7,000 of the most fluorescent events from the population based on both the BODIPY and PE emission spectra were collected as described under Results (59, 107). The antibody genes (scFv or dAb) from the collected spheroplasts were by amplified by PCR using primers BRH06 (5'-GCGGATAACAATTTCACACAGG-3') and AHX89 (5'-CGCAGTAGCGGTAAACGGC-3') (59). The amplified DNA was analyzed on a 1% agarose gel under UV light. The band intensities were determined by densitometry analysis software.

Flow Cytometry

E. coli Jude-1 containing pMoPac12, pMoPac16, pAPEx1, and pAK200 plasmids encoding the anti-PA M18.1 scFv, and the plasmid pAPEx1 encoding 26.10 were individually cultured and converted to spheroplasts as described above. E. coli Jude-1 containing pMAZ360-IgG encoding for M18.1 IgG and also with and without pBAD33-NlpA-ZZ, were cultured in 2 ml of LB medium supplemented with 2% glc and Amp200 (and Cm30 for with pBAD33-NlpA-ZZ) overnight at 30 ºC. The cells were diluted into 2 ml of TB media supplemented with 2% glc, Amp100, and Cm30 to an A600 0.2, grown to A600 ~0.8-1.2 at 30 ºC, pelleted by centrifugation and resuspended in fresh media as above but also containing 1 mM IPTG to induce protein expression. After 16 h of incubation at 25 ºC, NlpA-ZZ protein expression was induced from pBAD33-NlpA-ZZ by the addition of 0.2% arabinose (w/v) and the cells were incubated for an additional 3 hours at 25 ºC. Subsequently, the cells were converted to spheroplasts as described above and labeled with 200 nM PA63-FITC (List Biological Laboratories, Campbell, CA) in PBS for 1 h at 25 ºC. Labeled spheroplasts were washed with PBS and analyzed on a FACSCalibur (Becton Dickinson Biosciences, San Jose, CA) flow cytometer by exciting

with a 488-nm laser and measuring the fluorescence emission spectrum of FITC with a 530/40 band-pass filter.

Chapter 4.

Affinity Maturation of an Anti-V Antigen IgG Expressed *In Situ* Via Adenovirus Gene Delivery Confers Enhanced Protection Against *Yersinia pestis* Challenge

INTRODUCTION

Yersinia pestis is the etiologic agent of the plague and has been responsible for pandemic outbreaks occurring throughout the course of history. Although advances in our current living conditions, public health practices, and antibiotic therapies make future pandemics unlikely, outbreaks of plague resulting from biological warfare are a real threat. The features of *Y. pestis* that make it an attractive option for use as a biological weapon include availability of the organism, capacity for aerosol dissemination, potential for spread of secondary cases, and the high fatality rate of the pneumonic form of plague. In endemic regions of the world, the bacterium survives by causing chronic disease in animal reservoirs. It is spread among these animals and occasionally to humans predominantly through a flea vector, such as *Xenopsylla cheopis* (21, 147). Without prompt antibiotic therapy, approximately 50% of bubonic plague infections are fatal and can progress to the more dangerous pneumonic plague (147). Respiratory droplets from a pneumonic infected individual promote rapid spread through a susceptible population. Symptoms develop in 1 to 6 days post-infection and the disease progresses rapidly from a flu-like illness to severe pneumonia with coughing, chest pain, and bloody sputum. To be effective, antibiotic therapy must be administered early. If treatment is delayed more than 24 hours following the onset of symptoms, the fatality rate is extremely high (165). Additionally, the presence of antibiotic-resistant strains of *Y. pestis* renders antibiotic

therapy unreliable. Fro these reasons, *Y. pestis* is a likely agent to be used as a biological weapon since aerosolized bacteria can confer widespread pneumonic plague (147).

Of the 11 *Yersinia* species, only *Y. pestis*, *Y. enterocolitica*, and *Y. pseudotuberculosis* are human pathogens. *Y. pestis* is a gram-negative, non-motile, non-spore-forming bacterium that replicates intracellularly during the early stages of infection and grows predominantly extracellularly at later stages of the infectious cycle (147). At present, no plague vaccine has been approved for use in the US. Passive immunization with antibodies specific for the LcrV protein (V antigen) is an attractive alternative to vaccines and have been shown to be effective against lethal challenges with *Y. pestis* (67-69, 149). The V antigen plays a central role in plague pathogenesis. It activates the type III secretion system and thus mediates translocation of effector proteins (Yops) into host macrophages. It is also released from the bacteria and has immunosuppressive functions manifested by increasing levels of the anti-inflammatory cytokine interleukin 10 and decreasing levels of TNF-α (147). A recently developed anti-V antigen monoclonal antibody (mAb) 2C14.4 has been shown to confer protection against lethal challenge with intranasally administered *Y. pestis* in a dose-dependent manner (149).

For several neutralizing antibodies the degree of protection against challenge with pathogen correlates with antigen binding affinity (5, 101, 105, 162). For example, while monoclonal antibodies and antibody fragments to the Protective Antigen (PA) of *Bacillus anthracis* with a K_D=11 nM fail to confer protection against challenge with the holotoxin or with intranasally administered spores, engineered antibody variants displaying 40- to 200-fold higher affinities were protective in different animal models (98, 105). Notably, protection appeared to be mediated by blocking the ability of PA to bind to its receptor since PEGylated antibody fragments exhibiting a K_D=35 pM but lacking an Fc domain, and hence incapable of engaging innate immunity mechanisms of pathogen clearance,

were protective (98). Engineering antibodies with high affinity has been shown to improve protection for other protein toxins and viruses including Botulism, human immunodeficiency virus (HIV), and human respiratory syncytial virus (RSV) and have increased efficacy when targeting inflammatory cytokines such as TNF-α (5, 101, 105, 126, 131, 162).

In this study, we evaluated whether Ad-mediated delivery of an engineered 2C14.4 IgG exhibiting markedly increased affinity directed towards the V antigen can improve protection against *Y. pestis* challenge in mice (149). Mutations needed to confer higher affinity could have unexpected effects on protein expression from the Ad delivered IgG DNA or biodistribution of the IgG, thus making it difficult to predict how protection to pathogen challenge might be affected. A scFv fragment incorporating the V_H and V_L domains of the 2C14.4 IgG was constructed and subjected to affinity maturation by screening a library generated by random mutagenesis for high affinity variants. The latter was performed using an *E. coli* display technique called Anchored Periplasmic Expression (APEx) coupled with fluorescent activated cell sorting (FACS) (59). In APEx, the protein library is tethered to the periplasmic side of the inner membrane of the bacterium via fusion to the 6 N-terminus amino acids of the native lipoprotein NlpA. The resulting NlpA-scFv fusion is lipidated *in vivo* and thus becomes attached to the inner membrane. Following permealization of the *E. coli* outer membrane by chemical and enzymatic means, the cells are labeled with fluorescent antigen and the brightest cells are isolated by FACS. A single round of random mutagenesis and APEx screening resulted in the isolation of a clone, H8, displaying a K_D=100 pM which is 35-fold higher affinity than the parental 2C14.4. The H8 V_H and V_L domains were used to exchange those of 2C14.4 IgG in the adenoviral vector AdαV giving rise to AdαH8. We show that delivery of the two vectors *in vivo* resulted in approximately the same Ab

serum titers and that mice immunized with 10^{10} pu AdαH8 conferred a statistically significant increase in protection relative to the parental AdαV.

RESULTS

Engineering high affinity anti-V antigen antibodies

The variable heavy chain (V_H) and light chain (V_K) domains of the *Y. pestis* neutralizing mAb 2C12.4 were amplified by PCR (149) and used to create a single chain variable fragment (scFv) by incorporating a sequence encoding a $(Gly_4Ser)_4$ linker between the C termini of the V_H sequence and the N termini of the V_K sequence. The gene encoding the scFv was cloned into pMoPac16 for soluble expression of the antibody fragment in the single chain antibody (scAb) format (65). The scAb format is comprised of a scFv in which the C termini of the variable light chain domain is fused to the human kappa constant domain, resulting in improved expression characteristics in *E. coli* without altering the antibody binding affinity (62). Lysates from cells expressing the 2C14.4 scAb were confirmed to express full length protein via Western blotting and displayed binding activity as determined via ELISA using purified *Y. pestis* V antigen.

The gene encoding the scFv version of 2C12.4 was subjected to one round of random mutagenesis by error-prone PCR. Amplified DNA was cloned into pFLAG-APEx and the ligation product was transformed into *E. coli* Jude-1 cells yielding >2 X 10^6 independent transformants. DNA sequencing of 10 clones selected at random revealed an average of 1.75% nucleotide substitutions with a standard deviation of 0.75%. Cells were grown in liquid culture, protein expression was induced, and 4 hours later, the cells were harvested and converted into spheroplasts. The spheroplasted cells were then labeled with 5 μg/ml anti-Flag-PE and 500 nM V antigen-BODIPY to

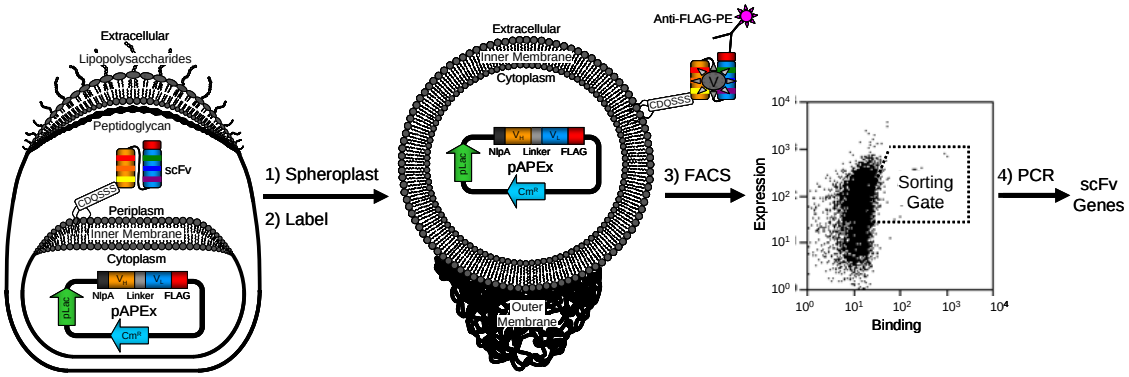

Figure 4.1. Schematic diagram of APEx
Libraries of antibody fragments are expressed from a single plasmid (pFLAG-APEx) as N-terminal fusions to NlpA(1-6) and are anchored to the periplasmic face of the cytoplasmic membrane of *E. coli*. This vector also encodes for a C-terminal FLAG epitope peptide. The cells are converted to spheroplatst through chemical and enzymatic degradation of the outer membrane and peptidoglycan layer allowing fluorescently labeled exogenous antigen to interact with the antibodies displayed on the surface of the inner membrane. Spheroplasts containing antibodies specific for the antigen are enriched from the total population by FACS and their antibody genes recovered by PCR.

determine full-length scFv expression levels and antigen binding, respectively (Figure 4.1). A total of 8 X 10^7 cells (40-fold library coverage) were subjected to high-throughput fluorescence activated cell sorting (FACS) and the top 2% events in terms of PE and BODIPY fluorescence emissions were collected (Figure 4.2). The collected spheroplasts were immediately resorted as above without additional labeling to maximize the isolation of antibodies with slow dissociation rate constants toward V antigen (59). The scFv genes in the spheroplasts collected during the resort were amplified by PCR, and the DNA was subcloned back into the pFLAG-APEx vector. Following transformation, the cells were subjected to two additional rounds of sorting using increasingly stringent collection criteria, namely a higher fluorescence threshold. After the third round of sorting, the number of events falling within the window used for the 1st round increased from 2% to 23% (Figure 4.2).

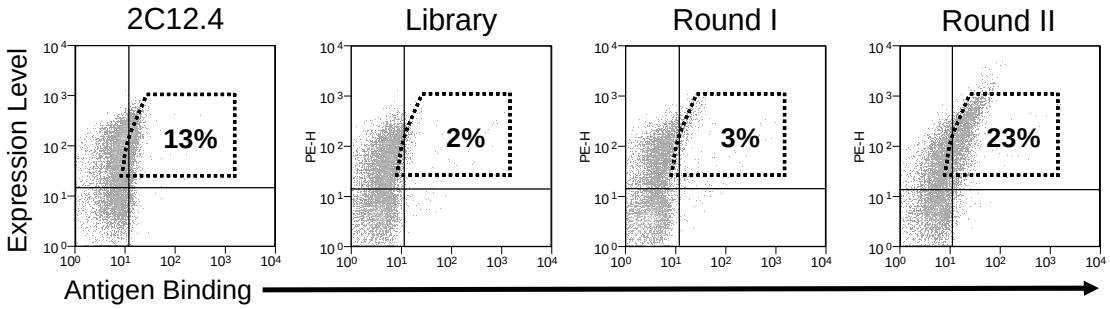

Figure 4.2. FACS analysis of affinity maturation using APEx.
FACS analysis of *E. coli* spheroplasts expressing anti-V antigen 2C12.4 scFv, the library of random mutants, and the populations recovered following two rounds of FACS. Spheroplasts were labeled with 500 nM V antigen-BODIPY and 5 μg/ml anti-FLAG-PE. The dashed box represents the gate used to isolate cells by FACS from the original library. The percentage of the spheroplast in this gate for each population is indicated.

The scFv gene pool from the third round of sorting was amplified by PCR and cloned into pMoPac16 for expression in the scAb format. SPR was used to rank order the dissociation rate constants of individual clones in crude cell lysate (Figure 4.3). Of the 72 colonies tested, 41 (57%) expressed scAbs that displayed significant binding towards V antigen immobilized on the Biacore chip. Of these 41 clones, four clones exhibited dissociation rate constants at least 10-fold slower than parental antibody (Figure 4.4). The reproducibility of the method is demonstrated in Figure 4.5.

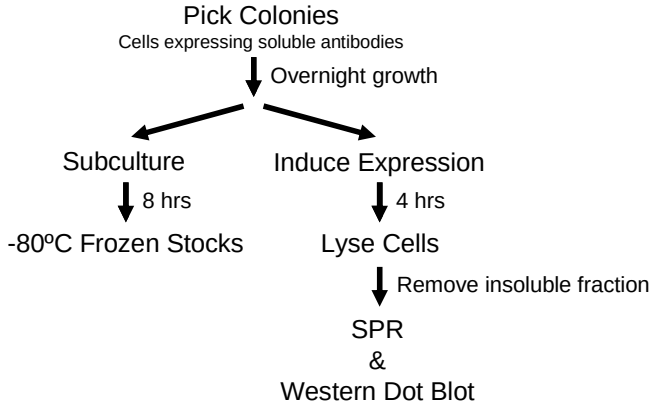

Figure 4.3. Process flow diagram for semi-high throughput SPR analysis

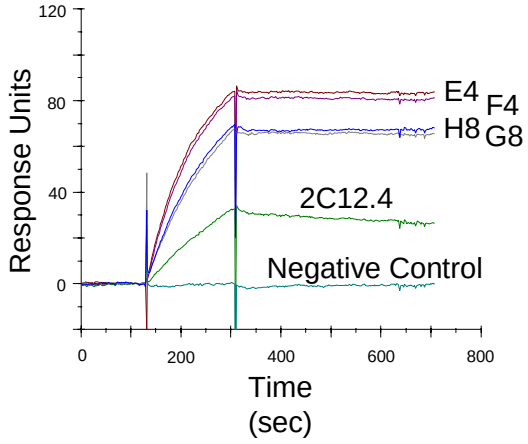

Wild-Type	k_{off} (s^{-1})	Relative k_{off}
2C12.4	3.9×10^{-4}	1
G8	2.8×10^{-5}	14
F4	3.5×10^{-5}	11
E4	2.7×10^{-5}	20
H8	$< 5 \times 10^{-6}$	>75

Figure 4.4. SPR analysis of four clones with low k_{off}
Crude cell lysates containing scAbs from 72 different clones were analyzed by SPR to determine their dissociation rate constants. Accurate values for H8 were not determined because the calculated k_{off} were lower than the sensitivity of the Biacore 3000 (163).

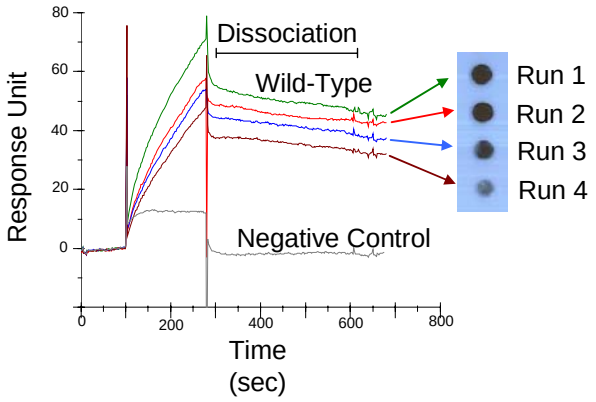

Wild-Type	k_{off} (s^{-1})	k_{off} Relative to Purified
Purified	3.2×10^{-4}	1.0
Run 1	3.3×10^{-4}	1.0
Run 2	3.9×10^{-4}	1.2
Run 3	4.0×10^{-4}	1.3
Run 4	4.1×10^{-4}	1.3

Figure 4.5. Reproducibility of k_{off} analysis by SPR
Four colonies each expressing 2C12.4 scAb were individually picked and processed according to the method described here. The dissociation rate constant for each sample was compared to the actual value obtained using purified 2C12.4 scAb monomers.

These four scAbs, as well as the 2C141.4 and 26.10 scAbs, were expressed at the 500 ml scale in shake flasks, the periplasmic fraction was isolated by osmotic shock, and monomeric scAb proteins were purified by immobilized metal affinity chromatography (IMAC) and size exclusion FPLC. Consistent with the isolation of the respective clones

based on increased PE fluorescence, the protein yields for all four scAbs was higher than that of the parental 2C14.4 scAb (Table 1). All antibodies exhibited at least 10-fold lower equilibrium dissociation constants (K_D) relative to the parental 2C14.4 scAb (Table 4.1) which is consistent with the measurements obtained using crude cell lysates (Figure 4.5). The highest affinity clone, H8, exhibited an affinity of 100 pM that translates to a 35-fold improvement compared to the parental antibody 2C12.4. The improved affinity for all clones was almost exclusively the result of a decrease in the dissociation rate constant whereas the association rate constant remained essentially unchanged. The four variants, H8, E4, F4 and G8, contained either 7 or 9 amino acid mutations compared to the parental antibody (Table 4.2) of which two were common: L49S in framework 2 of the V_H, which is immediately prior to complementary determining region 2 (CDR2); and Y32F in CDR1 of the light chain (102). Further, three of the variants contained an additional four common mutations (D1N, T5S, R24K, T97R) in the light chain.

Table 4.1. Kinetic analysis of anti-V antigen antibody fragments

Antibody	k_{on} ($M^{-1}s^{-1}$)	k_{off} (s^{-1})	K_D (pM)	Affinity Improvement[a]	Expression Improvement[b]
2C12.4	9.2×10^{4}	3.2×10^{-4}	3500	1x	1x
H8	1.2×10^{5}	1.2×10^{-5}	100	35x	4x
E4	1.0×10^{5}	1.8×10^{-5}	180	20x	5x
F4	1.2×10^{5}	2.6×10^{-5}	220	16x	3x
G8	9.8×10^{4}	2.4×10^{-5}	250	14x	2x

[a]Affinity improvement relative to the parental antibody 2C12.4

[b]Yield of purified scAb (mg/L A_{600}) compared to 2C12.4

Table 4.2. Sequence analysis of anti-V antigen antibody fragments

	Variable Heavy Chain[a]										Variable LightChain[a]											
	FW1		CDR1	FW2		CDR2		FW3			FW1		CDR1	FW2		CDR2		FW3			CDR3	
Clone	3	11	32	45	49	51	65	67	82		1	5	24	32	39	53	72	84	97			
2C12.4	T	I	S	L	L	I	S	L	I		D	T	R	Y	K	N	T	A	T			
H8					S	V					N	S	K	F					R			
E4		V	P		S									F	R	S		T				
F4	A			P	S			V			N	S	K	F					R			
G8					S		G		T		N	S	K	F			A		R			

[a]Amino acid substitutions based on Kabat numbering (102). FW, framework; CDR, complementary determining region

Genetic immunization using IgG encoding adenovirus vectors and challenge with *Y. pestis*

The VH and VK domains of a replication-defective serotype 5 human Ad gene transfer vector encoding the 2C12.4 mouse IgG2b (AdαV) were replaced with those from the highest affinity antibody variant, H8, to create AdαVH8 (149). Mice were immunized with varying numbers of particle units (pu) of AdαV, AdαVH8, or, as controls with either the highest level (10^{11} pu) of AdαPA, an adenovirus vector encoding a mouse IgG mAb specific for the B. anthracis PA or PBS. Serum anti-V antigen antibody titers were measured via ELISA three days post immunizations (Figure 4.6). A similar dose dependent response was observed for both AdαV and AdαVH8. The titers for equivalent immunization levels were within 2-fold for both AdαV and AdαVH8. Both AdαPA and PBS controls did not result in any measurable anti-V antibody titers. Three days after immunization, the mice were challenged intranasally with 363 LD50 of Y. pestis CO92 (Figure 4.7). All mice immunized with the highest dosage (10^{11} pu) of AdαV and

AdαVH8 survived. However, at a 10-fold lower dose (10^{10} pu), none of the mice immunized with AdαV survived while 80% (4 out of 5, P < _) of the mice immunized with this dose of AdαVH8 survived. None of the mice immunized with the lowest dose (10^{9} pu) of AdαV or AdαVH8 or with either control survived.

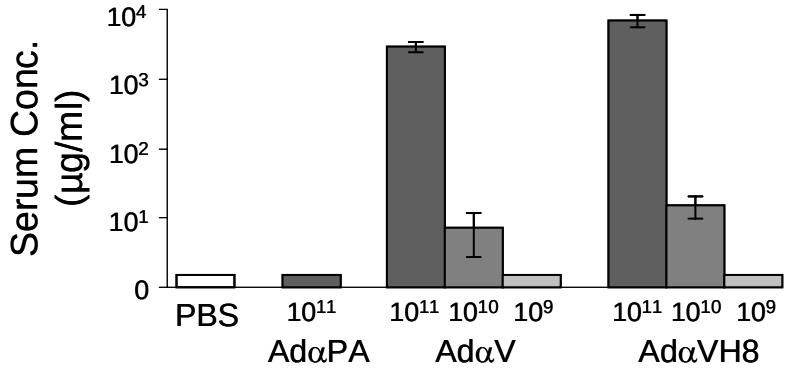

Figure 4.6. Mice titers following immunization with Ad vectors
Anti-V antigen IgG titers in mice following immunization with Ad vectors. C57BL/6 mice (*n* = 5/group for AdαV and AdαVH8; *n* = 1/group for AdαPA and PBS) were administered intravenously with the indicated Ad vectors or PBS. Serum anti-V antigen antibody titers were measured three days post immunization via ELISA. PBS, negative control; AdαPA, vector encoding an IgG specific for the *B. anthracis* PA; AdαV, vector encoding the 2C12.4 IgG; AdαVH8, vector encoding the 2C12.4 IgG mutant H8.

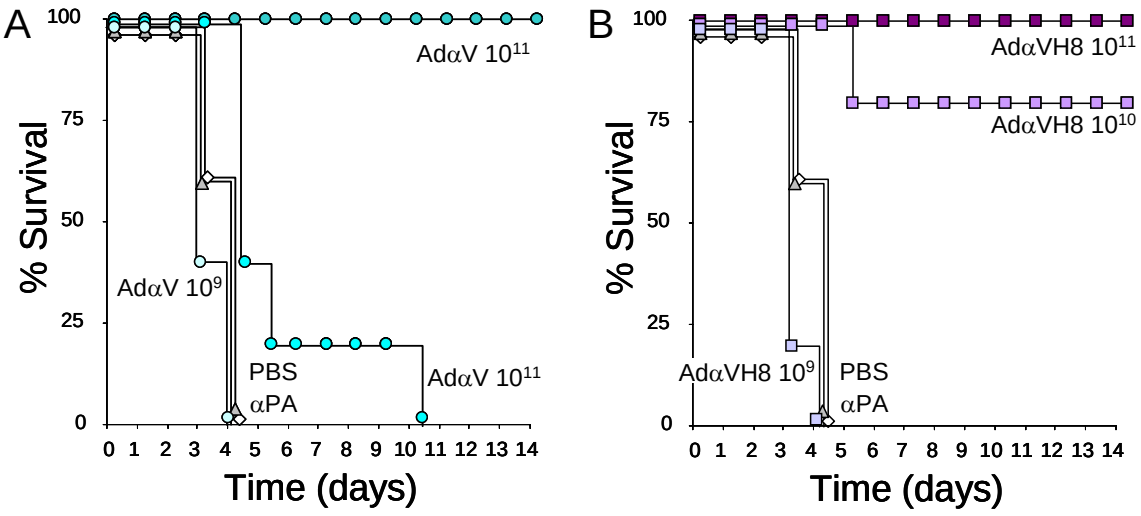

Figure 4.7. Survival of mice challenged with *Y. pestis*
Survival of mice challenged with *Y. pestis* following prophylactic administration of Ad vectors. Three days following intravenous administration of Ad vectors or PBS, C57BL/6 mice (n = 5/group for AdαV and AdαVH8; n = 1/group for AdαPA and PBS) were challenged with a lethal dose of *Y. pestis* intranasally. Survival of the mice was monitored for 14 days following challenge. (A) Immunization with AdαV compared to AdαPA and PBS. (B) Immunization with AdαVH8 compared to AdαPA and PBS.

DISCUSSION

Passive immunization with engineered antibodies displaying enhanced antigen affinity have been shown to increase the neutralization efficacy of a number of bacterial or viral pathogens and toxins (5, 101, 105, 126, 131, 162). However, to the best of our knowledge, neither the effect of antigen affinity for antibodies expressed *in situ* following viral transfer of the antibody gene, nor the relationship between V antigen affinity and protection to the potential biowarfare agent *Y. pestis,* have been examined. Here we found that increasing the affinity of the *Y. pestis* neutralizing antibody 2C14.4 from 3.5 nM to 100 pM (35-fold) could confer significant protection against a lethal challenge with *Y. pestis* at a 10-fold lower viral load for genetic delivery of the antibody.

The affinities of antibodies generated by the natural immune system are constrained by the kinetics of *in vivo* selection (45). Most high affinity mouse monoclonal antibodies display nanomolar affinities and this is the case for the anti-V antigen antibody 2C12.4 for which we measured a K_D=3.5 nM by SPR. Combinatorial mutagenesis and library screening by phage display or other high throughput techniques has been employed for affinity maturation of the variable domains of monoclonal antibodies (5, 101, 105, 126, 131, 162). In earlier studies, we used random mutagenesis and screening of *E. coli* displayed libraries by APEx to isolate picomolar affinity antibodies to the *B. anthracis* PA which in turn proved to have markedly improved neutralization potency *in vitro* and in various animal models (98, 105, 115). Key advantages of this strategy are the ease with which libraries of random mutants can be constructed in *E. coli* and screened by FACS. FACS is a high-throughput screening technique that enables real-time quantitative multi-parameter analysis on a cell by cell basis. Therefore, multiple properties can be monitored simultaneously to specifically isolate antibodies with desired characteristics.

In this work antibody fragments were tagged with a C-terminal FLAG peptide epitope that allowed simultaneous monitoring of both antigen affinity (using V-antigen labeled green) and expression level (using an anti-FLAG antibody labeled red, Fig. 1). Clones isolated from the last round of FACS were rank-ordered by comparing the dissociation rate constants in crude lysates (Supplementary Fig. 1). This approach significantly expedited the analysis of the clones obtained after screening, a process that often represents the rate limiting step in antibody affinity maturation. While it was not necessary to use in this case, the relative expression levels of the antibody variants can also be determined in high throughput using a 96-well dot blot apparatus and the data can then be used to estimate the association rate constant (k_{on}) (data not shown). In the end, a

single round of mutagenesis following by three rounds of FACS and dissociation rate constant analysis resulted in the isolation of antibodies displaying up to 35-fold higher affinities and higher expression yields (Fig. 1B, Table 1).

Genetic delivery of full-length antibodies *in vivo* has been carried out using adenovirus, adeno-associated virus and vaccinia virus vectors (9, 44, 82) and is an attractive alternative to the high cost of conventional methods which require production, purification, and storage of the monoclonal antibody (35, 82). This is compounded by problems relating to administration, bioavailability, and increased immunogenicity resulting from large dosages required by conventional methods (139). The administration of most monoclonal antibodies treatments requires hour long intravenous infusions every one to four weeks in order to maintain clinically relevant serum concentrations during this period (REF). A common complication are infusion reactions with symptoms ranging from mild to life-threatening and typically occur near the time of administration (31). Following infusions, complicated pharmacokinetics result in a continual decrease in serum concentrations which effects the bioavailability and the pharmacodynamic properties of the therapeutic antibody (83, 139). In addition, the initial large dosages required during infusions also increase the probability of generating an immune response against the therapeutic monoclonal antibody which can lead to rapid elimination and potentially severe allergic reactions (139). However, genetic delivery can provide immediate and sustained serum levels for several months from a single treatment with both adenovirus (Ad) and adeno-associated virus (AAV) vectors encoding the same monoclonal antibody (18). This approach has been demonstrated with a neutralizing antibody and offered almost immediate protection against anthrax toxin challenge *in vivo* which was sustained for 6 months (40). This approach circumvents many of the issues

associated with conventional methods and has the additional benefits of increasing patient quality of life and protecting soldiers entering combat for extended periods.

Here we demonstrate for the first time that the affinity of antibodies produced *in situ* following adenoviral gene transfer correlates with protection. Although the affinity of the antibody was improved 35-fold, only a 10-fold reduction in viral load could confer significant protection against a lethal challenge with *Y. pestis in vivo*. This was significant, but the lack of a direct correlation between affinity and efficacy may result from a decrease in antibody specificity attributed to a lysine to arginine substitution found in the affinity enhanced mutant (15). Arginine residues are correlated with increased non-specific binding which can alter biodistribution and result in this lower than expected viral load reduction of the mutant.

Engineering ultra-high affinity antibodies for *in situ* delivery may be one approach to circumvent preexisting immunity against Ad. Although human Ad serotype 5(Ad5) has been effectively used in a variety of animal models for genetic delivery, it has limited use because approximately 35 to 50% of humans have preexisting neutralizing antibodies against it (61). Even though human and non-human based Ad vectors can be effective in genetic delivery even in the presence of preexisting immunity, cross-reactive antibodies have been reported and are a major obstacle limiting the widespread use of Ad vector for gene therapy (61). An approach that has yet to be explored is to minimize the genetic delivery dosage levels in order to evade host immunity. This has been shown to occur when a low-dose infection with *Salmonella* evades host adaptive immunity (150). Ultra-high affinity antibodies have been reported (16) and may require very low Ad vector dosages that evade preexisting immunity while maintaining prophylactic/therapeutic benefit. The dosage levels can be further reduced by simultaneously engineering the Ad vectors to increase serum titers of the antibody for

which they encode (18). This combination approach can increase the application potential of the genetic delivery of antibodies as well as other proteins.

There are many pathogens to which an effective vaccine or antibiotic has yet to be produced and monoclonal antibodies remain the only alternative for protection. These antibodies frequently require engineering to enhance their affinities and expression levels in order to make them effective prophylactics/therapeutics from both a cost and efficacy perspective. This requires display systems and screening methodologies to expedite the discovery and engineering process. Even if a therapeutic antibody is generated, conventional methods for antibody production are expensive and high costs associated with therapy minimize their practical applications. However, genetic delivery of antibodies is an attractive alternative since it has the potential to be cheaper, safer, and increase patient quality of life.

MATERIALS AND METHODS

Bacterial strains and plasmid vectors

Escherichia coli Jude-1 (*E. coli* DH10B F^- *mcrA* Δ(*mrr-hsdRMS-mcrBC*) ϕ80d*lacZ* ΔM15 Δ*lacX74 recA1 araD139* Δ(*ara leu*)7697 *galU galK rpsL endA1 nupG* harboring an F′ from *E. coli* XL1-blue introduced by conjugation) used for all antibody engineering experiments. Plasmid pMoPac16 was used for soluble single-chain antibody fragment (scAb) expression and has been previously described (65). Plasmids pAPEx1 was used for *E. coli* display of soluble single-chain variable fragment antibodies (scFv) (59). pFLAG-APEx was constructed by replacing the polyhistidine and c-myc sequences in pAPEx1 via BamHI and NotI restriction sites with the FLAG peptide epitope sequence amplified by PCR using primers TVB100 (5’-

GTCGCTGCGGCCGCAGATTACAAAGACGACGATGACAAGTAGTGATATCGCA AGCTTGACC-3') and TVB101 (5'-CAGCGAGGATCCGTGACGCAGTAGCGGTAAACGGC-3').

Protein expression and purification

Recombinant V antigen was expressed and purified as previously described (149). Monomeric scAbs were expressed and purified according to published procedures (59, 65). Briefly, *E. coli* Jude-1 containing pMoPac16 derivatives encoding the desired scAb genes were streaked from frozen stocks onto agar plates containing Luria-Burtani Miller (LB) medium (Becton Dickinson Difco™, Sparks, MD) supplemented with 2% (wt/vol) glucose (2% glc) and 200 μg/ml ampicillin (Amp200) (20 h, 25 ºC). Individual colonies were cultured in 2 ml of Terrific Broth (TB) medium (Becton Dickinson Difco™, Sparks, MD) + 2% glc + Amp200 (8 h, 250 rpm, 30 ºC) then 1 ml was used to inoculate 500 ml of TB medium + 2% glc + Amp200 (250 rpm, 30 ºC). After overnight growth, cells were pelleted by centrifugation (15 min, 4,400 X g, 4 ºC) and resuspended in 500 ml of TB medium + Amp200 + 1 mM Isopropyl-β-d-thiogalactopyranoside (IPTG) (Sigma-Aldrich, St. Louis, MO) to induce protein expression. After 4 h of incubation at 25 ºC, the cells were pelleted by centrifugation (15 min, 4,400 X g, 4 ºC), and the periplasmic fraction from the cell pellet was isolated by osmotic shock according to published procedures (65). scAb proteins were purified from the shockate by immobilized metal affinity chromatography (IMAC) using Ni-NTA Agarose based on the manufacturer's protocol (Qiagen, Hilden, Germany), and monomeric scAbs were further isolated by size-exclusion FPLC (SEC) on a Superdex^{TM} 200 column (GE Healthcare, Uppsala, Sweden) using HBS-P (GE Healthcare, Uppsala, Sweden). Proteins were quantified based on the A_{280} measured using a NanoDrop^{TM} 1000 (Thermo Fisher Scientific, Wilmington, DE)

and the appropriate extinction coefficients calculated using Protein Calculator (http://www.scripps.edu/~cdputnam/protcalc.html, Putnam Lab at The Scripps Research Institute, La Jolla, CA). Relative concentrations were verified and purity determined by SDS-PAGE using a 4-20% gel (NuSep, Lawrenceville, GA) stained with GelCode Blue (Thermo Fisher Scientific, Rockford, IL). All scAbs used in this work were at least 90% pure.

Anti-V antigen antibody fragment cloning, expression, and analysis

Genes encoding the variable heavy chain (V_H) and the variable light chain (V_K) domains of anti-V antigen 2C12.4 IgG were amplified by PCR from the previously described adenovirus vector plasmid DNA (149) using primers TVB102 (5'-GCAGCGAGGCCCAGCCGGCCATGGCGCAGGTAACTCTGAAAGAGTCTG-3') and TVB103 (5'-AGAGCCGCC GCCGCCGCTACCACCACCACCAGAACCACCACCACCTGAGGAGACTGTGAGA GTGGTG-3') for V_H and TVB104 (5'-GGTGGTGGTGGTAGCGGCGGCGGCGGCTCTGGCGGCGGCGGCTCCGACATTG TGCTGACAC AGTCG-3') and TVB105 (5'-CGAATTCGGCCCCCGAGGCCCGTTTTACTTCCAGCTTGGTC-3') for V_K (149). The resulting PCR products were combined by overlap extension PCR and cloned into pMoPac16 via the non-compatible SfiI restriction sites for soluble expression as a scAb. The resulting ligation product was transformed into *E. coli* Jude-1, and scAb expression was performed as previously described (29, 65). Briefly, individual colonies were cultured overnight in 2 ml of TB medium + 2% glc + Amp200 at 30 °C. After overnight growth, cells were pelleted by centrifugation (10 min at 4,600 X g, 4 ºC) and resuspended in 2 ml of TB medium + Amp200 + 1 mM IPTG to induce protein expression. After 4 h

incubation at 25 ºC, 1 ml of cells were pelleted by centrifugation (10 min at 4,600 X g, 4 ºC), and the cell pellet was resuspended in 1 ml of lysis buffer which consisted of BugBuster™ HT Protein Extraction Reagent (Novagen, Madison, WI) diluted 1:4 in phosphate buffered saline (PBS) (107). The cells were incubated in lysis buffer while rotating on an inverter (30 min, 60 RPM, 25 ºC) then the insoluble fraction was removed by centrifugation (1 min, 10,000 X g, 4 ºC).

The soluble fraction was analyzed for the presence of full-length scAb specific for the V antigen by Western blot analysis and enzyme-linked immunosorbent assay (ELISA), respectively. Western blot analysis with anti-polyhistidine (anti-His) peroxidase (HRP) conjugate (Sigma-Aldrich, St. Louis, MO) was performed as previously described (132). ELISA was performed by coating Costar® high binding 96-well EIA/RIA plates (Corning, Corning, NY) overnight at 4º C with 50 µl of 5 µg/ml recombinant V antigen or bovine serum albumin (BSA) in PBS. The plates were washed three times with PBS followed by blocking with 400 µl PBS supplemented with 2% milk for 4 h at room temperature. Samples were diluted 1:1 in PBS with 2% milk and incubated for 1 h at room temperature. The plates were washed three times with PBS then an additional three times with PBS containing 0.1% Tween-20. Immunocomplexes were detected using an anti-human kappa light chain (anti-HuCκ) polyclonal serum HRP conjugate (Sigma, St. Louis, MO) applied at a 1:10,000 dilution and incubated for 30 min at room temperature. The plates were washed as described above and developed using the chromogenic HRP substrate TMB+ (Dako, Glostrup, Denmark) as described by the manufacturer. The A_{450} was measured with a mircroplate reader (BioTek, Winooski, VT).

Isolation of high affinity variants of the 2C14.4 scFv

The anti-V antigen 2C12.4 scFv and the anti-digoxin 26.10 scFv were cloned into pAPEx1 and pFLAG-APEx via the non-compatible SfiI restriction sites; *E. coli* Jude-1 transformed with the respective ligation products were used as controls for flow cytometry experiments (59). Purified recombinant V antigen was conjugated to BODIPY® using 6-((4,4-difluoro-5,7-dimethyl-4-bora-3a,4a-diaza-s-indacene-3-propionyl)amino)hexanoic acid succinimidyl ester (Invitrogen, Carlsbad, CA) at a molar ratio of 1:5 as described by the manufacturer. Free BODIPY FL-X SE was removed using a NAP-10 gel filtration column as described by the manufacturer (GE Healthcare, Uppsala, Sweden). The extent of conjugation was determined based on the ratio of A_{280} and A_{504} measured using a NanoDrop^{TM} 1000 and the appropriate extinction coefficients and correction factors as recommended by the manufacturer (Invitrogen, Carlsbad, CA; http://www.scripps.edu/~cdputnam/protcalc.html, Putnam Lab at The Scripps Research Institute, La Jolla, CA).

The anti-V antigen 2C12.4 scFv was subjected to random mutagenesis by error-prone PCR (50), the amplified DNA was cloned into pFLAG-APEx via the non-compatible SfiI restriction sites, and the ligation product was transformed into electrocompetent *E. coli* Jude-1 (59). Cells were cultured on agar plates containing LB medium + 2% glc + 30 μg/ml chloramphenicol (Cm30) (22 h, 25 ºC). Cells were transferred to LB medium + 2% glc + 15% glycerol (v/v) to A_{600} ~10 then stored at -80 ºC. Frozen cell stocks were thawed on ice and subcultured to A_{600} 0.1 in TB medium + 2% glc + Cm30 at 37 ºC, grown to A_{600} ~0.8-1.2, cooled for 30 min to 25 ºC, and protein expression was induced with the addition of 1mM IPTG. After 4h induction at 25 ºC, 1 ml of cells at A_{600} 5.0 were converted to spheroplasts using Tris/Sucrose/EDTA/lysozyme as previously described (59, 107). The spheroplasted cells

were first labeled with 5 μg/ml PhycoLink® anti-Flag® R-Phycoerythrin (anti-Flag PE) (Prozyme, San Leandro, CA) in PBS supplemented with 1% BSA (PBSB) (30 min, 150 rpm, 25 ºC). The spheroplasts were washed with PBSB and labeled with 500 nM V antigen conjugated to BODIPY (V antigen-BODIPY) in PBSB (1 h, 150 rpm, 25 ºC). Labeled spheroplasts were washed with PBSB and analyzed on a FACSAria (Becton Dickinson Biosciences, San Jose, CA) droplet deflection flow cytometer by exciting with a 488-nm laser and measuring the fluorescence emission spectrum of BODIPY and PE with 530/40 and 570/40 band-pass filters, respectively. Fluorescence compensation was performed using the APEx controls as previously described (107). The library population was gated to avoid aggregates as determined by the forward scatter (FSC) and side scatter (SSC) parameters, and the brightest 1-2% of the population based on both the BODIPY and PE emission spectrums was collected (59, 107). The collected spheroplasts were immediately resorted, and the scFv genes in the resort solution were by amplified by PCR using primers BRH06 (5'-GCGGATAACAATTTCACACAGG-3') and AHX89 (5'-CGCAGTAGCGGTAAACGGC-3') (59). The amplified DNA was cloned into pFLAG-APEx via the non-compatible SfiI restriction sites, and the ligation mixture was transformed into electrocompetent *E. coli* Jude-1. At least 10-fold excess of colonies relative to the number of events in the resort were obtained. Colonies were scraped from the agar plates into liquid media as above and subjected to an additional two rounds of sorting exactly as described above.

The scFv genes from the third round of sorting were subcloned into pMoPac16, and the ligation product was transformed into *E. coli* Jude-1 for expression of soluble scAb similar to above (59). In addition, *E. coli* Jude-1 containing pMoPac16 encoding 2C12.4 scAb was streaked from a frozen stock onto an agar plate containing LB medium + 2% glc + Amp200. Further, the anti-digoxin 26.10 scFv was cloned into pMoPac16 via

the non-compatible SfiI restriction sites, and the ligation product was transformed into *E. coli* Jude-1. 72 individual colonies from round III, 8 colonies of 2C12.4 scAb and 4 colonies of 26.10 scAb were picked and cultured overnight in sterile Costar® round bottom 96-well microtiter plates (Corning, Corning, NY) containing 200 µl of TB medium + 2% glc + Amp200 on a microtiter plate shaker. After overnight growth (150 rpm, 30 ºC), 4 µl aliquots were transferred to a master microtiter plate containing 156 µl of TB medium + 2% glc + Amp200, cultured on a plate shaker (8 h, 150 rpm, 30 ºC) and stored at 4 ºC for up to two weeks. The remaining cells were pelleted by centrifugation (10 min at 4,600 X g, 4 ºC) and resuspended in 200 µl of TB medium + Amp200 + 1 mM IPTG to induce protein expression. After 4 h induction at 25 ºC, cells were pelleted by centrifugation (10 min at 4,600 X g, 4 ºC), the cell pellet was resuspended in 1 ml of lysis buffer for 30 min at 25 ºC, and the insoluble fraction was removed by centrifugation (20 min at 4,600 X g, 4 ºC). The soluble fraction was further clarified using 96-well MultiScreen® HTS NA clearing filter plates (Millipore, Billerica, MA) as described by the manufacturer. Filtered lysates were transferred to Costar® non-binding 96-well plates (Corning, Corning, NY) and covered with microplate foil (GE Healthcare, Uppsala, Sweden). Relative expression levels of scAbs in filtered lysate were obtained using a Minifold® I Dot Blot System (Whatman, GE Healthcare, Uppsala, Sweden) by transferring 10 µl of filtered lysate diluted with 90 µl of PBS to a nitrocellulose membrane following the manufacturer guidelines. Western blot analysis of the nitrocellulose membrane was performed with anti-His HRP conjugate as previously described (132). The scAbs in filtered lysate were analyzed by SPR as described below.

Surface Plasmon resonance (SPR)

The scAbs in filtered lysate were analyzed via SPR using a Biacore^{TM} 3000 (GE Healthcare, Uppsala, Sweden) to obtain accurate dissociation rate constants of the scAb:V antigen complexes. Approximately 200 response units (RU) of V antigen in 10 mM sodium acetate, pH 5.0 were coupled to a CM5 chip (GE Healthcare, Uppsala, Sweden) by using 1-ethyl-3-(3-dimethylaminopropyl) carbodiimide/*N*-hydroxy succinimide chemistry. BSA was similarly coupled to the chip and used for in-line subtraction. Kinetic analysis was performed in HBS-P (GE Healthcare, Uppsala, Sweden) at a flow rate of 25 μl/min at 25 ºC unless indicated. Samples were injected for 3 min and dissociation was monitored for 5 min. The surface was regenerated with two 12 sec injections of 50 mM phosphoric acid. The antigen binding kinetics of purified monomeric scAb were determined in HBS-P at a flow rate of 50 μl/min. Samples were injected for 2 min and dissociation was monitored for 10 min. The surface was regenerated with two 12 sec injections of 50 mM phosphoric acid. Four 2-fold dilutions of each antibody beginning at 160 nM were performed in triplicate, double referenced with a blank, and globally fit to a 1:1 Langmuir binding model for the calculation of both k_{of} and k_{off} using BIAevaluation software (GE Healthcare, Uppsala, Sweden) (116).

Ad vectors

AdαV is a replication-defective human adenovirus (Ad) serotype 5, $E1^{-}E3^{-}$ gene transfer vector constructed to direct the expression of the heavy and light chains of the anti-V antigen monoclonal antibody 2C12.4 from a single promoter (149). The expression cassette contains (5' to 3') the cytomegalovirus (CMV) immediate early promoter/enhancer, the antibody IgG2b heavy chain gene, a 4 amino acid furin cleavage site, the 24 amino acid self-cleaving 2A peptide, the kappa light chain gene, and the

simian virus (SV) 40 polyadenylation signal. AdαV.H8 was constructed by assembling the genes encoding the variable heavy chain (V_H) and variable light chain (V_K) domains of the high affinity anti-V antigen 2C12.4 variant, H8, by overlap PCR using the AdαV IgG2b expression cassette as a template and the resulting fragment was used to replace the 2C12.4 coding sequence in AdαV. AdαPA is a similarly constructed gene transfer vector encoding an unrelated antibody (14B7-1H) against *Bacillus anthracis* protective antigen (PA) and was used as a negative control (40). AdαV, AdαV.H8, and AdαPA were produced in human embryonic kidney 293 cells (American Type Culture Collection, Manassas, VA) and purified by centrifugation twice through a CsCl gradient as described (137). The titer of each recombinant Ad preparation was determined spectrophotometrically and expressed as particle units (pu) as described (114).

Assessment of AdαV *in vivo*

Male C57BL/6 mice (n=5/group) (The Jackson Laboratory, Bar Harbor, ME) were housed under specific-pathogen-free conditions and used at 6 to 8 weeks of age. Mice were administered AdαV or AdαV.H8 (109, 1010, or 1011 pu) via the intravenous route. Naïve mice or mice injected with AdαPA (1011 pu) were used as negative controls. Ad vectors were diluted with saline to the specified dose. Serum was collected via the tail vein three days following vector administration, centrifuged at 8000x g for 20 min, and stored at -20 °C. Anti-V antigen serum titers were assessed by ELISA using flat bottomed 96-well EIA/RIA plates (Corning, New York, NY) coated with 100 µl 5 µg/ml recombinant V antigen in 0.05 M carbonate buffer, pH 7.4 overnight at 4 °C. The plates were washed with PBS containing 0.05% Tween-20 (PBST) and blocked with 400 µl PBS supplemented with 5% milk for 1 hr at 23 °C. Serial serum dilutions were added to each well and incubated for 1 hr at 23°C. The plates were washed four times with PBST,

immunocomplexes were detected using a sheep anti-mouse IgG HRP conjugate (Sigma, St. Louis, MO) applied at a 1:10,000 dilution in PBS supplemented with 1% milk incubated for 1 hr at 23 °C. The plates were washed four times with PBST and once with PBS, developed using 100 µl of peroxidase substrate (Bio-Rad, Hercules, CA) incubated for 15 min at 23 °C, and the reaction quenched by the addition of 100 µl 2% oxalic acid. The A415 was measured with a microplate reader (Bio-Rad, Hercules, CA). Antibody titers were calculated based on log(optical density)-log(dilution) normalized with purified anti-V antigen antibodies to account for affinity differences. Mice challenge studies were conducted at The Public Health Research Institute (PHRI) at the International Center for Public Health (Newark, NJ) under biosafety level 3 (BSL3) conditions. Y. pestis CO92 was grown aerobically in Heart Infusion Broth (Becton Dickinson DifcoTM, Sparks, MD) at 30 °C and diluted in saline solution for a challenge dose of 2 x 104 cfu which corresponds to 363 LD50. Twenty-five µl of bacterial suspension was used for intranasal infection of mice; bacterial dose was controlled by plating on Yersinia Selective Agar (YSA) (Oxoid, Hampshire, UK) and counting colonies for cfu determination. Survival was monitored daily for 14 days.

Statistical analysis

The data are presented as mean ± standard error of the mean. Statistical analyses were performed using the non-paired two-tailed Student's t-test, assuming equal variance. Survival evaluation was carried out using Kaplan-Meier analysis. Statistical significance was determined at $p<0.1$.

ACKNOWLEDGEMENTS

I would like to acknowledge our collaborators Julie Boyer, Ron Crystal, and Carolina Sofer-Podesta from the Weill Cornell Medical College, New York, New York for initiating this collaboration and conducting the *in vivo* experiments. I would also like to thank Mridula Rani for generating the sequencing encoding the glycine-serine linker for the antibody fragments.

Chapter 5.

Conclusions and Future Directions

CONCLUSIONS

This dissertation describes the implementation of a novel combinatorial library screening technology for the discovery and engineering of antibodies with unique binding properties. The anchored periplasmic expression (APEx) technology, as it is known, relies on anchoring antibody fragments onto the periplasmic side of the inner membrane of *E. coli* via fusion to either a transmembrane domain of an integral membrane protein or to the signal peptide and the first few N-terminal amino acids of an inner membrane lipoprotein, such as NlpA (59, 79). For the detection and subsequent isolation of antigen specific antibody fragments, the cells are converted to spheroplasts in order to disrupt the outer membrane and peptidoglycan layer, incubated with a fluorescently labeled antigen, and isolated by fluorescence activated cell sorting (FACS) based on high fluorescence. The APEx technology is also amenable for the isolation of full-length antibodies which assemble in the periplasm into aglycosylated IgGs that are fully functional for antigen binding and are non-covalently captured onto the inner membrane by an IgG binding protein co-expressed using APEx (106).

The limitations and relative merits of using different antibody formats in the combinatorial libraries by APEx was examined. The diversity of antibody binding sites obtained when the same library of V_H and V_L domains from an immunized animal was formatted as either an IgG or as a scFv was compared (Chapter 2). The two libraries were screened by APEx using similar cell labeling and FACS conditions, and a small panel of

antibodies specific for the Protective Antigen (PA) component from *Bacillus anthracis*, the causative agent of anthrax, were isolated. Overall, IgG display resulted in the isolation of a broader panel of V_H and V_L domain sequences exhibiting a wide range of affinities (K_D=21-440 nM), although, a binding site with a slightly higher affinity (K_D=6 nM) was isolated from the scFv library. Notably, several V domains isolated as IgGs displayed substantially reduced affinity when expressed as antibody fragments, which explains why they were not recovered from the scFv library. The results indicate that the antibody format used during *in vitro* selection affects which antibody variable domains can be isolated during screening. Therefore, the format required for the final application of the antibody is the preferred format for library generation and screening.

Several modifications of the APEx methodology were developed to allow for more efficient recovery of antibodies with desired properties (Chapter 3). Specifically, the system was reengineered to simultaneously account for antibody binding and expression levels by incorporating a C-terminal epitope peptide. The C-terminal epitope is recognized by a fluorescently labeled antibody for the detection of protein expression. This system, referred to as FLAG-APEx, was used to examine the effects of converting *E. coli* to spheroplasts and led to the development of optimal FACS settings. The combination of simultaneous detection of antibody binding and expression levels coupled with optimized FACS settings was shown to enable the isolation of antigen specific antibodies in a more efficient manner. Furthermore, additional strategies for protein display in *E. coli* were discovered (Chapter 3). Particularly, soluble proteins expressed in the periplasm of *E. coli* were found to be retained following conversion to spheroplasts. The degree to which soluble proteins were retained by spheroplasts was roughly proportional to their molecular weight. The lack of an anchoring motif resulted in a slight decrease in fluorescence, but nonetheless, the cell fluorescence was significantly higher

than background. Since an anchoring domain is not required, this approach enables more complex proteins consisting of multiple polypeptides to be "displayed" and engineered through library screening by FACS.

The FLAG-APEx system, coupled with the optimized FACS settings, was used to increase the affinity of an antibody by 35-fold resulting in a K_D of 100 pM following a single round of mutagenesis and three rounds of FACS (Chapter 4). Since clonal analysis following screening often represents the rate limiting step in antibody affinity maturation, this process was significantly expedited by rank-ordering clones isolated from the last round of FACS by comparing the dissociation rate constants of antibody fragments in crude lysates using surface Plasmon resonance (SPR). While it is well established that for many exogenous neutralizing antibodies increased antigen affinity correlates with protection (5, 101, 105, 162), the effect of antigen affinity on antibodies produced *in situ* following adenoviral gene transfer has not been examined. The variable domains from an affinity matured antibody (KD 100 pM) specific for the V antigen of *Yersinia pestis*, the etiological agent of the plague, and those variable domains from the antibody from which it was derived (K_D=3.5 nM) were formatted as mouse IgG2 antibodies in separate adenovirus gene delivery vectors. Genetic immunization of mice with these adenoviral vectors resulted in similar mouse serum titers of anti-V antigen antibodies 3 days post-immunization. Notably, the higher affinity antibody conferred increased protection against intranasal challenge with a 363 LD_{50} of *Y. pestis*. These results indicate that the affinity maturation of a neutralizing antibody delivered by genetic transfer may confer increased protection not only for *Y. pestis* challenge, but possibly for other pathogens.

In summary, in these studies we employed the APEx system for a variety of purposes: (*i*) antibody affinity maturation (59, 60) (Chapter 4), and antibody discovery applications (Chapter 2), (*ii*) to demonstrate that the antibody format used during *in vitro*

selection affects which antibody variable domains can be isolated during screening (Chapter 2). (*iii*) The system was modified to increase the isolation efficiency of antigen specific antibodies expressed in *E. coli* (Chapter 3).

FUTURE DIRECTIONS

The APEx system is a versatile display technology for antibody discovery and engineering applications. The work presented provides an additional example of how APEx can be used to isolate high affinity antibody variants following a single round of mutagenesis and a few round of FACS (59, 60). The simultaneous detection of antigen binding and antibody expression levels provides additional control during screening and enables efficient isolation of antibodies with desirable characteristics. This approach should be considered the preferred methodology for future library screening by FACS.

Further, the incorporation of SPR and small scale antibody expression without purification expedites the antibody discovery process following screening by FACS and should be used during future affinity maturation applications. This approach is superior to the analysis of individual clones by enzyme-linked immunosorbent assay (ELISA), which is the standard approach for characterizing clones isolated from screening. SPR facilitates the determination of accurate dissociation rate constants independent of protein expression levels, which is difficult to do via ELISA and is critical in order to isolate the highest affinity clones. This SPR approach was used again to identify an antibody toward the receptor binding domain of the SAR coronavirus exhibiting a 200-fold affinity improvement following FACS.

The improved *in vivo* neutralization potency of the highest affinity anti-V antigen antibody, H8, was shown to be approximately 10-fold higher than that of the antibody from which it was derived. A detailed analysis of the affinity contributions of

each amino acid mutation should be undertaken to eliminate mutations that do not contribute to the enhanced affinity and may decrease specificity.

APEx should continue to be used as a discovery platform for antibodies generated from immune libraries, and the antibody format used should be dictated by the final application of the antibody. For example, APEx is currently being used to isolate antibody fragments toward the complement protein C1s from immune libraries for use in inflammatory diseases. Antibody fragments, which lack the Fc region, are sought after since antibody mediated effector function through the Fc region can lead to an increase in inflammation, which is opposite of the desired therapeutic effect. APEx is also being used to isolate full-length antibodies toward the luteinizing hormone receptor for use in cancer therapy since the Fc mediated effector functions are desirable in this instance.

The ability to screen large naïve and synthetic libraries using APEx are currently under development as well. These approaches rely on APEx coupled with magnetic activated cell sorting (MACS) or phage display in order to downsize libraries containing more than 10^8 individual members, which are difficult to screen by FACS due to equipment limitations. Following downsizing, the power of FACS can be used for quantitative multi-parameter analysis to fine-tune which antibodies are selected for further screening and analysis. These alternative approaches will increase the application range of APEx.

Author's Publications

Van Blarcom T, Carroll S, Mazor Y, Kontos S, Iverson B, Georgiou G. (2009). A comparison of IgG and antibody fragments isolated by library screening. *Protein Engineering Design and Selection* (in preparation).

Van Blarcom T, Sofer-Podesta C, Crystal RG, Georgiou G, Boyer JL. (2009). Genetic delivery of an affinity matured anti-V antigen antibody provides increased protection against a lethal *Yersinia pestis* challenge. *Molecular Therapy* (in preparation).

Mazor Y, **Van Blarcom T**, Carroll S, Georgiou G. (2009). Selection of Full-Length IgG Antibodies by Tandem Display on *Filamentous* Phage and *E. coli* FACS Screening. *FEBS Journal* (submitted).

Van Blarcom T, Harvey BR. (2009). Bacterial Display. In *Therapeutic Antibodies: from Theory to Practice* (An Z, Strohl W, ed.), John Wiley & Sons Inc. (in press).

Mazor Y, **Van Blarcom T**, Iverson BL, Georgiou, G. (2009). Isolation of Full-Length IgG Antibodies from Combinatorial Libraries Expressed in *Escherichia coli*. In *Methods in Molecular Biology*, *Therapeutic Antibodies Methods and Protocols* (Dimitrov DS, Marks JD, ed.), Vol. 525. Humana Press.

Mazor Y, **Van Blarcom T**, Iverson BL, Georgiou G. (2008). E-clonal Antibodies: Selection of Full-Length IgG Antibodies using Bacterial Periplasmic Display. *Nature Protocols* **3**(11), 1766-1777.

Mazor Y, **Van Blarcom T**, Mabry R, Iverson BL, Georgiou G. (2007). Isolation of engineered, full-length antibodies from libraries expressed in Escherichia coli. *Nature Biotechnology* **25**(5), 563-565.

Ribnicky B, **Van Blarcom T**, Georgiou G. (2007). A scFv antibody mutant isolated in a genetic screen for improved export via the twin arginine transporter pathway exhibits faster folding. *Journal of Molecular Biology* **369**(3), 631-639.

References

1. **Ackerman, M., D. Levary, G. Tobon, B. Hackel, K. D. Orcutt, and K. D. Wittrup.** 2009. Highly avid magnetic bead capture: An efficient selection method for de novo protein engineering utilizing yeast surface display. Biotechnol Prog.
2. **Akamatsu, Y., K. Pakabunto, Z. Xu, Y. Zhang, and N. Tsurushita.** 2007. Whole IgG surface display on mammalian cells: Application to isolation of neutralizing chicken monoclonal anti-IL-12 antibodies. J Immunol Methods.
3. **Bae, W., W. Chen, A. Mulchandani, and R. K. Mehra.** 2000. Enhanced bioaccumulation of heavy metals by bacterial cells displaying synthetic phytochelatins. Biotechnol Bioeng **70:**518-524.
4. **Bae, W., R. K. Mehra, A. Mulchandani, and W. Chen.** 2001. Genetic engineering of Escherichia coli for enhanced uptake and bioaccumulation of mercury. Appl Environ Microbiol **67:**5335-5338.
5. **Barbas, C. F., 3rd, D. Hu, N. Dunlop, L. Sawyer, D. Cababa, R. M. Hendry, P. L. Nara, and D. R. Burton.** 1994. In vitro evolution of a neutralizing human antibody to human immunodeficiency virus type 1 to enhance affinity and broaden strain cross-reactivity. Proc Natl Acad Sci U S A **91:**3809-3813.
6. **Barbas, C. F., 3rd, A. S. Kang, R. A. Lerner, and S. J. Benkovic.** 1991. Assembly of combinatorial antibody libraries on phage surfaces: the gene III site. Proc Natl Acad Sci U S A **88:**7978-7982.
7. **Becerril, B., M. A. Poul, and J. D. Marks.** 1999. Toward selection of internalizing antibodies from phage libraries. Biochem Biophys Res Commun **255:**386-393.
8. **Beerli, R. R., M. Bauer, R. B. Buser, M. Gwerder, S. Muntwiler, P. Maurer, P. Saudan, and M. F. Bachmann.** 2008. Isolation of human monoclonal antibodies by mammalian cell display. Proc Natl Acad Sci U S A **105:**14336-14341.
9. **BenAmmar-Ceccoli, S., S. Humblot, R. Crouzier, B. Acres, M. P. Kieny, D. Herlyn, J. L. Pasquali, and T. Martin.** 2001. Recombinant vaccinia viruses expressing immunoglobulin variable regions efficiently and selectively protect mice against tumoral B-cell growth. Cancer Gene Ther **8:**815-826.
10. **Benhar, I.** 2007. Design of synthetic antibody libraries. Expert Opin Biol Ther **7:**763-779.
11. **Bereta, M., A. Hayhurst, M. Gajda, P. Chorobik, M. Targosz, J. Marcinkiewicz, and H. L. Kaufman.** 2007. Improving tumor targeting and therapeutic potential of Salmonella VNP20009 by displaying cell surface CEA-specific antibodies. Vaccine **25:**4183-4192.
12. **Berghman, L. R., D. Abi-Ghanem, S. D. Waghela, and S. C. Ricke.** 2005. Antibodies: an alternative for antibiotics? Poult Sci **84:**660-666.

13. **Bird, R. E., K. D. Hardman, J. W. Jacobson, S. Johnson, B. M. Kaufman, S. M. Lee, T. Lee, S. H. Pope, G. S. Riordan, and M. Whitlow.** 1988. Single-chain antigen-binding proteins. Science **242:**423-426.
14. **Birdsell, D. C., and E. H. Cota-Robles.** 1967. Production and ultrastructure of lysozyme and ethylenediaminetetraacetate-lysozyme spheroplasts of Escherichia coli. J Bacteriol **93:**427-437.
15. **Birtalan, S., Y. Zhang, F. A. Fellouse, L. Shao, G. Schaefer, and S. S. Sidhu.** 2008. The intrinsic contributions of tyrosine, serine, glycine and arginine to the affinity and specificity of antibodies. J Mol Biol **377:**1518-1528.
16. **Boder, E. T., K. S. Midelfort, and K. D. Wittrup.** 2000. Directed evolution of antibody fragments with monovalent femtomolar antigen-binding affinity. Proc Natl Acad Sci U S A **97:**10701-10705.
17. **Boder, E. T., and K. D. Wittrup.** 1997. Yeast surface display for screening combinatorial polypeptide libraries. Nat Biotechnol **15:**553-557.
18. **Boyer, J. L., G. Kobinger, J. M. Wilson, and R. G. Crystal.** 2005. Adenovirus-based genetic vaccines for biodefense. Hum Gene Ther **16:**157-168.
19. **Bradbury, A. R., and J. D. Marks.** 2004. Antibodies from phage antibody libraries. Journal of immunological methods **290:**29-49.
20. **Brey, R. N.** 2005. Molecular basis for improved anthrax vaccines. Adv Drug Deliv Rev **57:**1266-1292.
21. **Brouqui, P., and D. Raoult.** 2006. Arthropod-borne diseases in homeless. Ann N Y Acad Sci **1078:**223-235.
22. **Burnett, M. S., N. Wang, M. Hofmann, and G. Barrie Kitto.** 2000. Potential live vaccines for HIV. Vaccine **19:**735-742.
23. **Bussel, J. B., L. Giulino, S. Lee, V. L. Patel, C. Sandborg, and E. R. Stiehm.** 2007. Update on therapeutic monoclonal antibodies. Curr Probl Pediatr Adolesc Health Care **37:**118-135.
24. **Carter, P. J.** 2006. Potent antibody therapeutics by design. Nat Rev Immunol **6:**343-357.
25. **Casadevall, A., and M. D. Scharff.** 1994. Serum therapy revisited: animal models of infection and development of passive antibody therapy. Antimicrob Agents Chemother **38:**1695-1702.
26. **Chao, G., W. L. Lau, B. J. Hackel, S. L. Sazinsky, S. M. Lippow, and K. D. Wittrup.** 2006. Isolating and engineering human antibodies using yeast surface display. Nat Protoc **1:**755-768.
27. **Charbit, A., J. C. Boulain, A. Ryter, and M. Hofnung.** 1986. Probing the topology of a bacterial membrane protein by genetic insertion of a foreign epitope; expression at the cell surface. Embo J **5:**3029-3037.
28. **Chen, G., J. Cloud, G. Georgiou, and B. L. Iverson.** 1996. A quantitative immunoassay utilizing Escherichia coli cells possessing surface-expressed single chain Fv molecules. Biotechnol Prog **12:**572-574.
29. **Chen, G., A. Hayhurst, J. G. Thomas, B. R. Harvey, B. L. Iverson, and G. Georgiou.** 2001. Isolation of high-affinity ligand-binding proteins by periplasmic expression with cytometric screening (PECS). Nat Biotechnol **19:**537-542.

30. **Chen, W., and G. Georgiou.** 2002. Cell-Surface display of heterologous proteins: From high-throughput screening to environmental applications. Biotechnol Bioeng **79:**496-503.
31. **Chung, C. H.** 2008. Managing premedications and the risk for reactions to infusional monoclonal antibody therapy. Oncologist **13:**725-732.
32. **Cole, S. T., I. Sonntag, and U. Henning.** 1982. Cloning and expression in Escherichia coli K-12 of the genes for major outer membrane protein OmpA from Shigella dysenteriae, Enterobacter aerogenes, and Serratia marcescens. J Bacteriol **149:**145-150.
33. **Cooper, H. M., and Y. Paterson.** 2001. Production of polyclonal antisera. Curr Protoc Immunol **Chapter 2:**Unit 2 4.
34. **Curnow, P., P. H. Bessette, D. Kisailus, M. M. Murr, P. S. Daugherty, and D. E. Morse.** 2005. Enzymatic synthesis of layered titanium phosphates at low temperature and neutral pH by cell-surface display of silicatein-alpha. J Am Chem Soc **127:**15749-15755.
35. **Daugherty, A. L., and R. J. Mrsny.** 2006. Formulation and delivery issues for monoclonal antibody therapeutics. Adv Drug Deliv Rev **58:**686-706.
36. **Daugherty, P. S., G. Chen, B. L. Iverson, and G. Georgiou.** 2000. Quantitative analysis of the effect of the mutation frequency on the affinity maturation of single chain Fv antibodies. Proc Natl Acad Sci U S A **97:**2029-2034.
37. **Daugherty, P. S., G. Chen, M. J. Olsen, B. L. Iverson, and G. Georgiou.** 1998. Antibody affinity maturation using bacterial surface display. Protein Eng **11:**825-832.
38. **Daugherty, P. S., B. L. Iverson, and G. Georgiou.** 2000. Flow cytometric screening of cell-based libraries. J Immunol Methods **243:**211-227.
39. **Daugherty, P. S., M. J. Olsen, B. L. Iverson, and G. Georgiou.** 1999. Development of an optimized expression system for the screening of antibody libraries displayed on the Escherichia coli surface. Protein Eng **12:**613-621.
40. **De, B. P., N. R. Hackett, R. G. Crystal, and J. L. Boyer.** 2008. Rapid/sustained anti-anthrax passive immunity mediated by co-administration of Ad/AAV. Mol Ther **16:**203-209.
41. **Dessain, S. K., S. P. Adekar, J. B. Stevens, K. A. Carpenter, M. L. Skorski, B. L. Barnoski, R. A. Goldsby, and R. A. Weinberg.** 2004. High efficiency creation of human monoclonal antibody-producing hybridomas. J Immunol Methods **291:**109-122.
42. **Dufner, P., L. Jermutus, and R. R. Minter.** 2006. Harnessing phage and ribosome display for antibody optimisation. Trends Biotechnol **24:**523-529.
43. **Earhart, C. F.** 2000. Use of an Lpp-OmpA fusion vehicle for bacterial surface display. Methods Enzymol **326:**506-516.
44. **Fang, J., J. J. Qian, S. Yi, T. C. Harding, G. H. Tu, M. VanRoey, and K. Jooss.** 2005. Stable antibody expression at therapeutic levels using the 2A peptide. Nat Biotechnol **23:**584-590.
45. **Foote, J., and H. N. Eisen.** 1995. Kinetic and affinity limits on antibodies produced during immune responses. Proc Natl Acad Sci U S A **92:**1254-1256.

46. **Francisco, J. A., R. Campbell, B. L. Iverson, and G. Georgiou.** 1993. Production and fluorescence-activated cell sorting of Escherichia coli expressing a functional antibody fragment on the external surface. Proc Natl Acad Sci U S A **90:**10444-10448.
47. **Francisco, J. A., C. F. Earhart, and G. Georgiou.** 1992. Transport and anchoring of beta-lactamase to the external surface of Escherichia coli. Proc Natl Acad Sci U S A **89:**2713-2717.
48. **Francisco, J. A., C. Stathopoulos, R. A. Warren, D. G. Kilburn, and G. Georgiou.** 1993. Specific adhesion and hydrolysis of cellulose by intact Escherichia coli expressing surface anchored cellulase or cellulose binding domains. Biotechnology (N Y) **11:**491-495.
49. **Freudl, R., S. MacIntyre, M. Degen, and U. Henning.** 1986. Cell surface exposure of the outer membrane protein OmpA of Escherichia coli K-12. J Mol Biol **188:**491-494.
50. **Fromant, M., S. Blanquet, and P. Plateau.** 1995. Direct random mutagenesis of gene-sized DNA fragments using polymerase chain reaction. Anal Biochem **224:**347-353.
51. **Gao, C., S. Mao, H. J. Ditzel, L. Farnaes, P. Wirsching, R. A. Lerner, and K. D. Janda.** 2002. A cell-penetrating peptide from a novel pVII-pIX phage-displayed random peptide library. Bioorg Med Chem **10:**4057-4065.
52. **Gao, C., S. Mao, C. H. Lo, P. Wirsching, R. A. Lerner, and K. D. Janda.** 1999. Making artificial antibodies: a format for phage display of combinatorial heterodimeric arrays. Proc Natl Acad Sci U S A **96:**6025-6030.
53. **Georgiou, G., C. Stathopoulos, P. S. Daugherty, A. R. Nayak, B. L. Iverson, and R. Curtiss, 3rd.** 1997. Display of heterologous proteins on the surface of microorganisms: from the screening of combinatorial libraries to live recombinant vaccines. Nat Biotechnol **15:**29-34.
54. **Georgiou, G., D. L. Stephens, C. Stathopoulos, H. L. Poetschke, J. Mendenhall, and C. F. Earhart.** 1996. Display of beta-lactamase on the Escherichia coli surface: outer membrane phenotypes conferred by Lpp'-OmpA'-beta-lactamase fusions. Protein Eng **9:**239-247.
55. **Ghrayeb, J., and M. Inouye.** 1984. Nine amino acid residues at the NH2-terminal of lipoprotein are sufficient for its modification, processing, and localization in the outer membrane of Escherichia coli. J Biol Chem **259:**463-467.
56. **Goldsby, R. A., T. J. Kindt, B. A. Osborne, and J. Kuby.** 2003. Immunology, 5th ed. W. H. Freeman and Company, New York.
57. **Green, L. L., M. C. Hardy, C. E. Maynard-Currie, H. Tsuda, D. M. Louie, M. J. Mendez, H. Abderrahim, M. Noguchi, D. H. Smith, Y. Zeng, and et al.** 1994. Antigen-specific human monoclonal antibodies from mice engineered with human Ig heavy and light chain YACs. Nat Genet **7:**13-21.
58. **Hale, G.** 2006. Therapeutic antibodies--delivering the promise? Adv Drug Deliv Rev **58:**633-639.
59. **Harvey, B. R., G. Georgiou, A. Hayhurst, K. J. Jeong, B. L. Iverson, and G. K. Rogers.** 2004. Anchored periplasmic expression, a versatile technology for the

isolation of high-affinity antibodies from Escherichia coli-expressed libraries. Proc Natl Acad Sci U S A **101:**9193-9198.

60. **Harvey, B. R., A. B. Shanafelt, I. Baburina, R. Hui, S. Vitone, B. L. Iverson, and G. Georgiou.** 2006. Engineering of recombinant antibody fragments to methamphetamine by anchored periplasmic expression. J Immunol Methods **308:**43-52.
61. **Hashimoto, M., J. L. Boyer, N. R. Hackett, J. M. Wilson, and R. G. Crystal.** 2005. Induction of protective immunity to anthrax lethal toxin with a nonhuman primate adenovirus-based vaccine in the presence of preexisting anti-human adenovirus immunity. Infect Immun **73:**6885-6891.
62. **Hayhurst, A.** 2000. Improved expression characteristics of single-chain Fv fragments when fused downstream of the Escherichia coli maltose-binding protein or upstream of a single immunoglobulin-constant domain. Protein Expr Purif **18:**1-10.
63. **Hayhurst, A., and G. Georgiou.** 2001. High-throughput antibody isolation. Curr Opin Chem Biol **5:**683-689.
64. **Hayhurst, A., S. Happe, R. Mabry, Z. Koch, B. L. Iverson, and G. Georgiou.** 2003. Isolation and expression of recombinant antibody fragments to the biological warfare pathogen Brucella melitensis. J Immunol Methods **276:**185-196.
65. **Hayhurst, A., S. Happe, R. Mabry, Z. Koch, B. L. Iverson, and G. Georgiou.** 2003. Isolation and expression of recombinant antibody fragments to the biological warfare pathogen Brucella melitensis. Journal of Immunological Methods **276:**185-196.
66. **Heppel, L. A.** 1967. Selective release of enzymes from bacteria. Science **156:**1451-1455.
67. **Hill, J., C. Copse, S. Leary, A. J. Stagg, E. D. Williamson, and R. W. Titball.** 2003. Synergistic protection of mice against plague with monoclonal antibodies specific for the F1 and V antigens of Yersinia pestis. Infect Immun **71:**2234-2238.
68. **Hill, J., J. E. Eyles, S. J. Elvin, G. D. Healey, R. A. Lukaszewski, and R. W. Titball.** 2006. Administration of antibody to the lung protects mice against pneumonic plague. Infect Immun **74:**3068-3070.
69. **Hill, J., S. E. Leary, K. F. Griffin, E. D. Williamson, and R. W. Titball.** 1997. Regions of Yersinia pestis V antigen that contribute to protection against plague identified by passive and active immunization. Infect Immun **65:**4476-4482.
70. **Holliger, P., and P. J. Hudson.** 2005. Engineered antibody fragments and the rise of single domains. Nat Biotechnol **23:**1126-1136.
71. **Hoogenboom, H. R.** 2002. Overview of antibody phage-display technology and its applications. Methods Mol Biol **178:**1-37.
72. **Hoogenboom, H. R.** 2005. Selecting and screening recombinant antibody libraries. Nat Biotechnol **23:**1105-1116.
73. **Hoogenboom, H. R., A. D. Griffiths, K. S. Johnson, D. J. Chiswell, P. Hudson, and G. Winter.** 1991. Multi-subunit proteins on the surface of filamentous phage: methodologies for displaying antibody (Fab) heavy and light chains. Nucleic Acids Res **19:**4133-4137.

74. **Hoover, D. M., and J. Lubkowski.** 2002. DNAWorks: an automated method for designing oligonucleotides for PCR-based gene synthesis. Nucleic Acids Res **30:**e43.
75. **Hudson, P. J., and C. Souriau.** 2003. Engineered antibodies. Nat Med **9:**129-134.
76. **Jackson, A. M., J. Boutell, N. Cooley, and M. He.** 2004. Cell-free protein synthesis for proteomics. Brief Funct Genomic Proteomic **2:**308-319.
77. **Jakobovits, A., R. G. Amado, X. Yang, L. Roskos, and G. Schwab.** 2007. From XenoMouse technology to panitumumab, the first fully human antibody product from transgenic mice. Nat Biotechnol **25:**1134-1143.
78. **Jensen, K. B., M. Larsen, J. S. Pedersen, P. A. Christensen, L. Alvarez-Vallina, S. Goletz, B. F. Clark, and P. Kristensen.** 2002. Functional improvement of antibody fragments using a novel phage coat protein III fusion system. Biochem Biophys Res Commun **298:**566-573.
79. **Jeong, K. J., Y. Kawarasaki, J. Gam, B. R. Harvey, B. L. Iverson, and G. Georgiou.** 2004. A periplasmic fluorescent reporter protein and its application in high-throughput membrane protein topology analysis. Journal of Molecular Biology **341:**901-909.
80. **Jeong, K. J., M. J. Seo, B. L. Iverson, and G. Georgiou.** 2007. APEx 2-hybrid, a quantitative protein-protein interaction assay for antibody discovery and engineering. Proc Natl Acad Sci U S A **104:**8247-8252.
81. **Jespers, L. S., A. Roberts, S. M. Mahler, G. Winter, and H. R. Hoogenboom.** 1994. Guiding the selection of human antibodies from phage display repertoires to a single epitope of an antigen. Biotechnology (N Y) **12:**899-903.
82. **Jiang, M., W. Shi, Q. Zhang, X. Wang, M. Guo, Z. Cui, C. Su, Q. Yang, Y. Li, J. Sham, X. Liu, M. Wu, and Q. Qian.** 2006. Gene therapy using adenovirus-mediated full-length anti-HER-2 antibody for HER-2 overexpression cancers. Clin Cancer Res **12:**6179-6185.
83. **Joshi, A., R. Bauer, P. Kuebler, M. White, C. Leddy, P. Compton, M. Garovoy, P. Kwon, P. Walicke, and R. Dedrick.** 2006. An overview of the pharmacokinetics and pharmacodynamics of efalizumab: a monoclonal antibody approved for use in psoriasis. J Clin Pharmacol **46:**10-20.
84. **Karlsson, R.** 2004. SPR for molecular interaction analysis: a review of emerging application areas. J Mol Recognit **17:**151-161.
85. **Klein, U., and R. Dalla-Favera.** 2008. Germinal centres: role in B-cell physiology and malignancy. Nat Rev Immunol **8:**22-33.
86. **Kohler, G., and C. Milstein.** 1975. Continuous cultures of fused cells secreting antibody of predefined specificity. Nature **256:**495-497.
87. **Krebber, A., S. Bornhauser, J. Burmester, A. Honegger, J. Willuda, H. R. Bosshard, and A. Pluckthun.** 1997. Reliable cloning of functional antibody variable domains from hybridomas and spleen cell repertoires employing a reengineered phage display system. J Immunol Methods **201:**35-55.
88. **Le, H. V., and P. P. Trotta.** 1991. Purification of secreted recombinant proteins from Escherichia coli. Bioprocess Technol **12:**163-181.

89. **Leary, J. F.** 1994. Strategies for rare cell detection and isolation. Methods Cell Biol **42 Pt B:**331-358.
90. **Lee, C. V., S. S. Sidhu, and G. Fuh.** 2004. Bivalent antibody phage display mimics natural immunoglobulin. J Immunol Methods **284:**119-132.
91. **Lee, P. A., D. Tullman-Ercek, and G. Georgiou.** 2006. The bacterial twin-arginine translocation pathway. Annu Rev Microbiol **60:**373-395.
92. **Leysath, C. E., A. F. Monzingo, J. A. Maynard, J. Barnett, G. Georgiou, B. L. Iverson, and J. D. Robertus.** 2009. Crystal structure of the engineered neutralizing antibody M18 complexed to domain 4 of the anthrax protective antigen. J Mol Biol **387:**680-693.
93. **Link, A. J., K. J. Jeong, and G. Georgiou.** 2007. Beyond toothpicks: new methods for isolating mutant bacteria. Nat Rev Microbiol **5:**680-688.
94. **Little, S. F., S. H. Leppla, and E. Cora.** 1988. Production and characterization of monoclonal antibodies to the protective antigen component of Bacillus anthracis toxin. Infect Immun **56:**1807-1813.
95. **Lonberg, N.** 2005. Human antibodies from transgenic animals. Nat Biotechnol **23:**1117-1125.
96. **Lonberg, N., L. D. Taylor, F. A. Harding, M. Trounstine, K. M. Higgins, S. R. Schramm, C. C. Kuo, R. Mashayekh, K. Wymore, J. G. McCabe, and et al.** 1994. Antigen-specific human antibodies from mice comprising four distinct genetic modifications. Nature **368:**856-859.
97. **Low, N. M., P. H. Holliger, and G. Winter.** 1996. Mimicking somatic hypermutation: affinity maturation of antibodies displayed on bacteriophage using a bacterial mutator strain. J Mol Biol **260:**359-368.
98. **Mabry, R., M. Rani, R. Geiger, G. B. Hubbard, R. Carrion, Jr., K. Brasky, J. L. Patterson, G. Georgiou, and B. L. Iverson.** 2005. Passive protection against anthrax by using a high-affinity antitoxin antibody fragment lacking an Fc region. Infect Immun **73:**8362-8368.
99. **Maggon, K.** 2007. Monoclonal antibody "gold rush". Curr Med Chem **14:**1978-1987.
100. **Marasco, W. A., and J. Sui.** 2007. The growth and potential of human antiviral monoclonal antibody therapeutics. Nat Biotechnol **25:**1421-1434.
101. **Marks, J. D.** 2004. Deciphering antibody properties that lead to potent botulinum neurotoxin neutralization. Mov Disord **19 Suppl 8:**S101-108.
102. **Martin, A. C.** 1996. Accessing the Kabat antibody sequence database by computer. Proteins **25:**130-133.
103. **Mattanovich, D., and N. Borth.** 2006. Applications of cell sorting in biotechnology. Microb Cell Fact **5:**12.
104. **Maynard, J., and G. Georgiou.** 2000. Antibody engineering. Annu Rev Biomed Eng **2:**339-376.
105. **Maynard, J. A., C. B. Maassen, S. H. Leppla, K. Brasky, J. L. Patterson, B. L. Iverson, and G. Georgiou.** 2002. Protection against anthrax toxin by recombinant antibody fragments correlates with antigen affinity. Nat Biotechnol **20:**597-601.

106. **Mazor, Y., T. V. Blarcom, R. Mabry, B. L. Iverson, and G. Georgiou.** 2007. Isolation of engineered, full-length antibodies from libraries expressed in Escherichia coli. Nat Biotechnol **25:**563-565.
107. **Mazor, Y., T. Van Blarcom, B. L. Iverson, and G. Georgiou.** 2008. E-clonal antibodies: selection of full-length IgG antibodies using bacterial periplasmic display. Nat Protoc **3:**1766-1777.
108. **Mazor, Y., T. Van Blarcom, R. Mabry, B. L. Iverson, and G. Georgiou.** 2007. Isolation of engineered, full-length antibodies from libraries expressed in Escherichia coli. Nat Biotechnol **25:**563-565.
109. **McCafferty, J., A. D. Griffiths, G. Winter, and D. J. Chiswell.** 1990. Phage antibodies: filamentous phage displaying antibody variable domains. Nature **348:**552-554.
110. **McGregor, D. P., P. E. Molloy, C. Cunningham, and W. J. Harris.** 1994. Spontaneous assembly of bivalent single chain antibody fragments in Escherichia coli. Mol Immunol **31:**219-226.
111. **McHeyzer-Williams, M. G., G. J. Nossal, and P. A. Lalor.** 1991. Molecular characterization of single memory B cells. Nature **350:**502-505.
112. **Meselson, M., J. Guillemin, M. Hugh-Jones, A. Langmuir, I. Popova, A. Shelokov, and O. Yampolskaya.** 1994. The Sverdlovsk anthrax outbreak of 1979. Science **266:**1202-1208.
113. **Minshull, J., and W. P. Stemmer.** 1999. Protein evolution by molecular breeding. Curr Opin Chem Biol **3:**284-290.
114. **Mittereder, N., K. L. March, and B. C. Trapnell.** 1996. Evaluation of the concentration and bioactivity of adenovirus vectors for gene therapy. J Virol **70:**7498-7509.
115. **Mohamed, N., M. Clagett, J. Li, S. Jones, S. Pincus, G. D'Alia, L. Nardone, M. Babin, G. Spitalny, and L. Casey.** 2005. A high-affinity monoclonal antibody to anthrax protective antigen passively protects rabbits before and after aerosolized Bacillus anthracis spore challenge. Infect Immun **73:**795-802.
116. **Myszka, D. G.** 1999. Improving biosensor analysis. J Mol Recognit **12:**279-284.
117. **Newcombe, C., and A. R. Newcombe.** 2007. Antibody production: polyclonal-derived biotherapeutics. J Chromatogr B Analyt Technol Biomed Life Sci **848:**2-7.
118. **O'Connell, D., B. Becerril, A. Roy-Burman, M. Daws, and J. D. Marks.** 2002. Phage versus phagemid libraries for generation of human monoclonal antibodies. Journal of molecular biology **321:**49-56.
119. **Osbourn, J., M. Groves, and T. Vaughan.** 2005. From rodent reagents to human therapeutics using antibody guided selection. Methods **36:**61-68.
120. **Pepper, L. R., Y. K. Cho, E. T. Boder, and E. V. Shusta.** 2008. A decade of yeast surface display technology: where are we now? Comb Chem High Throughput Screen **11:**127-134.
121. **Perez, O. D., and G. P. Nolan.** 2002. Simultaneous measurement of multiple active kinase states using polychromatic flow cytometry. Nat Biotechnol **20:**155-162.

122. **Presta, L. G.** 2006. Engineering of therapeutic antibodies to minimize immunogenicity and optimize function. Adv Drug Deliv Rev **58:**640-656.
123. **Price, P. W., E. C. McKinney, Y. Wang, L. E. Sasser, M. K. Kandasamy, L. Matsuuchi, C. Milcarek, R. B. Deal, D. G. Culver, and R. B. Meagher.** 2009. Engineered cell surface expression of membrane immunoglobulin as a means to identify monoclonal antibody-secreting hybridomas. J Immunol Methods.
124. **Rada, C., S. K. Gupta, E. Gherardi, and C. Milstein.** 1991. Mutation and selection during the secondary response to 2-phenyloxazolone. Proc Natl Acad Sci U S A **88:**5508-5512.
125. **Rainey, G. J., and J. A. Young.** 2004. Antitoxins: novel strategies to target agents of bioterrorism. Nat Rev Microbiol **2:**721-726.
126. **Rajpal, A., N. Beyaz, L. Haber, G. Cappuccilli, H. Yee, R. R. Bhatt, T. Takeuchi, R. A. Lerner, and R. Crea.** 2005. A general method for greatly improving the affinity of antibodies by using combinatorial libraries. Proc Natl Acad Sci U S A **102:**8466-8471.
127. **Rathanaswami, P., S. Roalstad, L. Roskos, Q. J. Su, S. Lackie, and J. Babcook.** 2005. Demonstration of an in vivo generated sub-picomolar affinity fully human monoclonal antibody to interleukin-8. Biochem Biophys Res Commun **334:**1004-1013.
128. **Reason, D., J. Liberato, J. Sun, W. Keitel, and J. Zhou.** 2009. Frequency and domain specificity of toxin-neutralizing paratopes in the human antibody response to anthrax vaccine adsorbed. Infect Immun **77:**2030-2035.
129. **Reichert, J. M., C. J. Rosensweig, L. B. Faden, and M. C. Dewitz.** 2005. Monoclonal antibody successes in the clinic. Nat Biotechnol **23:**1073-1078.
130. **Reichert, J. M., and V. E. Valge-Archer.** 2007. Development trends for monoclonal antibody cancer therapeutics. Nat Rev Drug Discov **6:**349-356.
131. **Riano-Umbarila, L., V. R. Juarez-Gonzalez, T. Olamendi-Portugal, M. Ortiz-Leon, L. D. Possani, and B. Becerril.** 2005. A strategy for the generation of specific human antibodies by directed evolution and phage display. An example of a single-chain antibody fragment that neutralizes a major component of scorpion venom. Febs J **272:**2591-2601.
132. **Ribnicky, B., T. Van Blarcom, and G. Georgiou.** 2007. A scFv antibody mutant isolated in a genetic screen for improved export via the twin arginine transporter pathway exhibits faster folding. J Mol Biol **369:**631-639.
133. **Rich, R. L., and D. G. Myszka.** 2007. Higher-throughput, label-free, real-time molecular interaction analysis. Anal Biochem **361:**1-6.
134. **Richins, R. D., I. Kaneva, A. Mulchandani, and W. Chen.** 1997. Biodegradation of organophosphorus pesticides by surface-expressed organophosphorus hydrolase. Nat Biotechnol **15:**984-987.
135. **Rodi, D. J., and L. Makowski.** 1999. Phage-display technology--finding a needle in a vast molecular haystack. Curr Opin Biotechnol **10:**87-93.
136. **Roopenian, D. C., and S. Akilesh.** 2007. FcRn: the neonatal Fc receptor comes of age. Nat Rev Immunol **7:**715-725.
137. **Rosenfeld, M. A., K. Yoshimura, B. C. Trapnell, K. Yoneyama, E. R. Rosenthal, W. Dalemans, M. Fukayama, J. Bargon, L. E. Stier, L. Stratford-**

Perricaudet, and et al. 1992. In vivo transfer of the human cystic fibrosis transmembrane conductance regulator gene to the airway epithelium. Cell **68:**143-155.

138. **Rosovitz, M. J., P. Schuck, M. Varughese, A. P. Chopra, V. Mehra, Y. Singh, L. M. McGinnis, and S. H. Leppla.** 2003. Alanine-scanning mutations in domain 4 of anthrax toxin protective antigen reveal residues important for binding to the cellular receptor and to a neutralizing monoclonal antibody. J Biol Chem **278:**30936-30944.
139. **Samaranayake, H., T. Wirth, D. Schenkwein, J. K. Raty, and S. Yla-Herttuala.** 2009. Challenges in monoclonal antibody-based therapies. Ann Med**:**1-10.
140. **Seo, M. J., K. J. Jeong, C. E. Leysath, A. D. Ellington, B. L. Iverson, and G. Georgiou.** 2009. Engineering antibody fragments to fold in the absence of disulfide bonds. Protein Sci **18:**259-267.
141. **Shapiro, H. M., and John Wiley & Sons.** 2003, posting date. Practical flow cytometry. Wiley-Liss 4th. [Online.]
142. **Shi, H., and W. Wen Su.** 2001. Display of green fluorescent protein on Escherichia coli cell surface. Enzyme Microb Technol **28:**25-34.
143. **Sidhu, S. S.** 2001. Engineering M13 for phage display. Biomol Eng **18:**57-63.
144. **Siegrist, C. A., and R. Aspinall.** 2009. B-cell responses to vaccination at the extremes of age. Nat Rev Immunol **9:**185-194.
145. **Silverstein, A. M.** 2004. Labeled antigens and antibodies: the evolution of magic markers and magic bullets. Nat Immunol **5:**1211-1217.
146. **Skerra, A., and A. Pluckthun.** 1988. Assembly of a functional immunoglobulin Fv fragment in Escherichia coli. Science **240:**1038-1041.
147. **Smiley, S. T.** 2008. Immune defense against pneumonic plague. Immunol Rev **225:**256-271.
148. **Smith, G. P.** 1985. Filamentous fusion phage: novel expression vectors that display cloned antigens on the virion surface. Science **228:**1315-1317.
149. **Sofer-Podesta, C., J. Ang, N. R. Hackett, S. Senina, D. Perlin, R. G. Crystal, and J. L. Boyer.** 2009. Adenovirus-mediated Delivery of an Anti-V Antigen Monoclonal Antibody Protects Mice Against a Lethal Yersinia pestis Challenge. Infect Immun.
150. **Srinivasan, A., J. Foley, R. Ravindran, and S. J. McSorley.** 2004. Low-dose Salmonella infection evades activation of flagellin-specific CD4 T cells. J Immunol **173:**4091-4099.
151. **Stephens, D. L., M. D. Choe, and C. F. Earhart.** 1995. Escherichia coli periplasmic protein FepB binds ferrienterobactin. Microbiology **141 (Pt 7):**1647-1654.
152. **Villemagne, D., R. Jackson, and J. A. Douthwaite.** 2006. Highly efficient ribosome display selection by use of purified components for in vitro translation. J Immunol Methods **313:**140-148.
153. **Vora, K. A., K. Tumas-Brundage, and T. Manser.** 1999. Contrasting the in situ behavior of a memory B cell clone during primary and secondary immune responses. J Immunol **163:**4315-4327.

154. **Walsh, G.** 2006. Biopharmaceutical benchmarks 2006. Nature biotechnology **24:**769-776.
155. **Wan, H. M., B. Y. Chang, and S. C. Lin.** 2002. Anchorage of cyclodextrin glucanotransferase on the outer membrane of Escherichia coli. Biotechnol Bioeng **79:**457-464.
156. **Wang, A. A., A. Mulchandani, and W. Chen.** 2001. Whole-cell immobilization using cell surface-exposed cellulose-binding domain. Biotechnol Prog **17:**407-411.
157. **Wang, J. Y., and Y. P. Chao.** 2006. Immobilization of cells with surface-displayed chitin-binding domain. Appl Environ Microbiol **72:**927-931.
158. **Wark, K. L., and P. J. Hudson.** 2006. Latest technologies for the enhancement of antibody affinity. Adv Drug Deliv Rev **58:**657-670.
159. **Wetzel, R.** 1988. Active immunoglobulin fragments synthesized in E. coli--from Fab to scantibodies. Protein Eng **2:**169-170.
160. **Winau, F., and R. Winau.** 2002. Emil von Behring and serum therapy. Microbes Infect **4:**185-188.
161. **Winter, G., and C. Milstein.** 1991. Man-made antibodies. Nature **349:**293-299.
162. **Wu, H., D. S. Pfarr, S. Johnson, Y. A. Brewah, R. M. Woods, N. K. Patel, W. I. White, J. F. Young, and P. A. Kiener.** 2007. Development of motavizumab, an ultra-potent antibody for the prevention of respiratory syncytial virus infection in the upper and lower respiratory tract. J Mol Biol **368:**652-665.
163. **Wu, H., D. S. Pfarr, Y. Tang, L. L. An, N. K. Patel, J. D. Watkins, W. D. Huse, P. A. Kiener, and J. F. Young.** 2005. Ultra-potent antibodies against respiratory syncytial virus: effects of binding kinetics and binding valence on viral neutralization. J Mol Biol **350:**126-144.
164. **Yan, X., and Z. Xu.** 2006. Ribosome-display technology: applications for directed evolution of functional proteins. Drug Discov Today **11:**911-916.
165. **Zhou, D., Y. Han, and R. Yang.** 2006. Molecular and physiological insights into plague transmission, virulence and etiology. Microbes Infect **8:**273-284.

Vita

Thomas John Van Blarcom was born in Hackensack, New Jersey on May 23rd, 1979, the son of Thomas and Dorothy Van Blarcom. After attending Ramapo High School in Franklin Lakes, New Jersey, he enrolled at North Carolina Sate University in Raleigh, North Carolina in 1997. During this time, he studied at The University of Melbourne, Australia for one semester and worked at Amgen, Incorporated for almost two years. Upon receiving his Bachelor of Science in Chemical Engineering with a minor in Biotechnology in 2003, he was immediately accepted into the Department of Chemical Engineering at The University of Texas at Austin to pursue a doctoral degree in Chemical Engineering. During this time, he was associated with several publications in peer reviewed journals and a book chapter.

Permanent address: 17 Albatross Point, Bayville, New Jersey, 08721

This dissertation was typed by Thomas John Van Blarcom.